ISTANBUL TECHNICAL UNIVERSITY ★ ENERGY INSTITUTE

ON THE DISCRETE NATURE OF THERMODYNAMICS

M.Sc. THESIS

Alhun AYDIN

Energy Science and Technology Division

Energy Science and Technology Programme

MAY 2014

ISTANBUL TECHNICAL UNIVERSITY ★ ENERGY INSTITUTE

ON THE DISCRETE NATURE OF THERMODYNAMICS

M.Sc. THESIS

Alhun AYDIN
(301121003)

Energy Science and Technology Division

Energy Science and Technology Programme

Thesis Advisor: Prof. Dr. Altuğ ŞİŞMAN

MAY 2014

İSTANBUL TEKNİK ÜNİVERSİTESİ ★ ENERJİ ENSTİTÜSÜ

TERMODİNAMİĞİN KESİKLİ DOĞASI ÜZERİNE

YÜKSEK LİSANS TEZİ

Alhun AYDIN
(301121003)

Enerji Bilim ve Teknoloji Anabilim Dalı

Enerji Bilim ve Teknoloji Programı

Tez Danışmanı: Prof. Dr. Altuğ ŞİŞMAN

MAYIS 2014

Alhun AYDIN, a M.Sc. student of ITU Energy Institute 301121003 successfully defended the thesis entitled **"ON THE DISCRETE NATURE OF THERMODYNAMICS"**, which he prepared after fulfilling the requirements specified in the associated legislations, before the jury whose signatures are below.

Thesis Advisor :   **Prof. Dr. Altuğ ŞİŞMAN**   ....
Istanbul Technical University

Jury Members :   **Prof. Dr. Tekin DERELİ**   ....
Koç University

Asst. Prof. Dr. Fatih ÖZTÜRK   ....
Istanbul Technical University

Date of Submission :   **5 May 2014**
Date of Defense :   **27 May 2014**

To the shoulders of giants,

FOREWORD

In this Master of Science thesis, intrinsic discrete nature of thermodynamics is introduced and examined as a consequence of quantum size effects. I would like to express my deepest gratitude to my advisor Prof. Dr. Altuğ Şişman who sincerely trusted in and tirelessly guided me during my thesis with his scientific knowledge and experience. His great sincerity, kindness and valuable discussions and suggestions was indispensable for me. I would like to thank also the members of Nano Energy Research Group (NERG) and all academic, administrative and employee staff of ITU Energy Institute for their helps and supports. Lastly, I would like to thank my family for their invaluable efforts on me.

I hope this thesis can put a drop into the ocean of knowledge.

MAY 2014   Alhun AYDIN
                                                                                                      Physicist

x

TABLE OF CONTENTS

ABBREVIATIONS

0D   **:** Zero-dimensional
1D   **:** One-dimensional
2D   **:** Two-dimensional
3D   **:** Three-dimensional
BE   **:** Bose-Einstein
FD   **:** Fermi-Dirac
FWHM **:** Full Width at Half Maximum
Li   **:** Polylogarithm function
MB   **:** Maxwell-Boltzmann
PSF   **:** Poisson Summation Formula
QBL   **:** Quantum Boundary Layer
QSE   **:** Quantum Size Effects
Var   **:** Variance

LIST OF TABLES

LIST OF FIGURES

LIST OF SYMBOLS

A	:	Area
C	:	Circumference
C_V	:	Heat capacity at constant volume
D	:	Dimension
E	:	Energy
f	:	Distribution function
F	:	Free Energy
g	:	Energy level
G	:	Gibbs free energy
h	:	Planck's constant
$\hbar$	:	Reduced Planck's constant
H	:	Enthalpy
He	:	Helium
i	:	Momentum state
I	:	Imaginary unit
k	:	Wave number
k_B	:	Boltzmann's constant
K	:	Kelvin
L	:	Length
L_c	:	A scale factor based on de Broglie wavelength
m	:	Mass
N	:	Number of particles
p	:	Momentum
P	:	Pressure
Q	:	Heat
S	:	Entropy
T	:	Temperature
U	:	Internal energy
V	:	Volume
W	:	Work
$\aleph$	:	Number of eigenvalues
α	:	Confinement parameter
δ	:	Full width at half maximum
ε	:	Energy eigenvalue
γ_e	:	Proportionality constant of electronic heat capacity
γ_L	:	Proportionality constant of lattice heat capacity

Γ	:	Gamma function
$\mathcal{G}$	:	Density of states
λ_{th}	:	Thermal de Broglie wavelength
Λ	:	Dimensionless chemical potential
μ	:	Chemical potential
∇	:	Vector differential operator
ψ	:	Wave function
Ψ	:	Total wave function
Θ	:	Heaviside step function
Ω	:	Macrostate multiplicity
$\mathcal{Z}$	:	Grand partition function

ON THE DISCRETE NATURE OF THERMODYNAMICS

SUMMARY

Thermodynamics is one of the oldest and most significant disciplines in natural sciences. Mainly it concerns with energy and its relation to entropy and work. Since we are surrounded by energy, almost every thing in nature is related with thermodynamics in some way. Before the quantum revolution in 1920's, thermodynamics was one of the most well-established discipline in the scientific world. On the other side, with the understanding and insight that quantum mechanics gives us now, it might be the time to reconsider some things even in well-established areas of physics like the thermodynamics itself.

For centuries, it was assumed that thermodynamic quantities have continuous nature, since they represent macroscopic properties of the system. For the first time, we showed for Fermi gases that thermodynamic quantities intrinsically have discrete nature which reveals itself properly in nano scale where quantum effects dominate the system. One cannot separate quantum mechanics from thermodynamics at nano scale and below. Although continuum approximation is very useful to study thermodynamics of macro systems, in nano scale it apparently fails. Therefore, thermodynamic properties of nano systems cannot be calculated by classical and conventional methods.

The proper calculation of thermodynamic quantities in nano scale confined structures have to be done by using the exact summations of thermodynamic state functions. Converting them to integrals by using density of states concept is not valid in strongly degenerate and confined structures, since that process eventually vanishes size effects. As confinement increases, wavefunctions of particles start to be affected prominently by the boundaries of the domain due to quantum mechanical reasons. This leads to a stepwise behavior in the summation of Fermi-Dirac distribution function and since all thermodynamic properties contains the distribution function inside the summations, all of them are affected by the confinement and present discrete behaviors.

Two distinct type of discrete behaviors observed in thermodynamic quantities; stepwise and peakwise behaviors. Stepwise behaviors observed in variations of number of particles, internal energy, free energy and pressure with chemical potential, whereas peakwise behaviors observed in variations of entropy and heat capacity with chemical potential, number of particles, confinement parameter and domain size in one direction. The ones exhibit stepwise behavior contains the summation over distribution function which generates steps and others that exhibit peakwise behavior contains the summation over the derivative of distribution function (or variance function) which generates peaks. Detailed examination of peakwise behavior in entropy and heat

capacity showed that Fermi line and Fermi surfaces are also discrete. These odd phenomena come directly from the quantum nature of Fermi-Dirac statistics.

Behaviors of thermodynamic state functions also depend on the dimension of the momentum space. In one-dimensional structures, thermodynamic quantities have regular discrete nature whereas for multi-dimensional structures, they have quasi-irregular nature due to the degeneracy of energy levels.

Effects introduced in this thesis may lead to the development of new nano devices that stores thermal energy at nano scale in a more efficient way. Finally, proposal of an experimental verification of discrete and oscillatory nature in thermodynamic quantities is discussed.

TERMODİNAMİĞİN KESİKLİ DOĞASI ÜZERİNE

ÖZET

Temelde sistemin enerjisinin ısı ve iş alış-verişi ile ilişkilerini inceleyen termodinamik disiplini, doğa bilimlerinin en eski ve en önemlilerinden biridir. Yaşadığımız bu dünyada veya daha genel olarak evrende tüm süreçlere enerji alış-verişi eşlik ettiğinden aslında her şey bir bakıma termodinamik ile ilgilidir. 1920'lerdeki kuantum devriminden önce bilim camiasında termodinamik en sağlam ve köklü disiplinlerden biri olarak görülmekteydi. Günümüzde ise, kuantum mekaniğinin bize kazandırdığı anlayış sayesinde, fiziğin en oturmuş kabul edilen alanlarından biri olan termodinamikte bile bazı şeyleri yeniden gözden geçirmenin zamanının geldiği anlaşılmaktadır.

Termodinamik büyüklüklerin yıllardır sürekli değişkenler oldukları varsayılmıştı. Büyük ölçekli sistemler için doğru olan bu yaklaşım, nano ölçekte kuantum davranışların da sebebi olan maddenin dalga karakterinin önemli hale gelmesi nedeniyle geçerliliğini yitirmektedir. Tezde ilk defa Fermi gazları için termodinamik büyüklüklerin içsel bir kesikli doğası olduğu ve bu özelliğin kuantum etkilerin sistemde hakim olduğu nano ölçeklerde daha belirgin bir şekilde ortaya çıktığı gösterilmiştir. Kuantum etkilerin sistemdeki hakimiyetinden dolayı, nano ölçek ve altında sistemin termodinamiği, kuantum mekaniğinden ayrı incelenemez. Süreklilik yaklaşımı her ne kadar büyük ölçekte ve hatta orta ölçeklerde kullanışlı olsa da, nano sistemlerde geçerli olmayıp hatalı sonuçlar verir. Bu nedenle, nano sistemlerin termodinamik özellikleri hesaplanırken alışılagelmiş klasik yöntemlerin kullanılması doğru olmaz.

Parçacık sayısı, iç enerji, entropi, basınç, serbest enerji ve ısı sığası gibi termodinamik büyüklükler tanımları gereği toplam formülleri ile ifade edilir. Klasik termodinamikte hesap ve işlem kolaylığı açısından toplamlar süreklilik yaklaşımı altında integrallerle yer değiştirilir. Bu yer değiştirme sırasında hal yoğunluğu kavramından yararlanılır. Kuantum etkilerinin önemsenmediği büyük ölçekli yapılarda bu işlem hem oldukça iyi sonuçlar verir, hem de termodinamik özelliklerin analitik olarak ifade edilmesini ve bu sayede aralarındaki ilişkilerin kolay görülmesini sağlar. Diğer yandan, kuantum mekaniğinin doğasının bir sonucu olarak küçük ölçekli yapılarda örneğin nano ölçekte kuantum ölçek etkileri termodinamik özellikler üzerinde rol oynamaya başlar.

Kuantum mekaniğinin sonucu olarak, tutuklanma arttıkça termodinamik özellikler de ölçeğe ve biçime bağlı hale gelir. Doğal olarak tutuklanma ve/veya parçacık yoğunluğu ne kadar fazlaysa, bu etki o kadar güçlenir.

Tez kapsamında; tezin amacının, literatür araştırmasının ve tezin önemli sonuçlarının listelendiği giriş niteliğindeki ilk bölümün ardından ikinci bölümde, tezi anlamak

için gerekli olan tüm bilgiler sistemli bir şekilde verilmeye çalışılmıştır. Kuantum istatistiğine giriş yapılmış, dağılım fonksiyonları türetilmiş ve termodinamik büyüklükler tanıtılmıştır. Literatürde toplam formüllerinin integrallerle nasıl yer değiştirildiği incelenmiş ve buna göre termodinamik büyüklükler farklı boyutlarda türetilmiştir. Ardından termodinamik toplamların analitik gösterimine olanak sağlayan Poisson toplam formülü tanıtılmıştır. Tutuklanma değişkeni tanımlanmış ve farklı tutuklanma değerlerinde Poisson toplam formülünün terimleri incelenmiş ve kesikli yapının matematiksel gösterimi yapılmıştır.

Termodinamik özelliklerin kesikli doğası, 3., 4., ve 5. bölümlerde sırasıyla 1, 2 ve 3 boyutlu domenlerde ayrı ayrı incelenmiştir. Her bölümde termodinamik büyüklüklerdeki basamaklı ve tepeli yapı ayrı altbaşlıklar altında incelenmiş ve bu yapılara neden olan etmenler açıklanmıştır. Bunlardan kısaca bahsedersek; kuantum etkilerin bir sonucu olan termodinamiğin kesikli yapısı, termodinamik büyüklükler üstünde etkisini basamaklı ve tepeli olmak üzere iki farklı şekilde gösterir. Parçacık sayısı, iç enerji, basınç ve serbest enerji gibi termodinamik büyüklüklerin kimyasal potansiyel ve parçacık sayısı ile değişimlerinde basamaklı bir yapı gözlenmiştir. Bu basamaklı yapı temel olarak Fermi-Dirac dağılım fonksiyonunda Fermi gazlarının ayırt edici bir özelliği olan Pauli dışarlama ilkesi ve kütleli parçacıkların bir özelliği olan ikinci dereceden enerji-momentum ilişkisinin aşırı yoğun ve ileri derece tutuklanmış durumlarda çok belirgin hale gelmesi sonucu gözlemlenir. Belli termodinamik özelliklerin türevleri ile bulunan entropi ve ısı sığası gibi termodinamik büyüklüklerde ise Fermi-Dirac dağılım fonksiyonunun değişimi ya da türevinin tepeli doğası gereği tepeli davranışlar gözlenir. Entropi ve ısı sığasındaki parçacık sayısı ve tutuklanma şiddeti değişimine bağlı tepeli davranış 1, 2 ve 3 boyutta sırasıyla Fermi noktası, Fermi doğrusu ve Fermi yüzeyinin kesikli yapısının sonucu olarak açıklanmıştır.

Termodinamik hal fonksiyonlarının farklı değişkenler altında davranışları domenin kaç boyutlu olduğu ile de doğrudan ilişkilidir. Örneğin tek boyutlu yapılarda basamaklı ve tepeli yapılar düzenli bir halde ilerlerken, birden fazla boyutlu yapılarda aynı kuantum enerji seviyesinde birden fazla hal bulunabileceğinden basamaklı ve tepeli yapıların değişimi düzensiz bir hal alır. Fermi gazlarında entropi ve ısı sığası sıfır boyutlu bir yapıda tam olarak sıfır ve tek boyutlu yapılarda neredeyse sıfır iken, birden fazla boyutlu yapılarda anlamlı değerler almaya başlar. Ayrıca literatürde Fermi gazlarında yaklaşık olarak eşit kabul edilen entropi ve ısı sığasının, domendeki tutuklanma arttıkça birbirinden oldukça farklı davrandıkları ve eşit olmadıkları gösterilmiştir.

Bazı termodinamik özellikler için gerek sürekli davranışı, gerekse de kesikli davranışı temsil edebilen analitik bağıntılar türetilmiştir. Termodinamik özelliklerin tutuklanma değişkeni ve ölçek ile olan bağımlılıkları incelenmiş, 2 ve 3 boyuttaki eş yönlü olmayan tutuklanmalarda entropi ve ısı sığasında salınımlar gözlenmiştir. Eş yönlü değişimlerde ise bu salınımlar yerini daha pürüzsüz değişimlere bırakmıştır.

Tezin son bölümünde ısı sığasındaki tepelerden yola çıkarak nano ölçekte yüksek miktarlarda enerji depolamayı sağlayabilecek bir nano cihaz önerisi ve deneysel çalışma için koşulların bilgisi verilmiştir. Nano ölçekte domenin boyutlarındaki değişim, ısı sığasında literatürdekinin aksine salınımlı bir değişime yol açmaktadır. Tezde yapılan teorik öngörüler, günümüz deneysel koşullarında test edilebilir nicelikte görülmektedir. Isı sığasındaki domene bağlı salınımların deneysel doğrulaması,

termodinamik özelliklerin kesikli yapısının da ve tezdeki diğer sonuçların da doğrulaması olacaktır. Bunun yanısıra, günümüz enerji depolama tekniklerine alternatif olabilecek yüksek miktarda ısıl enerji depolama mümkün olabilecektir.

Son olarak tezin ek kısmında tezde gereken matematiksel ve termodinamik altyapı için gerekli bilgiler verilmiştir.

1. INTRODUCTION

Even though quantum theory has revolutionized our way of thinking about the nature, the results we encounter on quantum nature of matter still continue to surprise us. Advancements in nanosciences and nanotechnologies in recent years make it possible to examine the macroscopic manifestations of quantum mechanical behaviors of matter in laboratories. In fact, three of the last five years Nobel prizes in physics are given to the experimental developments in various areas of nanotechnology. As a matter of fact, experiments are going ahead of theory in nanoscience but its theoretical basis' are also open to improvement.

In practical context, nanoscience and nanotechnologies have great potential to bring innovations in energy harvesting. Quantum dot solar cells emerged recently to increase the efficiency of solar energy systems by tuning the band gaps closely so that benefiting from wide ranges of solar spectrum. Nano materials with large surface area like graphene and carbon nanotubes can be used to make supercapacitors, since increasing surface area of capacitor plates and decreasing their distance between, raises capacitance vastly.

The importance of nanostructures comes mainly from their quantum mechanical behaviors. Unlike bulk materials, in nano materials, quantum nature of matter become prominent and even dominates the behavior of material, which leads to some significant capabilities that macro materials does not have, like giant magneto-capacitance and the importance of topological structure.

In consideration of today's leap forwards, necessity of studying thermal properties of nano systems became ineluctable. Nano scale thermodynamics or nanothermo-dynamics, is a brand new as well as an important topic of nanoscience. Along with the fundamental perspective of quantum statistics, it allows us to examine the thermodynamic behaviors of nano systems.

1

1.1 Purpose of Thesis

Proper study of thermodynamics of nano structures in a theoretical manner became a need. All the years before nano-revolution, scientists used classical or conventional methods of thermodynamics. Even in mesoscales, classical thermodynamics works quite well. However, when we go down to nano scale, things become too bizarre to be studied in a classical way.

Appearance of quantum mechanical effects at nano scale makes thermodynamic properties size and shape dependent. When domain sizes are smaller than thermal de Broglie wavelength, surface, edge and corner effects reveal themselves. It is insecure to continue using classical thermodynamics in such cases [1–3].

The main aim of this thesis is, to show that there are considerable deviations from classical thermodynamics in degenerate quantum gases at nano scale. Specifically for Fermi gases, they lead to some novel effects like discrete and oscillatory behaviors in thermodynamic quantities [4, 5]. To be able to observe these behaviors, proper way of calculating thermodynamic quantities for nano systems is introduced. Thermodynamic quantities have being supposed to be continuous at macroscale since they are considered by definition as macroscopic quantities. However, for the first time here, it is shown that thermodynamic quantities of Fermi gases have intrinsic discrete nature as a consequence of a combination of several quantum mechanical effects.

1.2 Literature Review

General principles and classical derivations of thermodynamic properties of gases have been made by considering thermodynamic limit in many textbooks [6–8]. Nevertheless, studies about finite-size effects increased nowadays, in parallel with the developments in nanotechnology. Numerous researches have been done to discover the nature of gases confined in finite-size domains [1, 2, 9–14].

In 1998, Schneider and Wallis obtained some results that are in correlation with the study of this thesis [15]. For ultracold Fermi gases in a harmonic trap, they obtained chemical potential and specific heat from thermodynamic state sums, and in 2012,

Chen, Su and Chen, made the similar study for quartic traps, again just for extremely low temperatures [16].

In 2004, by performing Poisson Summation Formula (PSF) on partition function, for a rectangular geometry, Sisman and Muller showed that considering exact summations has several consequences like thermosize effects, anisotropic pressure tensor and non-additive global thermodynamic properties which are not predicted by classical thermodynamics [1]. Generalization of this concept on spherical and cylindrical geometries and interpretation of thermosize effects as surface dependency of thermodynamics via the geometric dependence from surface/volume ratio has been done by Sisman in 2004 [2].

In 2007, it is theoretically shown that there is a quantum surface tension due to inhomogeneous density distribution, which causes the quantum boundary layer (QBL) in Maxwellian gases confined in a finite domain even in thermodynamic equilibrium [17]. Generalization of QBL to spherical and cylindrical geometries and to irregular arbitrary geometries has been shown in 2009 [18, 19].

In 2004 and 2008, temperature dependence of heat capacity has been just numerically examined for non-interacting fermions with multifractal energy spectra [20, 21].

As shown by Ozturk and Sisman in 2009, QSE make small corrections on thermal and potential conductivities of ideal Maxwell, Fermi and Bose gases. In addition, QSE are responsible from geometric dependency of Wiedemann-Franz ratio in nano scale [22].

In 2013, by Firat and Sisman, existence of QSE and QBL is also shown for D-dimensional arbitrary domains by using Weyl's conjecture and in addition to that, experimental setup for the verification of these effects has been proposed [23].

Studies of nanothermodynamics are newly developing and few researches have been done as they are given here. In this sense, scope and results of this thesis can be considered as novel and even surprising.

1.3 Structure of Thesis

Exact expressions of physical quantities in thermodynamics are in notions of summations. In this thesis, it is shown that there is an intrinsic discrete nature in thermodynamic properties of Fermi gases. Although discrete behavior is inherent, it reveals itself in some extreme conditions like drastically degenerate and severely confined Fermi gas systems. We may sort the main outputs and unique results of the thesis as

- Intrinsic discrete nature in thermodynamic properties of Fermi gas

- Regular stepwise behavior of number of particles, internal energy, free energy and pressure in 1D Fermi gas

- Periodic peakwise behavior of entropy and heat capacity in 1D Fermi gas

- Analytic expressions for some thermodynamic properties representing their discrete nature

- Quasi-irregular stepwise behavior of number of particles, internal energy, free energy and pressure in 2D and 3D Fermi gases

- Non-periodic oscillatory-like peaks in entropy and heat capacity of 2D and 3D Fermi gases

- Discrete Fermi point, Fermi line and Fermi surface

- Both behaviors and magnitudes of entropy and heat capacity of Fermi gases at nano scale are quite different from each other

- Strong size dependency of thermodynamic properties at nano scale

- Experimental proposal for the verification of new effects introduced in the thesis

- Proposition of nano scale thermal energy storage devices based on quantum size effects

After this introduction, in chapter two, a brief review of quantum statistical thermodynamics is given together with a summary of supplementary explanations for

the sake of better understanding of some concepts that are used in the thesis. Then, in chapters three, four and five, discussions of 1D, 2D and 3D Fermi gases are done respectively and effects of discrete nature are introduced and examined in detail with their explanations. Possible experimental verification and useful application in energy storage are discussed in the last chapter. In addition, some necessary mathematical information about the formulas, methods and functions that are used in thesis are given in Appendix A and glossaries of thermodynamics, quantum mechanics and laws of thermodynamics are given in Appendix B.

2. THERMODYNAMIC QUANTITIES OF IDEAL QUANTUM GASES

In this informative chapter, thermodynamics of non-interacting or in other words ideal quantum gases are briefly reviewed. Emergence of two types of particles with completely different statistical characters, as a direct result of their quantum wavefunctions, are discussed. Derivation of distribution functions and fundamental thermodynamic quantities are done in both exact and approximate forms for any dimension and any domain.

2.1 Exact Expressions of Thermodynamic Quantities

Thermodynamic quantities are represented in summation forms by definition. In classical thermodynamics, it is convenient to replace summations with integrals by using continuum approximation to obtain analytical and simple expressions which provide easiness for calculations and algebraic manipulations. Conversion from summation to integral is useful in thermodynamic limit where the system is considered as having infinite volume. On the other hand, for finite-size systems it is unsafe to use integrals, since they give considerably different results than summations. To study the thermodynamics of low dimensional quantum structures or extremely confined nano structures, it is more appropriate to use exact state sums instead of integrals. Therefore, exact definitions of thermodynamic properties of ideal quantum (Fermi or Bose) gases based on infinite sums are considered in most parts of this thesis. Note that, since masses and velocities of particles in nanostructures are extremely low in most cases, gravitational and relativistic effects are neglected as a matter of course.

2.1.1 Nature of Quantum Statistics

To study the thermodynamics of nano scale ideal gases, it is necessary to use quantum statistics; Fermi-Dirac (FD) or Bose-Einstein (BE), instead of classical Maxwell-Boltzmann (MB) statistics. In this section, by starting from the most

fundamental concepts, derivation of thermodynamic quantities for quantum gases are given in grand canonical ensemble which is the most general statistical ensemble.

Unlike classical mechanics, particles are *indistinguishable* in quantum mechanics. So an electron here is no different than an electron there. As quoted from David J. Griffiths,

> It is not merely that *we* don't know which electron is which; *God* doesn't know which is which, because there is no such thing as "this" electron, or "that" electron. [24]

Indistinguishability of particles bring a different statistical nature to quantum systems. To examine the statistical behavior of particles in quantum mechanics, let's take the simplest system of two particles with wavefunctions $\psi_a(x_1)$ and $\psi_b(x_2)$. From the joint probability of independent events, product of their individual wavefunctions gives the wavefunction of the system, $\psi(x_1, x_2)$. As a statistical fact, square of the absolute value of the wavefunction will not change under the exchange of particles,

$$|\psi(x_1, x_2)|^2 = |\psi(x_2, x_1)|^2 \tag{2.1}$$

which gives two different solutions,

$$\psi(x_1, x_2) = \pm \psi(x_2, x_1) \tag{2.2}$$

where "$+$" and "$-$" respectively denote the *symmetric* and *antisymmetric* wavefunctions under exchange. This result shows that in quantum mechanics there are two different types of particles in terms of their statistical behavior. The particle with the symmetric wavefunction is called Boson, and the antisymmetric wavefunction is called Fermion. Although it may look a bit trivial at first sight, the sign change leads to completely different statistical behaviors. For example when we add wavefunctions of two Fermions to their wavefunction under the exchange, it gives zero which means there is no wavefunction, in other words, the probability that two Fermions share the same quantum state is zero.

$$\psi(x_1, x_2) + [-\psi(x_2, x_1)] = 0 \tag{2.3}$$

8

This result is known as Pauli exclusion principle. On the contrary, since their wavefunction is symmetric, Bosons have tendency to accumulate to the same quantum state, which shows itself as Bose-Einstein condensate.

2.1.2 Distribution Functions in Quantum Statistics

In order to examine the statistical behaviors of Fermions and Bosons, we derive distribution functions for FD and BE statistics. Distribution function as the name implies defines how a statistical system of particles distributes. To find them, we first define their combinatoric functions. By assuming that all states are equally likely, number of micro states corresponding to a macro state, Ω, is the product of the combination functions which are defined as the number of ways to arrange N_i particles into g_i states. As we can deduce the combinatoric nature of FD and BE statistics from the nature of their particle's wavefunctions, Ω_{FD} and Ω_{BE} are written as

$$\Omega_{FD} = \prod_i \frac{g_i!}{N_i!(g_i - N_i)!} \tag{2.4}$$

$$\Omega_{BE} = \prod_i \frac{(N_i + g_i - 1)!}{N_i!(g_i - 1)!} \tag{2.5}$$

where i is the quantum state, g_i is the number of states corresponding to the same energy level (in other words the degeneracy of quantum energy levels) and N_i is the number of particles in an energy level ε_i. To satisfy the equilibrium condition of thermodynamics, we maximize entropy, which is defined by Boltzmann as[1]

$$S = k_B \ln \Omega \tag{2.6}$$

where k_B is the Boltzmann's constant, which is just an invented constant and the result of our choice of temperature scale (Kelvin scale).[2] It is convenient to use Stirling's approximation for factorials given in Eqs. (2.4) and (2.5), after all it also reserves the condition to make statistics and saves us from fluctuations.

$$x >> 1 \Rightarrow \ln x! \approx x \ln x - x \tag{2.7}$$

---

[1]For the derivation of the Boltzmann entropy formula, please look at Appendix A.

[2]Boltzmann's constant relates energy with temperature and it depends on our temperature scale. If we choose our temperature scale same as our energy units, there would be no such constant, k would equal to 1.

Using the Stirling's approximation and assuming $N_i >> 1$ for the Bose case gives,

$$\ln \Omega_{FD} = \sum_i g_i \ln g_i - N_i \ln N_i - (g_i - N_i) \ln(g_i - N_i) \qquad (2.8)$$

$$\ln \Omega_{BE} = \sum_i (N_i + g_i) \ln(N_i + g_i) - N_i \ln N_i - (g_i - 1) \ln(g_i - 1) \qquad (2.9)$$

To find the most probable distribution for equilibrium condition, we'll maximize entropy by using Lagrange multipliers, which is a method for finding the extremum of a function subject to some constraints. Maximizing Eqs. (2.8) and (2.9) by equating their partial derivatives with respect to N_i leads,

$$\frac{\partial \ln \Omega}{\partial N_i} = \sum_i \ln \left(\frac{g_i \mp N_i}{N_i} \right) = 0 \qquad (2.10)$$

where here "$-$" sign for FD, "$+$" sign for BE derivation.[3] Assuming total number of particles N and total energy U are fixed, Ω function has two constraints,

$$\sum_i N_i = N \qquad (2.11)$$

$$\sum_i \varepsilon_i N_i = U \qquad (2.12)$$

and maximizing them gives,

$$\frac{\partial N}{\partial N_i} = 0 = \sum_i dN_i \qquad (2.13)$$

$$\frac{\partial U}{\partial N_i} = 0 = \sum_i \varepsilon_i dN_i \qquad (2.14)$$

where ε_i is the energy of ith state. Introducing Lagrange multipliers λ_1 and λ_2 to the function,

$$d \ln \Omega = \lambda_1 dN + \lambda_2 dU \qquad (2.15)$$

$$\sum_i \ln \left(\frac{g_i \mp N_i}{N_i} - \lambda_1 - \lambda_2 \varepsilon_i \right) dN_i = 0 \qquad (2.16)$$

---

[3]Please pay attention to $\mp$ and $\pm$ signs. Their order changes along the derivation.

which becomes,

$$\frac{g_i \mp N_i}{N_i} = e^{\lambda_1} e^{\lambda_2 \varepsilon_i} \qquad (2.17)$$

Hence, number of particles in an energy level becomes,

$$N_i = \frac{g_i}{e^{\lambda_1 + \lambda_2 \varepsilon_i} \pm 1} \qquad (2.18)$$

where now "+" sign indicates FD, whereas "−" sign indicates BE. Now, to find Lagrange constants λ_1 and λ_2, from the first and second laws of thermodynamics, in constant volume,

$$dU = TdS + \mu dN \qquad (2.19)$$

where T is temperature and μ is chemical potential. By inserting Boltzmann's entropy formula and equating Eq. (2.19) to Eq. (2.15),

$$k_B T d \ln \Omega + \mu dN - dU = d \ln \Omega - \lambda_1 dN - \lambda_2 dU \qquad (2.20)$$

λ_1 and λ_2 are found as

$$\lambda_1 = -\frac{\mu}{k_B T}, \qquad \lambda_2 = -\frac{1}{k_B T} \qquad (2.21)$$

We have found N_i that is the number of particles in an energy level. To find the number of particles in a momentum state, we divide Eq. (2.18) to g_i and inserting λ_1 and λ_2 we get distribution functions for FD (with "+" sign) and BE (with "−" sign)[4]

$$f_i = \frac{1}{e^{(\varepsilon_i - \mu)/k_B T} \pm 1} \qquad (2.22)$$

or equivalently,

$$f_i = \frac{1}{e^{\tilde{\varepsilon}_i - \Lambda} \pm 1} \qquad (2.23)$$

where energy eigenvalues and chemical potential are written in their dimensionless forms as $\tilde{\varepsilon}_i = \varepsilon_i / k_B T$ and $\Lambda = \mu / k_B T$. It is apparent from the result that for FD, occupation probability of a state is $0 < f_i < 1$ regardless of the magnitudes of variables

---

[4]For convenience it is common to neglect spin degrees of freedom g_i, since for instance for a free electron gas or He$_3$ it is just a factor of 2, in the absence of an external magnetic field.

as Pauli exclusion principle restricted. On the other hand, there is no such restriction for BE as expected.

2.1.3 Thermodynamic Quantities Based On Infinite Sums

Now we are ready to derive thermodynamic properties. Summing the number of particles in all momentum states gives the total number of particles written as

$$N = \sum_i f_i \qquad (2.24)$$

where the thermodynamic summations are always from one to infinity. Summation of the energies of all momentum states gives the total internal energy,

$$U = \sum_i \varepsilon_i f_i \qquad (2.25)$$

From the definition of entropy by Eq. (2.6), taking the integral of Eq. (2.10) and inserting $\ln \Omega$, we get,

$$S = k_B \left[\sum_i N_i \ln \left(\frac{g_i}{N_i} \mp 1 \right) \mp g_i \ln(N_i \mp g_i) \right] \qquad (2.26)$$

Turning Eq. (2.26) into a sum over momentum states gives,

$$S = k_B \left[\sum_i (f_i \mp 1)(\varepsilon_i - \mu) \mp \ln f_i \right] \qquad (2.27)$$

Eq. (2.27) is the entropy in its exact, infinite summation form where "$-$" for FD and "$+$" for BE. Now, all other thermodynamic properties can be derived by using N, U and S. For example Helmholtz free energy (or simply called free energy) is defined as $F = U - TS$ and since we know how to calculate all these variables, we can find free energy easily. From the first law of thermodynamics, $dU = dQ + dW$ taking the derivative of internal energy equation given in Eq. (2.25) gives,

$$dU = \sum_i \varepsilon_i df_i + \sum_i f_i d\varepsilon_i \qquad (2.28)$$

In Eq. (2.28), the first term on the right hand side represents the heat term dQ and the second term represents the work term dW. Using Eq. (2.28) and considering a simple

12

system so that $dW = -PdV$, we can write pressure as

$$P = -\sum_i f_i \frac{\partial \varepsilon_i}{\partial V} \tag{2.29}$$

where V is volume for a 3D system. It will be area for 2D and line for 1D systems. Now by inserting energy eigenvalues to the equation above[5] pressure is,

$$P = \frac{2}{3V} \sum_i \varepsilon_i f_i = \frac{2U}{3V} \tag{2.30}$$

The other important thermodynamic quantity is the heat capacity which is defined as

$$C = \frac{dQ}{dT} \tag{2.31}$$

in constant volume. From the first law of thermodynamics, it becomes,

$$C_V = \frac{dU}{dT} \tag{2.32}$$

Now let's derive heat capacity of a Fermi gas at constant volume by differentiating Eq. (2.25) with respect to T as

$$\frac{dU}{dT} = \sum_i \frac{\partial \varepsilon_i}{\partial T} f_i + \sum_i \varepsilon_i \frac{\partial f_i}{\partial T} \tag{2.33}$$

Since $\partial \varepsilon_i / \partial T = 0$, first term of the right hand side of Eq. (2.33) vanishes. Then,

$$\frac{dU}{dT} = -\sum_i \varepsilon_i f_i (1 \mp f_i) \left[\left(\frac{\partial \tilde{\varepsilon}_i}{\partial T} \right)_V - \left(\frac{\partial \Lambda}{\partial T} \right)_V \right] \tag{2.34}$$

where $(\partial \tilde{\varepsilon}_i / \partial T)_V = -\varepsilon_i / k_B T^2$. Only unknown term is $(\partial \Lambda / \partial T)_V$ on the Eq. (2.34). To find it let's use the fact that derivative of number of particles with respect to temperature is zero. By the Eq. (2.24),

$$\frac{\partial N}{\partial T} = 0 = \sum_i f_i (1 \mp f_i) \left[-\frac{\varepsilon_i}{k_B T^2} - \left(\frac{\partial \Lambda}{\partial T} \right)_V \right] \tag{2.35}$$

Derivative of Λ becomes,

$$\left(\frac{\partial \Lambda}{\partial T} \right)_V = -\frac{\sum_i \frac{\varepsilon_i}{k_B T^2} f_i (1 \mp f_i)}{\sum_i f_i (1 \mp f_i)} \tag{2.36}$$

---

[5]In the following subsections, energy eigenvalues will also be derived so that one can confirm this result.

Inserting Eq. (2.36) into Eq. (2.34),

$$\frac{dU}{dT} = k_B \sum_i \frac{\varepsilon_i^2}{k_B^2 T^2} f_i(1 \mp f_i) - \frac{k_B \sum_i \varepsilon_i f_i(1 \mp f_i) \sum_i \frac{\varepsilon_i}{k_B^2 T^2} f_i(1 \mp f_i)}{\sum_i f_i(1 \mp f_i)} \tag{2.37}$$

Finally, C_V becomes,

$$C_V = k_B \left[\sum_i (\tilde{\varepsilon}_i)^2 f_i(1 \mp f_i) - \frac{[\sum_i \tilde{\varepsilon}_i f_i(1 \mp f_i)]^2}{\sum_i f_i(1 \mp f_i)} \right] \tag{2.38}$$

In the derivation of heat capacity, to be able to interchange derivative operator with summation, sum has to converge uniformly. Although speed of convergence of the our summation depends on its variables, comparison of analytical and numerical derivative perfectly matches with each other, so there is no uniform convergency problem in these summations.

We introduced and derived three basic thermodynamic quantities (N, U and S) in terms of infinite summations from their definitions and also showed that all thermodynamic state functions (like F, P and C_V) can be derived based on them.

2.1.4 Thermodynamic Potentials and Conjugate Variables

Thermodynamic potentials are scalar quantities that represent the certain types of energy of the system in terms of relevant variables. The main thermodynamic potential is internal energy, U and the fundamental thermodynamic equation is written as

$$dU = TdS - PdV + \mu dN \tag{2.39}$$

Other thermodynamic potentials can easily be reproduced from internal energy, U by using Legendre transformations,

$$dF = -SdT - PdV + \mu dN \tag{2.40}$$

$$dH = TdS + VdP + \mu dN \tag{2.41}$$

$$dG = -SdT + VdP + \mu dN \tag{2.42}$$

14

where F is Helmholtz free energy, H is enthalpy and G is Gibbs free energy.

In thermodynamics, there are three conjugate variables in pairs of temperature-entropy (T-S), pressure-volume (P-V) and chemical potential-number of particles (μ-N), which are representing thermal, mechanical and chemical parameters of a thermodynamic system respectively. Here P, T and μ are intensive properties that means independent from the amount of substance and V, S, N are extensive properties depending on the amount of substance.

Pressure is the thermodynamic driving force that causes displacement in volume. Analogously, temperature and chemical potential might be considered as driving forces of displacements in entropy and particle number respectively, though they are not actually forces in a usual sense. As heat moves from higher temperature to lower temperature to increase the entropy of the system, particles move from higher to lower chemical potential. Pressure, temperature and chemical potential can be written as the gradient of thermodynamic potentials.

2.2 Conventional Expressions of Thermodynamic Quantities

Before examining thermodynamic properties at nano scale, it is appropriate to go over their conventional forms to understand in which ways they differ from macro scale. For this reason, in this section, conventional thermodynamic quantities are derived in thermodynamic limit (without considering finite-size effects) by taking the most general definitions for thermal de Broglie wavelength and density of states.

2.2.1 General Definition of Thermal de Broglie Wavelength

According to quantum mechanics, matter exhibits wave properties and has a wavelength corresponding to its matter wave. This wavelength is called de Broglie wavelength, and average de Broglie wavelength of ideal gas particles with a specified temperature is called thermal de Broglie wavelength. When domain size is much larger than thermal de Broglie wavelength, it is useful to neglect quantum effects and consider energy levels as if they are continuous. Here λ_{th} for a general energy-momentum

dispersion relation $E = ap^s$, is written as

$$\lambda_{th}(D,s) = \frac{h}{\sqrt{\pi}}\left(\frac{a}{k_B T}\right)^{1/s}\left[\frac{\Gamma(D/2+1)}{\Gamma(D/s+1)}\right]^{1/D} \qquad (2.43)$$

where D denotes dimension of the domain, a is energy-momentum dispersion constant and s is energy-momentum dispersion order [25]. For massive particles, energy-momentum dispersion relation is $E = p^2/2m$, so $a = 1/2m$ and $s = 2$. Since $s = 2$ removes dimensional dependency, for any dimension Eq. (2.43) becomes,

$$\lambda_{th} = \frac{h}{\sqrt{2\pi m k_B T}} \qquad (2.44)$$

where h is the Planck's constant and m is the mass of the particle.

2.2.2 Density of States for a D-dimensional Arbitrary Domain

As you may noticed, there are three common variables (ε, T, μ) appear in all thermodynamic state functions. ε is the energy eigenvalues that are solved from relevant differential equation, in this case (quantum gas) Schrödinger equation, a special type of Helmholtz partial differential equation,

$$\nabla^2 \psi + k^2 \psi = 0 \qquad (2.45)$$

which turns to time-independent Schrödinger equation when wavenumber is $k = \sqrt{2m\varepsilon}/\hbar$,

$$-\frac{\hbar^2}{2m}\nabla^2 \psi = \varepsilon \psi \qquad (2.46)$$

where $\hbar = h/2\pi$ is the reduced Planck's constant and external potential is zero.

In spectral theory, asymptotic behaviors of eigenvalues of Helmholtz-like partial differential equations for an arbitrary domain are given by Weyl's conjecture [23, 26]. In D-dimensions, the number of eigenvalues within an arbitrary domain is written as

$$\aleph_D(k) = \frac{Vk^3}{6\pi^2}\Theta(D-3) + (-1)^D\frac{Ak^2}{4^{D-2}4\pi}\Theta(D-2) + (-1)^{D-1}\frac{Ck}{4^{D-1}\pi}\Theta(D-1)$$

$$+ (-1)^{D-2}\frac{N_C}{4^D}$$

$$(2.47)$$

16

where k is the wavenumber, D denotes dimension, V is volume, A is surface area, C is circumference, N_C is the number of corners and holes in the domain and Θ is Heaviside step function which is defined as

$$\Theta(x) = \begin{cases} 0 & , x < 0 \\ 1 & , x \geq 0 \end{cases} \tag{2.48}$$

Then, density of states in k-space is,

$$\mathcal{G}_D(k) = \frac{\partial \aleph_D(k)}{\partial k} = \frac{Vk^2}{2\pi^2}\Theta(D-3) + (-1)^D \frac{Ak}{4^{D-2}2\pi}\Theta(D-2)$$
$$+ (-1)^{D-1}\frac{C}{4^{D-1}\pi}\Theta(D-1) \tag{2.49}$$

To convert density of states to ε-space we first insert $k = \sqrt{2m\varepsilon}/\hbar$ in Eq. (2.47),

$$\aleph_D(\varepsilon) = \frac{V}{6\pi^2}\left(\frac{2m}{\hbar^2}\right)^{3/2}\varepsilon^{3/2}\Theta(D-3) + (-1)^D \frac{Am\varepsilon}{4^{D-2}2\pi\hbar^2}\Theta(D-2)$$
$$+ (-1)^{D-1}\frac{C\sqrt{2m\varepsilon}}{4^{D-1}\pi\hbar}\Theta(D-1) + (-1)^{D-2}\frac{N_C}{4^D} \tag{2.50}$$

Then, taking the derivative with respect to ε gives the density of states in ε-space,

$$\mathcal{G}_D(\varepsilon) = \frac{V}{4\pi^2}\left(\frac{2m}{\hbar^2}\right)^{3/2}\sqrt{\varepsilon}\Theta(D-3) + (-1)^D \frac{Am}{4^{D-2}2\pi\hbar^2}\Theta(D-2)$$
$$+ (-1)^{D-1}\frac{C}{4^{D-1}2\pi\hbar}\sqrt{\frac{2m}{\varepsilon}}\Theta(D-1) \tag{2.51}$$

or equivalently,

$$\mathcal{G}_D(\varepsilon) = 2\pi V\left(\frac{2m}{h^2}\right)^{3/2}\sqrt{\varepsilon}\Theta(D-3) + (-1)^D \frac{2Am\pi}{4^{D-2}h^2}\Theta(D-2)$$
$$+ (-1)^{D-1}\frac{C}{4^{D-1}h}\sqrt{\frac{2m}{\varepsilon}}\Theta(D-1) \tag{2.52}$$

where the first, second and third terms of Eqs. (2.51) or (2.52) are conventional density of states equations for 3D, 2D and 1D domains, respectively represented by $\mathcal{G}_3(\varepsilon)$,

$\mathcal{G}_2(\varepsilon)$ and $\mathcal{G}_1(\varepsilon)$. Under continuum approximation, sums can be replaced by integrals as

$$\sum_i (...) \longrightarrow \int (...)\mathcal{G}(\varepsilon)d\varepsilon \qquad (2.53)$$

All we need for the derivation of thermodynamic properties of continuous domains are given in their most general forms in this subsection. Now let's examine thermodynamic quantities for 3D, 2D and 1D cases, separately.

2.2.3 Thermodynamic Quantities of a 3D Quantum Gas

Substantially, all structures are 3-dimensional. However, confinement of the domain in a direction, can result to a quasi-reduction of that dimension. Although the domain is still 3-dimensional, it may behave as if it's lower-dimensional. Ordinarily, 3-dimensional structures are called bulk structures. Number of particles N for a 3D domain under continuum approximation is written as

$$N_3 = \int_0^\infty \frac{\mathcal{G}_3(\varepsilon)d\varepsilon}{e^{(\varepsilon-\mu)/k_BT} \pm 1} \qquad (2.54)$$

where subscripts of $3,2$ and 1 throughout this section indicate the numbers of dimensions of the domain. Taking the 3D density of states only, that is the first term of Eq. (2.51), and inserting it into Eq. (2.54) gives,

$$N_3 = \mp \frac{V}{4\pi^2} \left(\frac{2mk_BT}{\hbar^2} \right)^{3/2} \frac{\sqrt{\pi}}{2} Li_{3/2}(\mp e^{\mu/k_BT}) \qquad (2.55)$$

By arranging it and inserting Eq. (2.44) we can represent number of particles in terms of thermal de Broglie wavelength as

$$N_3 = \mp \frac{V}{\lambda_{th}^3} Li_{3/2}(\mp e^{\mu/k_BT}) \qquad (2.56)$$

By using the first terms of asymptotic expansions of polylogarithm functions in degenerate Fermi limit ($\mu \gg 1$), for Fermi gas, number of particles becomes,

$$N_3 = \frac{4V\pi}{3} \left(\frac{2m}{h^2} \right)^{3/2} \mu_{F3}^{3/2} \qquad (2.57)$$

18

where μ_F is the chemical potential at Fermi level. Note that since we didn't consider temperature correction terms in the expansions of polylogarithm functions yet, μ turns into μ_F in this equation. We'll consider temperature corrections in the derivations of entropy and heat capacity. From Eq. (2.57), by replacing N/V with denisty n, chemical potential at Fermi level is found as

$$\mu_{F_3} = \frac{h^2}{2m}\left(\frac{3n_3}{4\pi}\right)^{2/3} \tag{2.58}$$

Similarly, internal energy is written in its integral form,

$$U_3 = \int_0^\infty \frac{\varepsilon \mathcal{G}_3(\varepsilon) d\varepsilon}{e^{(\varepsilon-\mu)/k_B T} \pm 1} \tag{2.59}$$

Then inserting again the first term of Eq. (2.51) gives,

$$U_3 = \mp \frac{V k_B T}{4\pi^2}\left(\frac{2m k_B T}{\hbar^2}\right)^{3/2}\frac{3\sqrt{\pi}}{4} Li_{5/2}(\mp e^{\mu/k_B T}) \tag{2.60}$$

By rearranging it and inserting thermal de Broglie wavelength, we have,

$$U_3 = \mp \frac{3V k_B T}{2\lambda_{th}^3} Li_{5/2}(\mp e^{\mu/k_B T}) \tag{2.61}$$

Using the first terms of asymptotic expansions of polylogarithm functions for Fermi limit gives,

$$U_3 = \frac{4V\pi}{5}\left(\frac{2m}{h^2}\right)^{3/2}\mu_{F_3}^{5/2} \tag{2.62}$$

By inserting Eq. (2.57) into Eq. (2.62), we get the very familiar result,

$$U_3 = \frac{3}{5}N_3\mu_{F_3} \tag{2.63}$$

From Eq (2.30) pressure is obtained as,

$$P_3 = \frac{2U_3}{3V} \tag{2.64}$$

Until now, in the derivations of conventional 3D thermodynamic quantities, we only considered the zeroth order approximations of polylogarithm functions, which was

enough for the derivations of N, U and P. However, when we try to calculate our other fundamental properties like entropy and then heat capacity, we'll find them zero, since we neglected the temperature correction terms in the asymptotic expansions of polylogarithm functions. To find the expressions for entropy and heat capacity, we have to consider at least the first order terms also. First order temperature correction to chemical potential in 3D domain gives[6]

$$\mu_3 = \mu_{F_3} \left(1 - \frac{\pi^2 k_B^2 T^2}{12 \mu_{F_3}^2} \right) \tag{2.65}$$

By adding the first order correction term to internal energy in Eq. (2.61) we get,

$$U_3 = \frac{3 V k_B T}{2 \lambda_{th}^3} \frac{8 \Lambda^{5/2}}{15 \sqrt{\pi}} \left(1 + \frac{5 \pi^2}{8 \Lambda^2} \right) \tag{2.66}$$

Adding chemical potential correction only to the term in the nominator by using the assumption $(1+x)^n \approx 1 + nx$,

$$U_3 = \frac{3 V k_B T}{2 \lambda_{th}^3} \frac{8 \Lambda_F^{5/2}}{15 \sqrt{\pi}} \left(1 - \frac{5 \pi^2}{24 \Lambda_F^2} \right) \left(1 + \frac{5 \pi^2}{8 \Lambda_F^2} \right) \tag{2.67}$$

where $\Lambda_F = \mu_F / k_B T$. Arranging it by neglecting fourth order terms emerged by multiplications gives,

$$U_3 = \frac{4 V k_B T}{5 \lambda_{th}^3 \sqrt{\pi}} \Lambda_F^{5/2} \left(1 + \frac{5 \pi^2}{12 \Lambda_F^2} \right) \tag{2.68}$$

Inserting N_3 from Eq. (2.57) into the Eq. (2.68) gives the internal energy expression with temperature correction,

$$U_3 = \frac{3}{5} N_3 \mu_{F_3} \left(1 + \frac{5 \pi^2 k_B^2 T^2}{12 \mu_{F_3}^2} \right) \tag{2.69}$$

Now let's derive our other fundamental property; entropy. It's expression was given in section (2.1.3) by Eq. (2.27). We can easily arrange it,

$$S_3 = k_B \left(\sum_i \varepsilon_i f_i - \mu_3 \sum_i f_i - \sum_i (\mu_3 - \varepsilon_i) - \sum_i \ln f_i \right) \tag{2.70}$$

---

[6]For the derivation of this, look at Appendix A.

Then it can be written as,

$$S_3 = k_B[U - N\mu - \sum_i \ln(1 - f_i)]$$

(2.71)

In the equation above, the last term corresponds to the partition function which is a sum over all states. I didn't introduce and use the partition function in the derivations of thermodynamic quantities to show you that it is not an obligation to define somewhat *"magic"* quantities to derive thermodynamic state functions. As you see, it emerges inside of the entropy function as a term and for brevity I'll just put it to clarify the notation. Again, pay attention that there is no need for a partition function to derive thermodynamic properties, as we derived them here without using it. Then converting sum to the integral,

$$-\sum_i \ln(1 - f_i) \longrightarrow -\int \mathcal{G}_3 \ln(1 - f_i) d\varepsilon = \mathcal{Z}_3$$

(2.72)

and applying density of states concept gives,

$$\mathcal{Z}_3 = -\frac{V k_B T}{\lambda_{th}^3} Li_{5/2}(\mp e^{\mu/k_B T})$$

(2.73)

By adding temperature correction of chemical potential we obtain,

$$\mathcal{Z}_3 = \frac{8V\pi}{15} \mu_{F_3}^{5/2} \left(1 - \frac{5\pi^2}{24\Lambda_F^2}\right) \left(1 + \frac{5\pi^2 k_B^2 T^2}{8\mu_{F_3}^2}\right)$$

(2.74)

Inserting N_3 inside the Eq. (2.74) gives,

$$\mathcal{Z}_3 = \frac{2}{5} N_3 \mu_{F_3} \left(1 + \frac{5\pi^2 k_B^2 T^2}{12\mu_{F_3}^2}\right)$$

(2.75)

Now putting Eqs. (2.69), (2.65) and (2.75) respectively into Eq. (2.71),

$$S_3 = k_B \left[\frac{3}{5} N_3 \mu_{F_3} \left(1 + \frac{5\pi^2 k_B^2 T^2}{12\mu_{F_3}^2}\right) - N_3 \mu_{F_3} \left(1 - \frac{\pi^2 k_B^2 T^2}{12\mu_{F_3}^2}\right)\right.$$

$$\left. + \frac{2}{5} N_3 \mu_{F_3} \left(1 + \frac{5\pi^2 k_B^2 T^2}{12\mu_{F_3}^2}\right)\right]$$

(2.76)

Simplifying the above equation gives,

$$S_3 = \frac{\pi^2}{2\Lambda_F} N_3 k_B \tag{2.77}$$

Heat capacity[7] can easily be found by differentiating U_3 in Eq. (2.69) with respect to T as

$$C_V = \frac{\pi^2}{2\Lambda_F} N_3 k_B \tag{2.78}$$

Freakishly, neglecting other temperature corrections but most importantly ignoring size effect corrections leads to the equivalence of heat capacity and entropy in Fermi gases, which is, we'll see in next chapters, absolutely not true, although in literature ([6]) it is being used even in nano systems with incomprehensible complacency.

2.2.4 Thermodynamic Quantities of a 2D Quantum Gas

In 2D quantum gas, one direction is strongly confined so that system behaves as if it is 2-dimensional. Such systems are also called quantum wells. In the same way we derived the 3D quantities, let's derive them for a 2D domain. Number of particles for a 2D domain under continuum approximation is,

$$N_2 = \int_0^\infty \frac{\mathcal{G}_2(\varepsilon) d\varepsilon}{e^{(\varepsilon-\mu)/k_B T} \pm 1} \tag{2.79}$$

Inserting the second term of Eq. (2.52) which represents the 2D density of states gives,

$$N_2 = \mp \frac{2A\pi m}{h^2}(k_B T) Li_1(\mp e^{\mu/k_B T}) \tag{2.80}$$

Then for Fermions, by expanding polylogarithms to series we obtain the number of particles for a 2D Fermi gas,

$$N_2 = \frac{2A\pi m}{h^2}\mu_2 \tag{2.81}$$

And chemical potential is,

$$\mu_2 = \frac{h^2 n_2}{2\pi m} \tag{2.82}$$

---

[7]By heat capacity, we always mean the electronic contribution. Lattice contributions are out of scope of this thesis.

where $n_2 = N/A$. Two-dimensional internal energy is written in integral form as

$$U_2 = \int_0^\infty \frac{\varepsilon \mathcal{G}_2(\varepsilon)d\varepsilon}{e^{(\varepsilon-\mu)/k_BT} \pm 1} \tag{2.83}$$

Inserting 2D density of states and taking the integral gives,

$$U_2 = \mp \frac{2A\pi m}{h^2}(k_BT)^2 \, Li_2(\mp e^{\mu/k_BT}) \tag{2.84}$$

Expanding polylogarithms in degenerate Fermi limit,

$$U_2 = \frac{A\pi m}{h^2}\mu_2^2 \tag{2.85}$$

Then internal energy in 2D Fermi gas can be written as

$$U_2 = \frac{N_2\mu_2}{2} \tag{2.86}$$

From Eq. (2.29),

$$P_2 = \frac{U_2}{A} \tag{2.87}$$

Now, like we do in 3D case, let's insert the first order temperature corrections,

$$U_2 = \mathcal{Z}_2 = \frac{N_2\mu_2}{2}\left(1 + \frac{\pi^2 k_B^2 T^2}{3\mu^2}\right) \tag{2.88}$$

Here in 2D, internal energy and grand partition function become equal when we neglect higher order terms. Since $\mu_2 = \mu_{F_2}$ and there is no temperature correction also in number of particles in 2D, putting these into the entropy equation in Eq. (2.71) gives,

$$S_2 = \frac{N_2\mu_2}{2}\left(1 + \frac{\pi^2 k_B^2 T^2}{3\mu^2}\right) - N_2\mu_2 + \frac{N_2\mu_2}{2}\left(1 + \frac{\pi^2 k_B^2 T^2}{3\mu^2}\right) \tag{2.89}$$

which turns to

$$S_2 = \frac{\pi^2}{3\Lambda_F}N_2 k_B \tag{2.90}$$

Taking the derivative of Eq. (2.88) with respect to temperature, we get 2D heat capacity at constant area,

$$C_A = \frac{\pi^2}{3\Lambda_F}N_2 k_B \tag{2.91}$$

where A stands for area.

2.2.5 Thermodynamic Quantities of a 1D Quantum Gas

Now let's derive thermodynamic quantities of continuous 1D domains, namely quantum wires. Number of particles for a 1D domain in thermodynamic limit can be written as

$$N_1 = \int_0^\infty \frac{\mathcal{G}_1(\varepsilon)d\varepsilon}{e^{(\varepsilon-\mu)/k_B T} \pm 1} \tag{2.92}$$

Inserting the third term of Eq. (2.52) which represents the 1D density of states gives,

$$N_1 = \mp \frac{C}{h}\sqrt{2\pi m k_B T} \, Li_{1/2}(\mp e^{\mu/k_B T}) \tag{2.93}$$

Expanding polylogarithms gives,

$$N_1 = \frac{2C}{h}\sqrt{2m}\sqrt{\mu_1} \tag{2.94}$$

Then chemical potential becomes,

$$\mu_1 = \frac{h^2 n_1^2}{8m} \tag{2.95}$$

Internal energy in integral its form is written as

$$U_1 = \int_0^\infty \frac{\varepsilon \mathcal{G}_1(\varepsilon)d\varepsilon}{e^{(\varepsilon-\mu)/k_B T} \pm 1} \tag{2.96}$$

Taking the integral gives,

$$U_1 = \mp \frac{C}{h}\sqrt{2m}(k_B T)^{3/2}\frac{\sqrt{\pi}}{2} Li_{3/2}(\mp e^{\mu/k_B T}) \tag{2.97}$$

From Appendix A, inserting expansions of polylogarithm function leads,

$$U_1 = \frac{2C}{3h}\sqrt{2m}\mu_1^{3/2} \tag{2.98}$$

Then internal energy is,

$$U_1 = \frac{N_1 \mu_1}{3} \tag{2.99}$$

And here comes 1D pressure,

$$P_1 = \frac{2U_1}{C} \tag{2.100}$$

Let's consider first order temperature corrections to find entropy in 1D. Then relation between chemical potential at Fermi energy and chemical potential is,

$$\mu_1 = \mu_{F1}\left(1 + \frac{\pi^2 k_B^2 T^2}{12\mu_F^2}\right) \tag{2.101}$$

Internal energy in 1D with its first order temperature correction is,

$$U_1 = \frac{N_1\mu_1}{3}\left(1 + \frac{\pi^2 k_B^2 T^2}{8\mu_1^2}\right) \tag{2.102}$$

Putting correction of chemical potential into it,

$$U_1 = \frac{N_1\mu_1}{3}\left(1 + \frac{\pi^2 k_B^2 T^2}{8\mu_1^2}\right)\left(1 + \frac{\pi^2 k_B^2 T^2}{12\mu_1^2}\right)^{3/2}$$

$$= \frac{N_1\mu_1}{3}\left(1 + \frac{\pi^2 k_B^2 T^2}{8\mu_1^2}\right)\left(1 + \frac{\pi^2 k_B^2 T^2}{8\mu_1^2}\right) \tag{2.103}$$

$$= \frac{N_1\mu_1}{3}\left(1 + \frac{\pi^2 k_B^2 T^2}{4\mu_1^2}\right)$$

Number of particles and grand partition functions with first order temperature corrections are below respectively,

$$N_1 = \frac{2C}{h}\sqrt{2m\mu_1}\left(1 - \frac{\pi^2 k_B^2 T^2}{24\mu_1^2}\right) \tag{2.104}$$

$$\mathcal{Z}_1 = \frac{2}{3}N_1\mu_1\left(1 + \frac{\pi^2 k_B^2 T^2}{8\mu_1^2}\right) \tag{2.105}$$

From Eq. (2.71), entropy in 1D is written,

$$S_1 = k_B\left[\frac{N_1\mu_1}{3}\left(1 + \frac{\pi^2 k_B^2 T^2}{4\mu_1^2}\right) - \frac{2C}{h}\sqrt{2m\mu_1}\left(1 - \frac{\pi^2 k_B^2 T^2}{24\mu_1^2}\right)\right.$$

$$\left. + \frac{2}{3}N_1\mu_1\left(1 + \frac{\pi^2 k_B^2 T^2}{8\mu_1^2}\right)\right] \tag{2.106}$$

Entropy in 1D becomes,

$$S_1 = \frac{\pi^2}{6\Lambda}N_1 k_B \tag{2.107}$$

25

Then 1D heat capacity at constant circumference,

$$C_C = \frac{\pi^2}{6\Lambda} N_1 k_B \tag{2.108}$$

where C stands for circumference.

For 0D domain, a true quantum dot, one cannot talk about a Fermi gas. For example, in case the particles are electron, only two of them with opposite spins can occupy the 0D domain with zero-dimensional momentum space. Naturally, it is not meaningful to talk about statistics in such condition.

2.3 Confinement Parameter

Consider a rectangular 3D domain with dimensions L_1, L_2 and L_3. Since thermodynamics deals with equilibrium processes, time-independent Schrödinger equation will be considered here. Assuming that there is no penetration through domain walls, solution of the time-independent Schrödinger equation for boundary conditions $\psi(0) = \psi(L) = 0$ with normalization is,

$$\Psi_{i_n}(x_n) = \prod_{n=1}^{3} \sqrt{\frac{2}{L_n}} \sin\left(\frac{i_n \pi x_n}{L_n}\right), \text{ with } i_n = 1, 2, 3, ..., \tag{2.109}$$

where i_n represents quantum states with subscript denotes the directions $\{1, 2, 3\}$ of 3D domain and x_n stands for the position of the wavefunction. Then energy eigenvalues for a rectangular domain are,

$$\varepsilon_{i_n} = \frac{h^2}{8m} \sum_{n=1}^{3} \left(\frac{i_n}{L_n}\right)^2 \tag{2.110}$$

For convenience we shall define a confinement parameter, dimensionless inverse scale factor α as

$$\alpha = \frac{L_c}{L} = \frac{h}{\sqrt{8mk_B T L}} \tag{2.111}$$

where L_c is a scale factor based on de Broglie wavelength of particles. Here α indicates the rate of confinement, since when α increases, confinement also increases and vice versa. Comparison of continuous and confined domains can be roughly seen in Figure (2.1) below:

26
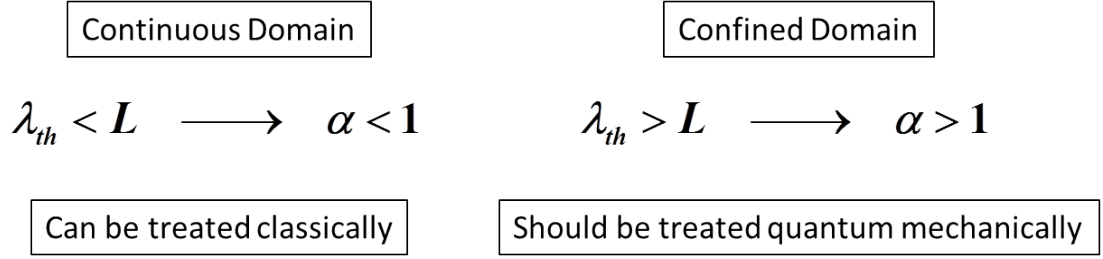
Figure 2.1: Comparison of continuous and confined domains.

Note that, separation of continuous and confined domains does not occur in one certain point and transition from continuous to discrete behavior is neither sharp, nor well-defined, just like in the case of transition from classical behavior to quantum mechanical one. However, it is possible to loosely separate the regions that are nearly free, relatively weakly confined and strongly confined by using the confinement parameter α, in Fig. (2.2).
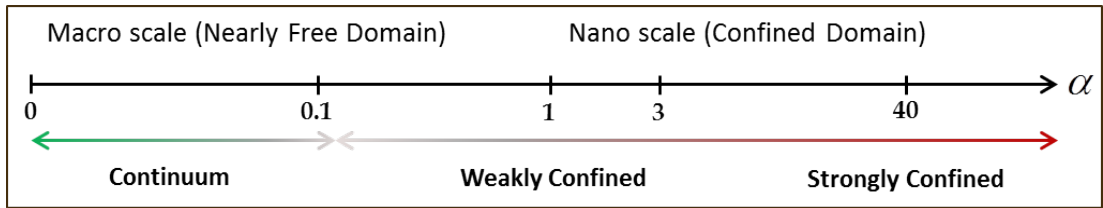
Figure 2.2: Loose separation of continuous and confined domains by confinement parameter.

Then, for 3D domain, energy eigenvalues can be expressed in terms of α's as

$$\frac{\varepsilon}{k_B T} = \tilde{\varepsilon} = [(\alpha_1 i_1)^2 + (\alpha_2 i_2)^2 + (\alpha_3 i_3)^2] \tag{2.112}$$

We'll use this notation in all thermodynamic state functions throughout the thesis, since it is possible to write all thermodynamic state functions in terms of dimensionless energy eigenvalues and dimensionless chemical potential and also it allows us to arrange the confinement through α easily.

2.4 Evaluation of Summations by Using Poisson Summation Formula

In order to evaluate summations, we used Poisson summation formula (PSF) which relates the summation of original function to the summation of its Fourier transform.

For even functions (that is the case for all thermodynamic state functions), PSF can be written as[8]

$$\sum_{i=1}^{\infty} f(i) = \underbrace{\int_0^{\infty} f(i)di}_{\text{Conventional Integral}} - \underbrace{\frac{f(0)}{2}}_{\text{Zero Correction}} + \underbrace{2\sum_{s=1}^{\infty} \int_0^{\infty} f(i)\cos(2\pi si)di}_{\text{Discrete Correction}} \qquad \textbf{(2.113)}$$

PSF is an exact summation formula and has some fortuitous advantages. It dissociates the sum into three terms and fabulously separates three regions with different physical outcomes. When thermodynamic state functions are applied into the PSF, the first term gives the conventional integral term and represents the classical region where the domain sizes are much larger than thermal de Broglie wavelength. The second term gives the zero correction term that excludes false contribution from the zeroth momentum state. This term becomes apparent in the transition region from classical to quantum and examined in literature as QSE [1, 2, 17]. The third term is the discrete correction term and reveals its contribution only in quantum scale where the domain size is smaller than the thermal de Broglie wavelength of particles in the domain.

Examination of the terms of PSF for different degeneracy (Λ) and confinement (α) values by choosing the kernel function as FD distribution function is shown in the Table (2.1) below.

Table 2.1: Exact sum and the terms of PSF for different degeneracy and confinement values:

Λ and α values	Sum	1st Term	2nd Term	3rd Term
$\Lambda = 0.1$, $\alpha = 0.1$	5.44	5.703	-0.2625	0
$\Lambda = 20$, $\alpha = 0.1$	44.175	44.675	-0.5	0
$\Lambda = 0.1$, $\alpha = 3$	0	0.1901	-0.2625	0.0724
$\Lambda = 20$, $\alpha = 3$	1	1.48916	-0.5	0.01084
$\Lambda = 1000$, $\alpha = 3$	10	10.5401	-0.5	-0.0401
$\Lambda = 200$, $\alpha = 40$	0	0.35355	-0.5	0.14645
$\Lambda = 10000$, $\alpha = 40$	2	2.49983	-0.5	0.00017

As we see before, summation over distribution function gives the total number of particles in the domain. Functional behaviors of the sum and the terms of PSF

---

[8]For the derivation of PSF for even and odd functions, you may look at to the Appendix A

is examined below in one-dimension for three cases; continuous, relatively weakly confined and strongly confined domains. The confinement rates of domains are calibrated through α, the confinement parameter. In Figs (2.3), (2.4) and (2.5) blue curves represent the exact summation over FD distribution function, namely the exact calculation of number of particles. Red curves represent the conventional integral term in PSF or in other words number of particles function that commonly used in literature. Yellow and green curves represent the second and third terms of PSF respectively. As PSF suggests, adding red, yellow and green curves gives exactly the blue curves.

Figure 2.3: Exact sum and terms of PSF in one dimension changing with dimensionless chemical potential for continuous domain ($\alpha = 0.1$).

As it is seen from Fig (2.3), even for nearly continuous case, there is a small difference between sum and integral which can be recovered by using just the second term of PSF. In literature, consequences of this small difference examined as QSE and QBL. When degeneracy increases, contribution of the third term of PSF vanishes for the continuous case.
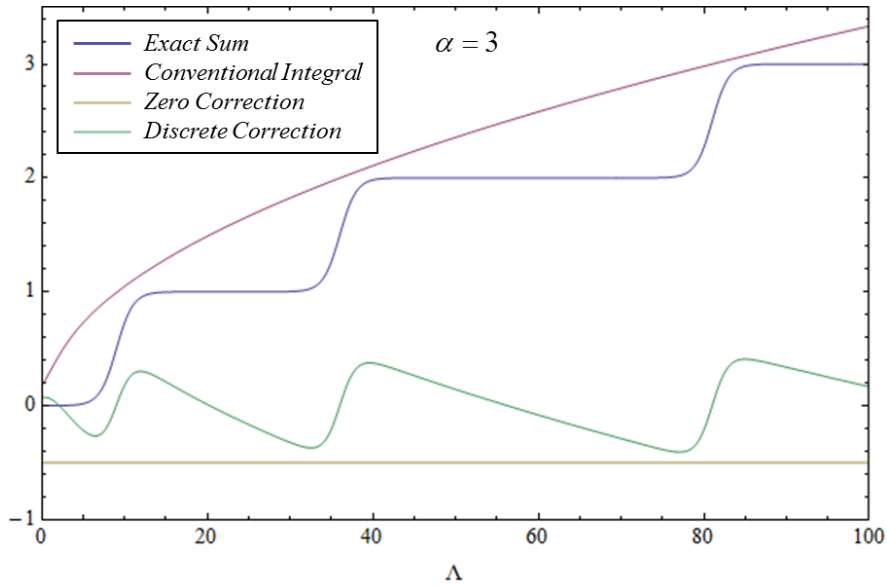
Figure 2.4: Exact sum and terms of PSF in one dimension changing with dimensionless chemical potential for relatively weakly confined domain ($\alpha = 3$).

In Fig. (2.4) domain size is three times smaller than the de Broglie wavelength of particles and as a consequence of this size confinement, discrete term reveals its oscillatory-like contribution. In Fig. (2.5) discreteness is even more apparent, where the domain is extremely confined.
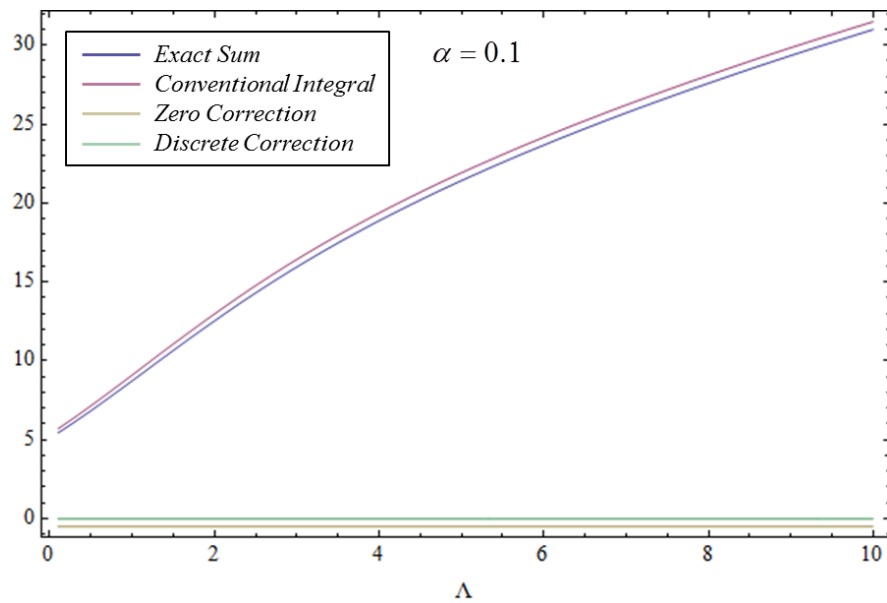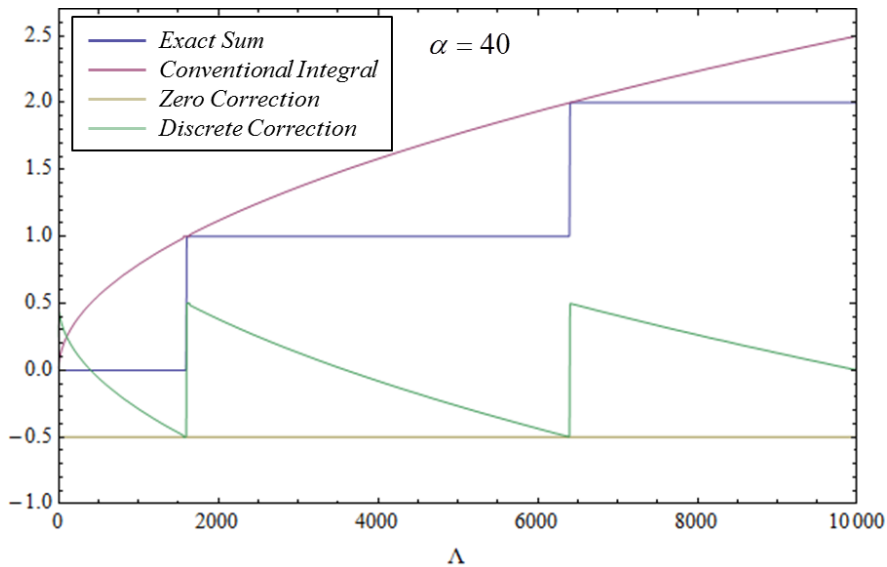

Figure 2.5: Exact sum and terms of PSF in one dimension changing with dimensionless chemical potential for strongly confined domain ($\alpha = 40$).

In Fig. (2.6) variation of the sum and the terms of PSF with confinement parameter α is shown for constant dimensionless chemical potential. This is a remarkable figure that shows exactly how PSF represents discreteness of FD distribution function properly. As confinement of the domain increases discrete contributions of the third term appears. Even around $\alpha = 0.3$ effects of confinement start to reveal itself and as the confinement become strong, deviations from the continuous behavior become more apparent.
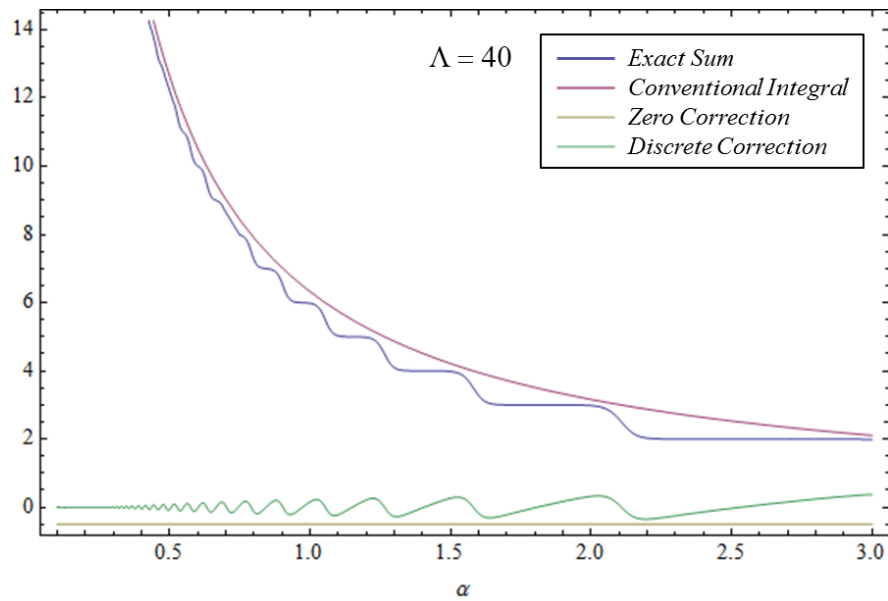
Figure 2.6: Exact sum and terms of PSF in one dimension changing with confinement parameter ($\Lambda = 40$).

Despite it looks like a purely mathematical equation[9], PSF marvelously symbolizes the quantum mechanical effects arises in confined structures. Even so, don't let the beauty of formula trick you, since its third term is exceedingly complicated to calculate analytically in many cases. That's why except some certain cases, we used the sum itself, instead of performing PSF on it.

In this chapter, a brief review of thermodynamics of ideal quantum gases has been done and all the information needed is given to proceed to the next chapter and understand the novel results of this thesis.

---

[9]In fact, it is not. Fundamentally it is a consequence of Parseval's theorem and Plancherel theorem that prove Fourier transform is unitary which means it preserves energy and information so that makes the whole signal processing phenomenon widely used in physics and engineering possible.

3. 1D FERMI GAS CONFINED IN AN ANISOMETRIC DOMAIN

In this chapter, the first case of the study, the 1D Fermi gas, is examined. As quantum mechanics points out, increasing or decreasing domain size changes boundary conditions of Schrödinger equation, and thus causes a change in energy levels. When domain size is reduced, gaps between energy levels increase. Confinement in a direction causes to a restriction in accessible momentum states in that direction, since some energy levels become too high to be occupied by particles. After a point, the confinement becomes so strong that no momentum states remain for particles to become excited. In such a case, for a D-dimensional structure, when there is no accessible state, except the ground state, in n number of directions, system is said to be $D - n$ dimensional in its momentum space. Of course if there is enough energy, particles can occupy the excited states, so technically all structures are always 3-dimensional in our world. However, for a definite range of variables some structures may practically behave as they are lower dimensional.

3.1 1D Thermodynamic Quantities with Regular Stepwise Behavior

To see the nature of thermodynamic quantities in nano scale, let's start with the most basic one, number of particles.

Number of particles in a Fermi gas is stated as the summation of FD distribution function over all momentum states in all directions,

$$N = \sum_{i_n=1}^{\infty} \frac{1}{e^{(\tilde{\varepsilon}-\Lambda)} + 1} \tag{3.1}$$

where the summation is a triple sum with $i_n = \{i_1, i_2, i_3\}$. In thermodynamic limit, one have to convert thermodynamic state sums to integrals, because upper limit of summations is infinite. Luckily, for finite-size systems, one can put an upper limit to

the summations, since after Fermi level[1] ($i_F = \sqrt{\Lambda}/\alpha$), contributions to summation decrease rapidly. To keep the safety, one can sum up to $i_{max} = 2i_F$, since contributions become completely negligible after the value i_{max}. Then number of particles can be expressed as

$$N = \sum_{i_1=1}^{i_{1max}} \sum_{i_2=1}^{i_{2max}} \sum_{i_3=1}^{i_{3max}} \frac{1}{e^{[(\alpha_1 i_1)^2 + (\alpha_2 i_2)^2 + (\alpha_3 i_3)^2 - \Lambda]} + 1} \tag{3.2}$$

Now, consider a domain which is strongly confined in two directions and relatively weakly confined in the other direction, as the one shown in Fig. (3.1).

1D Fermi Gas
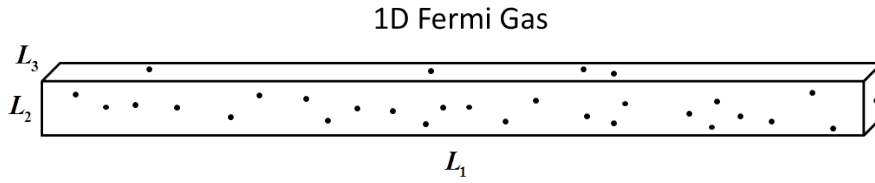
Figure 3.1: A prototype of an anisometric 1D domain with $\alpha_1 = 1$, $\alpha_2 = 40$ and $\alpha_3 = 40$.

Confinement parameters can be chosen as $\alpha_1 = 1$, $\alpha_2 = 40$ and $\alpha_3 = 40$ in such a case.[2] Then, in this case we can replace triple sums over momentum states in all directions by a single sum over only the first direction as long as $\Lambda < \Lambda_1 = (\alpha_1)^2 + (\alpha_2)^2 + (2\alpha_3)^2$. As it can be understood from the two factor in front of the α_3, Λ_1 is the value where the excitation of strongly confined directions starts.[3] Once excitation of states starts in a direction, then one can no longer neglect that direction and have to make summation at least up to the i_F or more safely to i_{max}. Then for the condition of $\Lambda < \Lambda_1$, Eq. (3.2) becomes,

$$N_{1D} = \sum_{i_1=1}^{i_{1max}} \frac{1}{e^{[(\alpha_1 i_1)^2 - \Lambda']} + 1} \tag{3.3}$$

On the other hand, for $\alpha_1 << 1$, PSF can be used to calculate number of particles analytically. It is sufficient to use the first two terms of PSF for $\alpha_1 << 1$ and number

---

[1]Fermi level is defined as the hypothetical energy level that makes the FD distribution function one half, namely when $\mu = \varepsilon$.

[2]It is ensured that 40 is not an unrealistic value for α, since for an electron confined in a graphene with 0.3 nm thickness at 20K, $\alpha = 43$ [27].

[3]Two factor comes from the first excited state and it indicates that the summation is begun. Since we chose the confinement rate of second and third directions, the factor may well be in front of the α_2 too, there is no difference. However, if α_2 and α_3 has not been equal, factor would be in front of the least confined direction.

of particles can be approximated as

$$N_{1D} \approx -\frac{\sqrt{\pi}}{2\alpha_1} Li_{1/2}(-e^{\Lambda'}) + \frac{1}{2} Li_0(-e^{\Lambda'}) \approx \frac{\sqrt{\Lambda'}}{\alpha_1} - \frac{1}{2} \qquad (3.4)$$

where $\Lambda' = \Lambda - \alpha_2^2 - \alpha_3^2$ and Li denotes the polylogarithm function. Transition in Eq. (3.4) is obtained by using asymptotic expansions of polylogarithms for $\Lambda >> 1$, which is the limit of degenerate Fermi gas. Conversely, for α_1 values that are not much less than unity, third term of PSF has also to be considered. With some mathematical operations whole terms of PSF can be analytically obtained for number of particles of 1D Fermi gases,

$$N_{1D}^{PSF} \cong \frac{\sqrt{\Lambda'}}{\alpha_1} - \frac{1}{2} + \frac{1}{\pi} \arctan \left[\cot \left(\frac{\pi \sqrt{\Lambda'}}{\alpha_1} \right) \right] \qquad (3.5)$$

where PSF superscript of N_{1D} refers that the whole terms of PSF is used to obtain this expression. Then number of particles N varies with dimensionless chemical potential Λ is obtained in Fig. (3.2) as
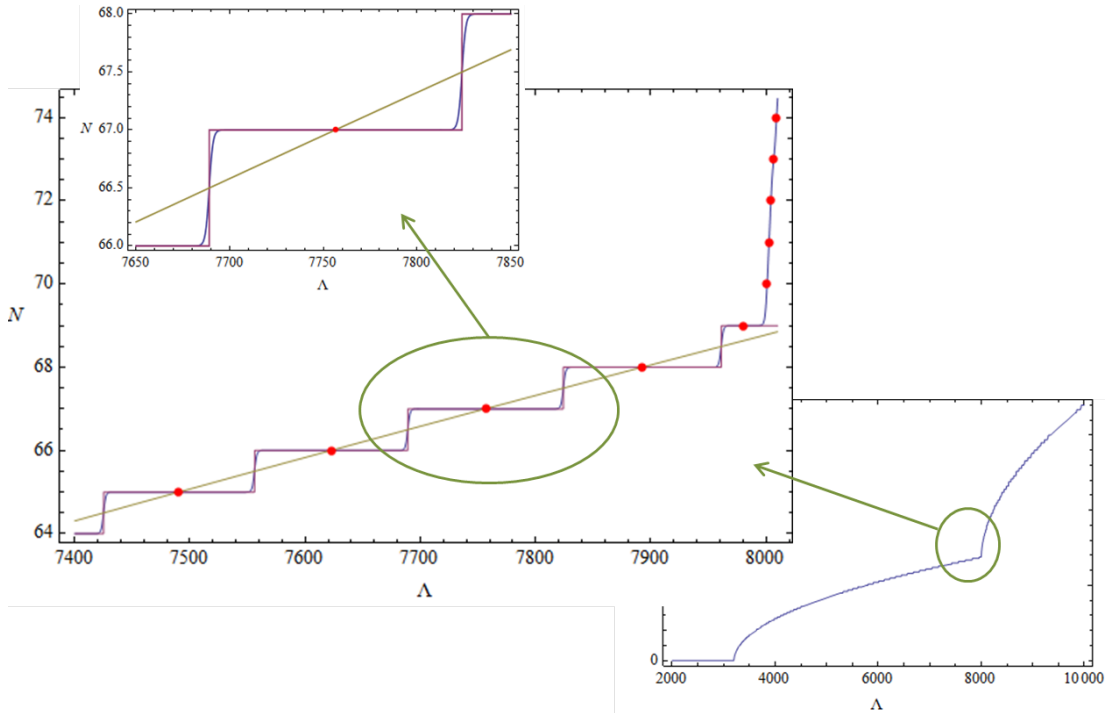

Figure 3.2: Number of particles vs dimensionless chemical potential for 1D Fermi gas with $\alpha_1 = 1$, $\alpha_2 = 40$ and $\alpha_3 = 40$.

In Fig. (3.2), striking intrinsic discrete nature is shown. There are three subfigures, which point out certain regions of $N - \Lambda$ relationship in detail. Blue, red and yellow

curves represent Eqs. (3.3), (3.5) and (3.4) respectively, except on the bottom subfigure blue curve is plotted by using Eq. (3.2). Red dots indicates the certain discrete chemical potential values that corresponding to the integer particle number. They are numerically solved from Eq. (3.3). On the bottom subfigure it is seen that after Λ_1, second momentum state (the first excited state) of a strongly confined direction starts to be occupied since there is enough chemical potential. Main subfigure in the middle shows the intrinsic discrete nature of $N - \Lambda$ relationship and the top subfigure zooms to a step to show the small difference of blue and red curves and to show how yellow curve passes exactly from the red points. As it is seen, except the sharpness of the edges of the steps, Eq. (3.5) represents the discrete nature pretty well. On the other hand, even though Eq. (3.4) cannot represent the intrinsic discrete nature, it passes from the points exactly where the number of particles is integer. Since as far as we know, particle number is integer, even Eq. (3.4) is a good approximation too.

It is seen from Eq. (3.5) that chemical potential Λ can be written as the functions of particle number N and confinement parameter α. Note that the third term of Eq. (3.5) is zero when number of particles is integer. There are two ways to define the formula, either equating the third term of Eq. (3.5) to zero and looking for its roots, or more easily solving Λ from the first two terms of Eq. (3.5). Hence, for large integer N,

$$\Lambda' = \alpha_1^2 \left(N + \frac{1}{2} \right)^2 \tag{3.6}$$

Since all thermodynamic state functions contains chemical potential, by using the formula above, one can express them in terms of N and α. It is also possible to define the chemical potential interval as

$$\Delta\Lambda' = 2\alpha_1^2(N+1) = 2\alpha_1\sqrt{\Lambda'} + \alpha_1^2 \tag{3.7}$$

which allows to specify the forbidden chemical potential values analytically for integer N. It is apparent that when confinement (α) or degeneracy (Λ) increase, intervals between discrete values of chemical potential also increase, which means the discrete nature becomes more apparent.

Another interesting feature of N-Λ function is that skewness of the steps are always same for the domains with same confinement parameter α. That means change in

number of particles corresponds to a same change in Λ and this is true even for the steps that corresponds to more than one particle changes in particle number in 2D and 3D systems. The reason of this can be understood by comparing Figs. (2.4) and (2.5). Note that in these figures, skewness of steps does not change with increasing Λ. To define a formula for the changes of steps in $N - \Lambda$, we used distribution function and defined a variable x, which is the value of distribution function where it is equal to a control variable x_c that we assign. Then for all systems, we have a same change in Λ corresponds to a stepwise change in particle number and Eq. (3.8) defines the upper (+) and lower (-) ranges of the function.

$$x_{\pm} = \alpha_1^2 + \alpha_2^2 + \alpha_3^2 \pm \operatorname{arcosh}(50x_c) \qquad (3.8)$$

For instance for $x_c = 0.99$ or $x_c = 0.01$, $\tau \cong \operatorname{arcosh}(49.5)$. We can assign any value to x_c to adjust the precision of x.

Now let's discuss our next fundamental thermodynamic property; internal energy, and its variation with chemical potential. Dimensionless internal energy is written from its definition,

$$\frac{U}{k_B T} = \widetilde{U} = \sum_{i_n=1}^{\infty} \frac{\widetilde{\varepsilon}}{e^{(\widetilde{\varepsilon}-\Lambda)} + 1} \qquad (3.9)$$

By the same way we do for number of particles, for 1D Fermi gases dimensionless internal energy can be analytically derived for integer N, by using the first two terms of PSF and asymptotic series expansions of polylogarithm functions,

$$\widetilde{U}_{1D} = \frac{(\Lambda')^{3/2}}{3\alpha_1} + \left(\frac{\sqrt{\Lambda'}}{\alpha_1} - \frac{1}{2} \right)(\alpha_2^2 + \alpha_3^2) \qquad (3.10)$$

Interestingly, Eq. (3.4) appears inside of the formula as a factor. As it is seen from Fig. (3.3), regular stepwise behavior in internal energy-chemical potential relationship is observed in 1D Fermi gases for number of particles from 65 to 74.
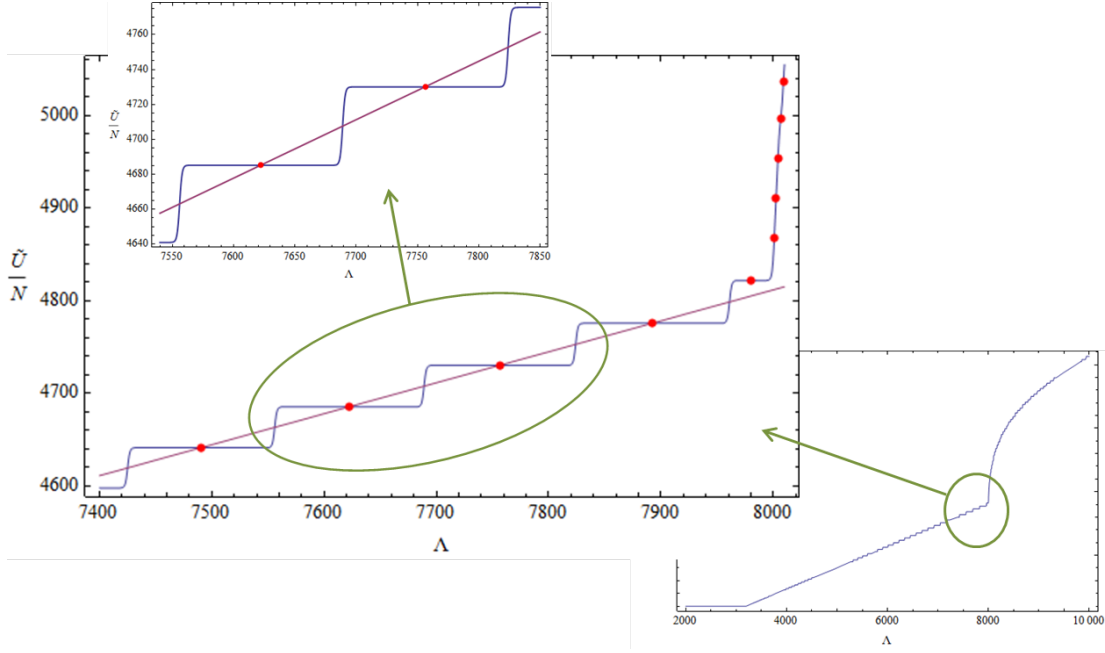
Figure 3.3: Dimensionless internal energy per particle vs dimensionless chemical potential for 1D Fermi gas with $\alpha_1 = 1, \alpha_2 = 40, \alpha_3 = 40$.

In Fig. (3.3), blue curve is obtained by dividing Eq. (3.9) to Eq. (3.3), since we are dealing with dimensionless internal energy per particle.[4] Red curve is the result of Eq. (3.10) divided by Eq. (3.4). As it is found in chapter 2 Eq. (2.99), relationship of internal energy per particle and chemical potential is linear in the 1D region, which can be seen in Fig. (3.3) in the bottom subfigure where before the value of Λ_1 indicates the 1D region. When the second modes in strongly confined directions can become excited, domain can no longer be considered 1D and linear behavior disappears, as it is expected. Even for the unit value of α, if N is sufficiently large, Λ' becomes so large that dimensionless internal energy can be written by using Eq. (3.6) and Eq. (3.10) as

$$\widetilde{U}_{1D} \cong \frac{\alpha_1^2}{3}\left(N + \frac{1}{2}\right)^3 + N(\alpha_2^2 + \alpha_3^2) \tag{3.11}$$

Dimensionless internal energy interval can be obtained from Eq. (3.11) as

$$\Delta\left(\frac{\widetilde{U}}{N}\right) \cong \frac{2}{3}\alpha_1^2\left(N + \frac{5}{4}\right) \tag{3.12}$$

---

[4]Of course, dimensionless internal energy itself has also discrete and stepwise nature. But, we discussed quantities per particle to show that the discreteness is not coming from the obvious fact of discreteness in particle number. Stepwise behavior observed even in quantities per particle.

It is clear from Eq. (3.12) that, when α goes to zero (in macro scale), stepwise nature practically disappears, although Eq. (3.9) intrinsically has discrete nature.

Regular stepwise behavior of number of particles and internal energy can be observed only in strongly degenerate and confined 1D Fermi gases and the behaviors are completely different than macroscopic (continuous) ones. Their continuous behavior in macro systems is shown in Fig. (3.4) where α_1 is chosen as 0.1, which means the first direction is not so confined (in fact it may be considered as nearly free). It is also interesting that, even for the confinement value of 0.1, system behaves as continuous. There is a drastic conversion from continuous behavior to discrete one around the unit value of the confinement parameter α. So, one can loosely separate the continuous and discrete behaviors as $\alpha < 1$ and $\alpha \geq 1$, though for the values of α very close to 1, discrete behaviors start to be seen. When domain sizes are getting far from α to opposite limits, the relevant nature become stronger and the transition region from continuous to discrete happens around α.
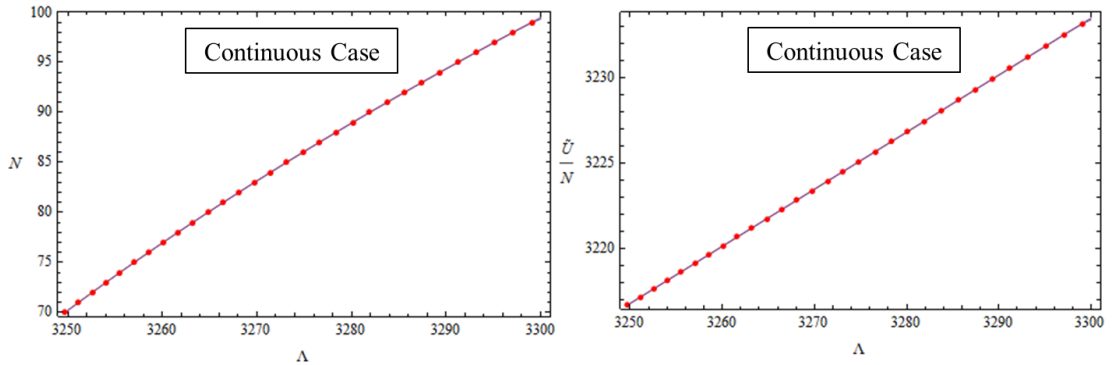
Figure 3.4: Variation of number of particles and dimensionless internal energy per particle with dimensionless chemical potential $\alpha_1 = 0.1, \alpha_2 = 40, \alpha_3 = 40$.

Variation of dimensionless energy per particle vs number of particles is also examined for discrete ($\alpha_1 = 1$) and continuous ($\alpha_1 = 0.1$) cases in 1D Fermi gas in Fig. (3.5). In contrast with the variations of N and U with the chemical potential Λ, surprisingly there is no stepwise behavior in their variations with number of particles even in discrete case where $\alpha_1 = 1$.

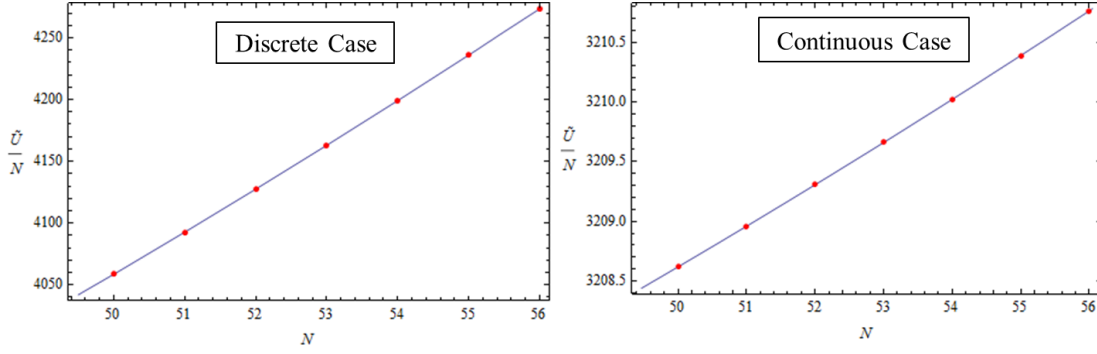**Figure 3.5**: Variation of dimensionless internal energy per particle for $\alpha_1 = 1$ (left subfigure) and $\alpha_1 = 0.1$ (right subfigure) with number of particles where $\alpha_2 = 40, \alpha_3 = 40$.

It is seen that number of particles and chemical potential relationship is intrinsically discrete as it is a stepwise function. This behavior of N is the result of the nature of FD distribution function which will be discussed at the end of this chapter. The reason why internal energy has also same nature is it differs from number of particles by just a factor ε. Free energy and pressure have also same stepwise nature. To prevent repetitions on figures, we didn't put their figures, but let's explain the reason why they have same stepwise nature. In strongly confined systems, as we shall see in the next subsection for 1D case, entropy is extremely low. From the definition of free energy ($F = U - TS$) it's seen that when temperature and entropy are sufficiently low, difference between free energy and internal energy become very small, so that $F \approx U$.

Other thermodynamic properties that are derived from dW, work term of the first law of thermodynamics, $dU = dQ + dW$, like free energy F and pressure P, have exactly same discrete, regular stepwise behavior and different with just a factor from internal energy. Consequently, we only gave the internal energy plots throughout the thesis, but be sure that free energy and pressure has exactly same behavior as internal energy.

3.2 1D Thermodynamic Quantities with Regular Peakwise Behavior

We discussed the stepwise behavior of some thermodynamic quantities in last section. The second type of behavior found in confined nano systems is the peakwise behavior which is observed in entropy and heat capacity.

Dimensionless entropy of a Fermi gas in its exact form

$$\frac{S}{k_B} = \widetilde{S} = \left[\sum_i (f_i - 1)(\varepsilon_i - \mu) - \ln f_i \right] \tag{3.13}$$

or equivalently it can be written in a more familiar form as

$$\widetilde{S} = \widetilde{U} - \widetilde{F} = \widetilde{U} - N\Lambda + \mathcal{Z} \tag{3.14}$$

$$\widetilde{S} = \sum_i \left[\varepsilon_i f_i - \Lambda f_i - \ln(1 - f) \right] \tag{3.15}$$

To write entropy in an analytical form for $\alpha_1 << 1$ we need $N, \widetilde{U}$ and $\mathcal{Z}$ with their first order temperature correction terms. They can be expressed from the first term of PSF and by using their temperature corrections as

$$N_1 \approx \frac{\sqrt{\Lambda'}}{\alpha_1} \left(1 - \frac{\pi^2}{24(\Lambda')^2} \right) \tag{3.16}$$

$$\widetilde{U_1} \approx \frac{(\Lambda')^{3/2}}{3\alpha_1} \left(1 + \frac{\pi^2}{8(\Lambda')^2} \right) \tag{3.17}$$

$$\mathcal{Z}_1 \approx \frac{2(\Lambda')^{3/2}}{3\alpha_1} \left(1 + \frac{\pi^2}{8(\Lambda')^2} \right) \tag{3.18}$$

From N, $\widetilde{U}$ and $\mathcal{Z}$, free energy becomes,

$$\widetilde{F_1} \approx \frac{(\Lambda')^{3/2}}{3\alpha_1} \left(1 - \frac{3\pi^2}{8(\Lambda')^2} \right) \tag{3.19}$$

By using Eqs. (3.16), (3.17), (3.18) and (3.19), entropy in 1D becomes in continuum limit,

$$S_1 \approx \frac{\pi^2}{6\alpha_1 \sqrt{\Lambda'}} \tag{3.20}$$

Variation of dimensionless entropy per particle with dimensionless chemical potential is given Figs. (3.6) and (3.7) for discrete and continuous cases respectively.
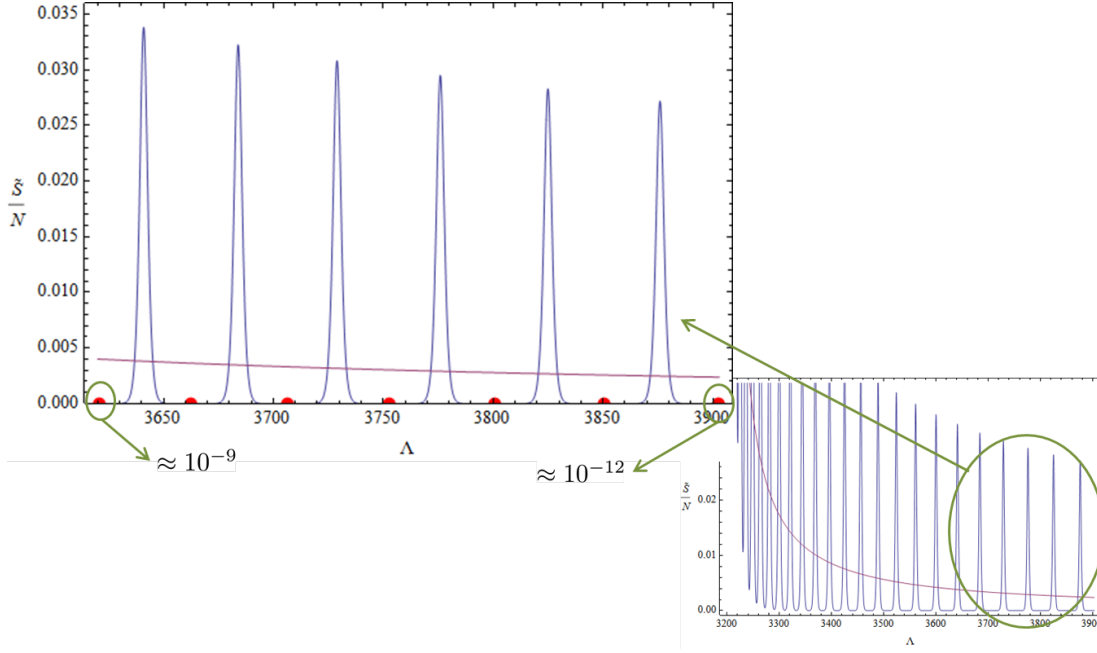
Figure 3.6: Variation of dimensionless entropy per particle with dimensionless chemical potential for 1D Fermi gas with $\alpha_1 = 1, \alpha_2 = 40, \alpha_3 = 40$.

In Fig. (3.6), blue curve is the exact entropy from Eq. (3.15) and red curve is the approximate entropy from Eq. (3.20). Red dots show the entropy values corresponding to the integer number of particles in the range from 20 to 26. In higher number of particles even around 50, entropy values become so small that (around 10^{-24} for 50 particles), plotting the graph without errors become impossible. So, in order to observe the nature we plotted the graph in such a low number of particle range. Although Eq. (3.20) matches exactly with the summation in continuous case given in Fig. (3.7), in discrete case, it passes from the integral averages of summations and cannot represent the peakwise nature as in Fig. (3.6). While exact entropy is crawling on the bottom with a range from $\approx 10^{-9}$ to $\approx 10^{-12}$, value of its approximation is on the order of 0.004. As it is seen from the huge deviation, using continuum approximation in such a confined nano structures will give completely wrong results.

Figure 3.7: Variation of dimensionless entropy per particle with dimensionless chemical potential for 1D Fermi gas with $\alpha_1 = 0.1, \alpha_2 = 40, \alpha_3 = 40$.

As in Fig. (2.6), difference of summation and integral approximations are shown for entropy and entropy per particle changing with confinement parameter for constant chemical potential[5] in Fig. (3.8). Before around the confinement value of 0.2 continuum approximation works well, but after that oscillations appear and deviations between summations and integrals are non-negligible.
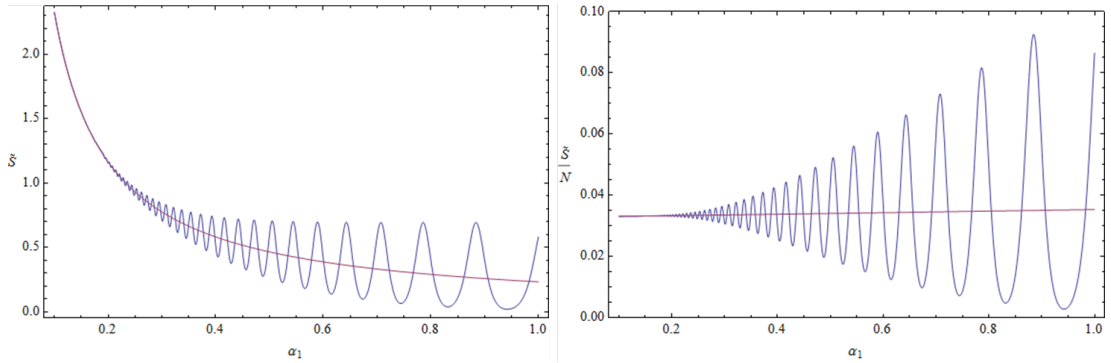
Figure 3.8: Dimensionless entropy and entropy per particle and its variation with confinement parameter in the first direction for $\Lambda = 3250$ and $\alpha_2 = 40, \alpha_3 = 40$.

---

[5]In fact this situation might be hard to physicalize since chemical potential is a function of confinement parameter also. However, examination of the difference between summation and integral is much clear in this way.

Heat capacity for Fermi gas from Eq. (2.38) in its summation form given as

$$\frac{C_V}{k_B} = \widetilde{C}_V = \sum_{i_n} (\tilde{\varepsilon})^2 f(1-f) - \frac{[\sum_{i_n} \tilde{\varepsilon} f(1-f)]^2}{\sum_{i_n} f(1-f)} \qquad (3.21)$$

In the Fig. (3.9) below, comparison of discrete and continuous cases for dimensionless heat capacity vs dimensionless chemical potential is given. The blue curve is the result of Eq. (3.21) and red dots show the values correspond to the integer particle number.
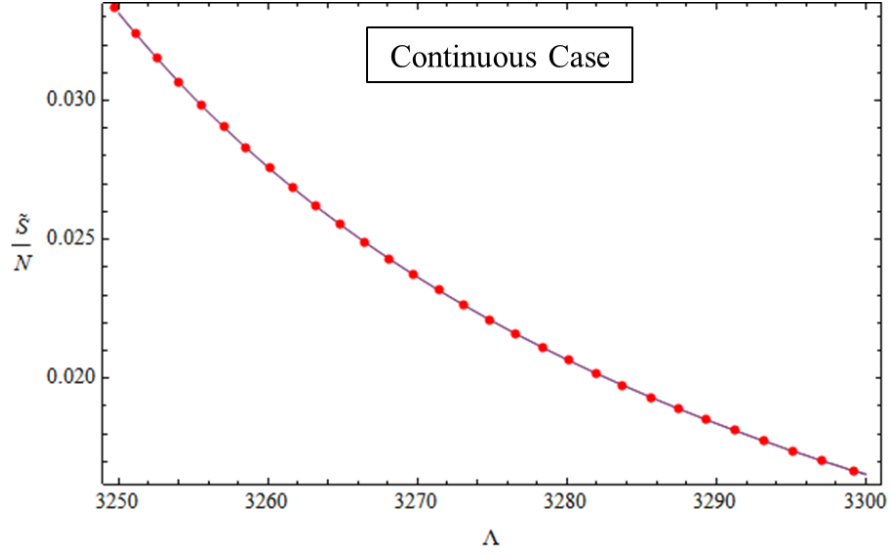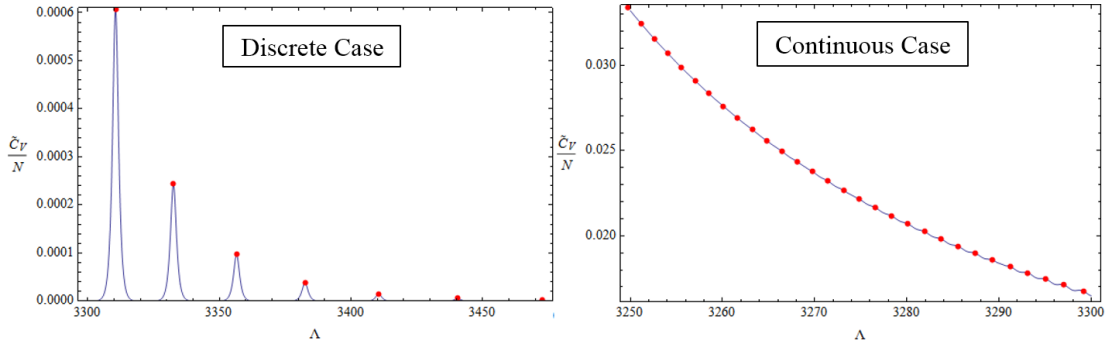

Figure 3.9: Variation of dimensionless heat capacity per particle with dimensionless chemical potential for 1D Fermi gas with $\alpha_1 = 1$ (left subfigure), $\alpha_1 = 0.1$ (right subfigure) and $\alpha_2 = 40, \alpha_3 = 40$.

Unlike other thermodynamic properties, in heat capacity, equation that is found by continuum approximation starts to deviate from even the integral representation of the trend of summation, as they are seen in Fig. (3.10). Although summation and integral approximation of it matches in low confinement values and represents the trend until around 0.4, after that it completely becomes different. This strangeness comes from the differences of very small values in the heat capacity equation. Note that, heat capacity is written as the difference of two terms. Although integrals of the summations inside the terms represent the trend behaviors of their summations individually and term by term, taking the difference leads to the strong deviation from the representation of the trend behavior.
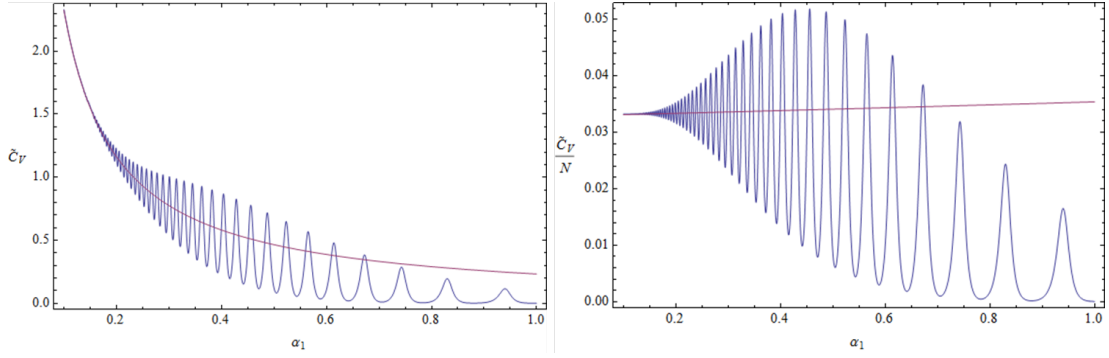
Figure 3.10: Dimensionless heat capacity and heat capacity per particle and its variation with confinement parameter in the first direction for $\Lambda = 3250$ and $\alpha_2 = 40, \alpha_3 = 40$.

In Fig. (3.11), variation of dimensionless heat capacity divided by dimensionless entropy is seen with confinement value from 0.1 to 1.
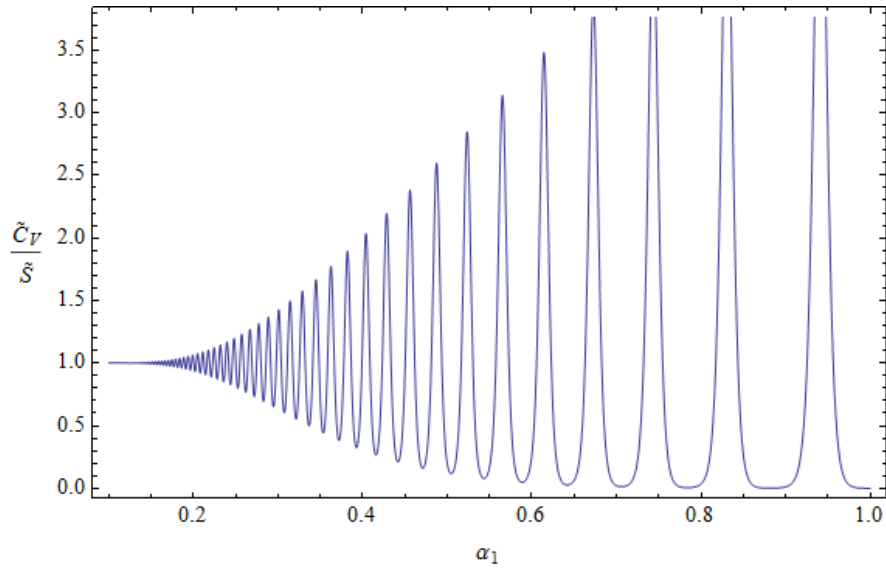
Figure 3.11: Dimensionless heat capacity divided by dimensionless entropy and its variation with confinement parameter in the first direction for $\Lambda = 3250$ and $\alpha_2 = 40, \alpha_3 = 40$.

Like we derived in chapter 2, their ratio equals to 1 in continuum limit. However, when confinement increases after around $\alpha_1 = 0.2$, strong deviations from this result appears, which shows that in real, entropy and heat capacity is not equal, as a matter of fact, completely different.

3.2.1 Nature of Fermi-Dirac Variance Function and Discrete Fermi Point

From the first law of thermodynamics, entropy can be written as

$$dQ = TdS \longrightarrow S = \int \frac{dQ}{T} \longrightarrow dQ = \sum_i \varepsilon_i df_i \longrightarrow S = \int \sum_i \frac{\varepsilon_i df_i}{T} \qquad \textbf{(3.22)}$$

Let's remember the definition of heat capacity and rewrite it by considering the first law of thermodynamics,

$$C_V = \frac{dQ}{dT} \longrightarrow dQ = \sum_i \varepsilon_i df_i \longrightarrow C_V = \sum_i \varepsilon_i \frac{df_i}{dT} \qquad \textbf{(3.23)}$$

Here in Eqs. (3.22) and (3.23), the derivative of distribution function (with respect to any of its variables such as T, Λ or ε) includes $f(1-f)$ which is the variance of distribution function or in short, variance function in FD statistics. The nature of this variance is quite interesting. For example, it has peaks in certain values when it is plotted versus dimensionless chemical potential. It is clear from Eqs. (3.22) and (3.23) that since S and C_V contains $f(1-f)$ inside the summations. Hence, contributions to entropy and heat capacity only comes from the peaks of the variance function, which correspond to the Fermi point, Fermi line and Fermi surface in 1D, 2D and 3D Fermi gases respectively. So, contributions from momentum states to entropy and heat capacity come from $D-1$ dimensional momentum space. As it is seen from Fig. (3.12) the state corresponding to the Fermi point is the state where distribution function is equal to one half. Also variance of the distribution function $f(1-f)$ makes its peak at one quarter. By equating the variance function to $1/8$, full band width at half maximum (FWHM) of the variance function can be expressed as

$$\delta_{1D} = \frac{\mathrm{arcosh}(17)}{2\alpha_1 \sqrt{\Lambda'}} \qquad \textbf{(3.24)}$$
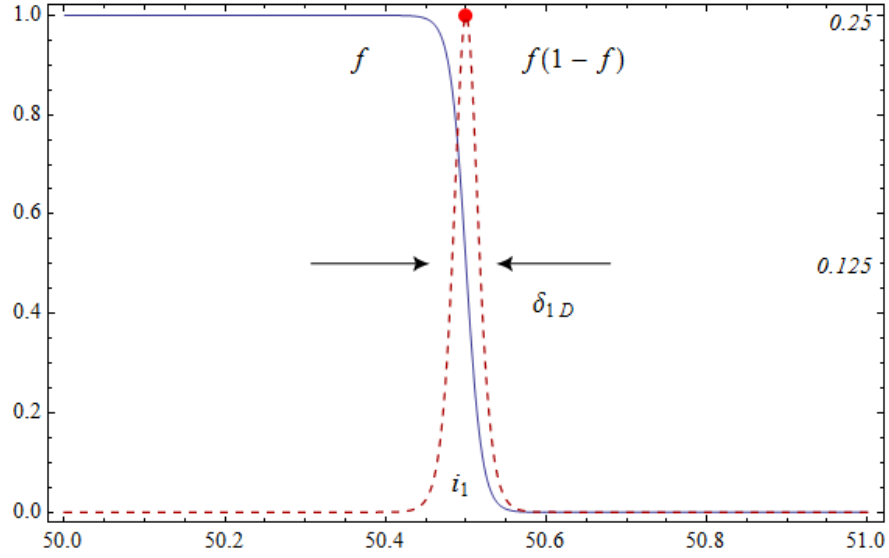
Figure 3.12: Distribution function (blue curve) and its variance (red curve) around Fermi point for 1D Fermi gas with $\alpha_1 = 1, \alpha_2 = 40, \alpha_3 = 40$ and $N = 50$.

For macro systems there are many states correspond to the variance of distribution function. However, for nano systems variance becomes too narrow that only few or no state can correspond to it. As it is clear from Eq. (3.24) that when confinement (α) or degeneracy (Λ) increases, FWHM decreases which means the peak of variance becomes too sharp. In Fig. (3.5) for a 1D Fermi gas with 50 particles, distribution function and its variance is plotted. As it is seen, it makes it peak at a half-state and there is no momentum state (integer value by definition) correspond to the non-vanishing values of variance. Since contributions of states around the peak of variance is nearly zero, entropy and heat capacity of 1D Fermi gas is also almost zero. In fact for a 0D system they are exactly zero, since summations die out for a 0D system and entropy and heat capacity equations gives exactly zero.

In Figs. (3.13) and (3.14), the nature of FD variance function is examined. Since $Var(f) = f(1-f)$, it can be written as the difference of distribution function and its square so that $f(1-f) = f - f^2$.
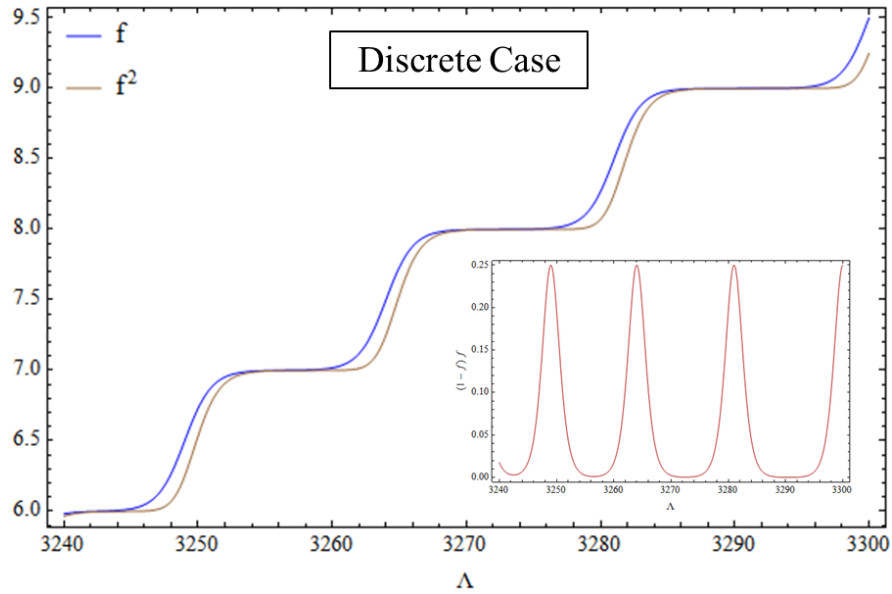
Figure 3.13: Examination of variance function vs dimensionless chemical potential for confined domains with $\alpha_1 = 1, \alpha_2 = 40, \alpha_3 = 40$.
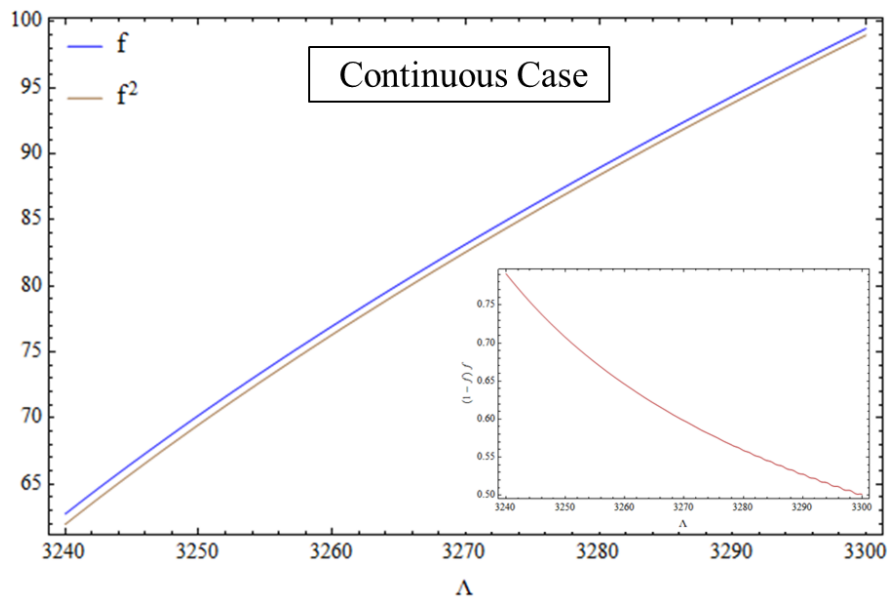
Figure 3.14: Examination of variance function vs dimensionless chemical potential for nearly free domains with $\alpha_1 = 0.1, \alpha_2 = 40, \alpha_3 = 40$.

The reason of the peaks in the variance is clear when we examine the difference in detail. However, as it is seen there is a huge difference in the natures of discrete and continuous cases where the domain is confined and nearly free respectively in Figs (3.13) and (3.14). The blue and brown curves represents the distribution function and

its square respectively, whereas red curves in subfigures shows the difference of blue and brown curves, in other words the variance.

Discreteness its repercussions like stepwise, peakwise and oscillatory behaviors, intrinsically come from the nature of FD distribution function. When we plot the summation over momentum states in distribution function vs confinement parameter α, we see that magnitude of confinement causes the appearance of discrete nature, Fig. (3.15).

Figure 3.15: Appearance of stepwise behavior due to size confinement, in FD distribution function, for constant chemical potential, $\Lambda = 3250$ and $\alpha_2 = \alpha_3 = 40$.

It is clear that why thermodynamic properties that include summation of distribution function (like particle number, internal energy, free energy and pressure) have stepwise nature. Because, distribution function itself gives a stepwise response to the confinement.

In Fig. (3.16), summation over momentum states of variance function vs confinement parameter is plotted and as it is expected, the nature is now not stepwise but peakwise. That's the reason why thermodynamic properties that contain summation of variance function (like entropy and heat capacity) have peakwise nature. Because, variance

function gives a peakwise response to the confinement, which is very natural since it is the derivative of the distribution function.

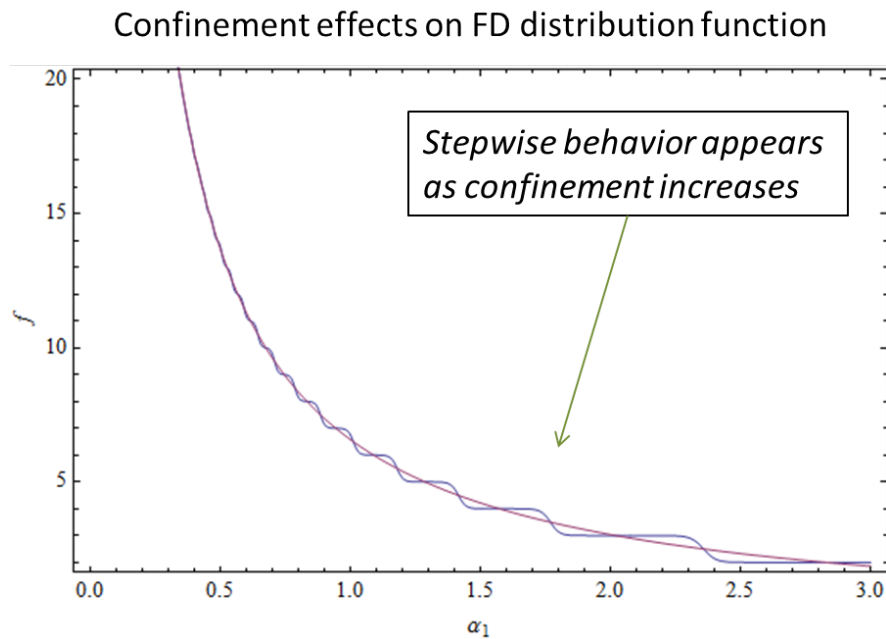### Confinement effects on FD variance function
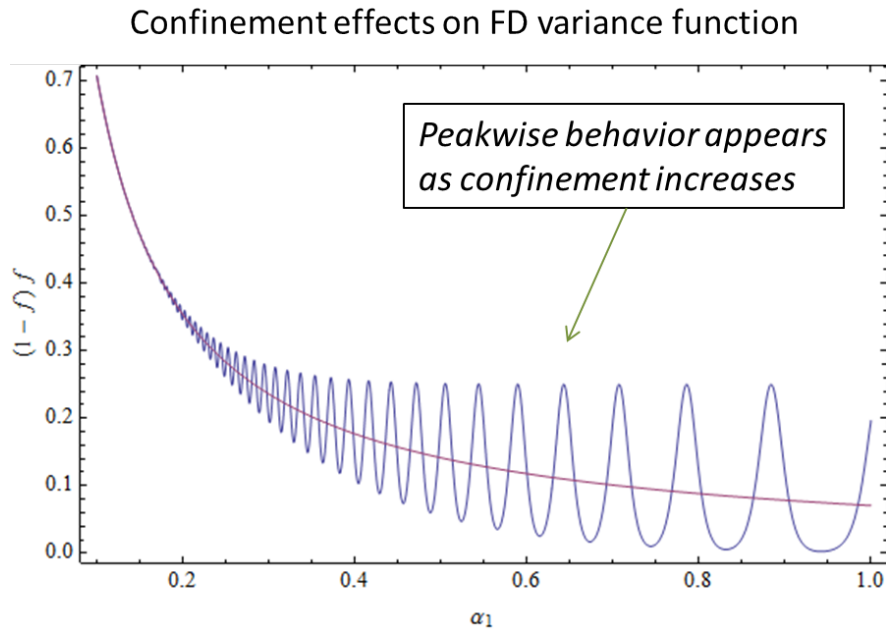
Figure 3.16: Appearance of peakwise behavior due to size confinement, in the FD variance function, for constant chemical potential, $\Lambda = 3250$ and $\alpha_2 = \alpha_3 = 40$.

As it shown in Fig (3.17), from the first law of thermodynamics, stepwise behavior is observed in thermodynamic properties that are derived from "work term" which contains the summation of FD distribution function. On the other hand, peakwise behavior is observed in properties that are derived from "heat term" that includes the summation of the derivative of FD distribution function (or equivalently FD variance function).

$$dU = dQ + dW$$

$$dU = \sum_i \varepsilon_i df_i + \sum_i f_i d\varepsilon_i$$
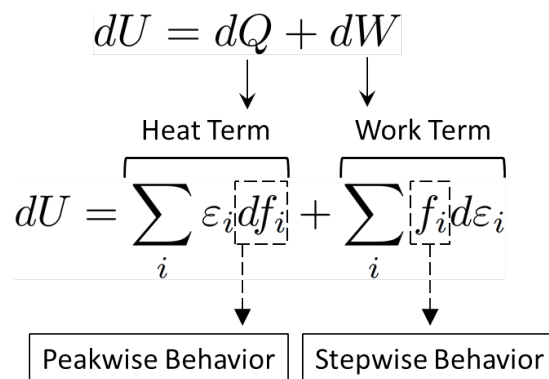
Figure 3.17: Comparison of stepwise and peakwise natures over the 1st law of thermodynamics.

In Fig. (3.18), the appearance of the discrete nature is charted.
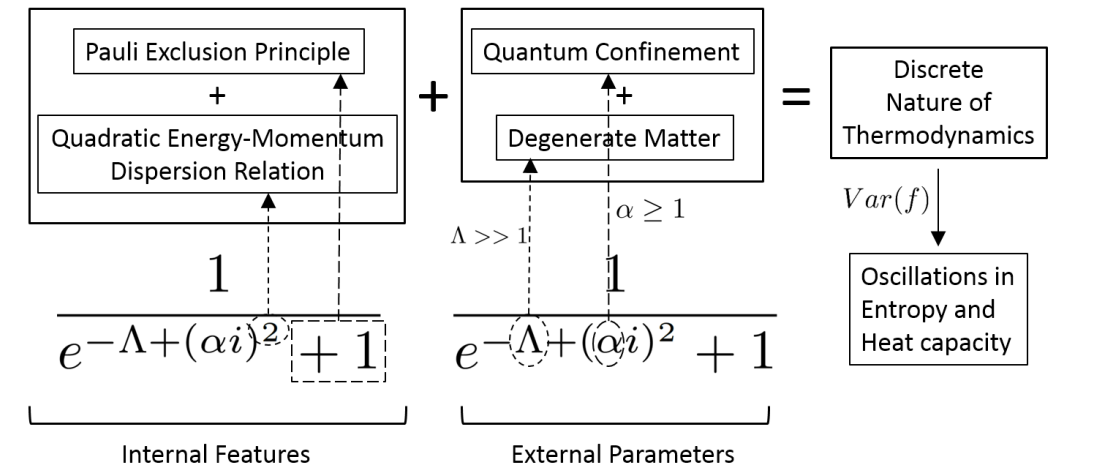
Figure 3.18: How discrete nature appears?

To see the reasons for the discrete nature, let's interpret the FD distribution function in detail. First of all, $+1$ term in the denominator is the result of Pauli exclusion principle that prohibits more than one fermion on the same quantum state. Also dispersion relation between energy and momentum is quadratic for all massive particles. These two are the internal features of the statistics of Fermions and neglecting them (for instance ignoring $+1$ like in Maxwell-Boltzmann statistics or lowering the order of dispersion relation) causes discrete nature to disappear. These internal features are always there for all Fermi gases. However, they may not enough to reveal the discrete nature as in macro scale. There are two external parameters that can be arranged; confinement of the domain and the degeneracy of the matter. α in FD distribution function indicates the rate of confinement of the domain. More strongly the domain is confined, more severely the discrete nature appears. Λ refers to degeneracy in other words the density of the matter in the domain. Increasing density of the matter also make a positive effect on the appearance of discrete nature. When these internal and external effects combined together in strongly confined and degenerate Fermi gases, discrete nature reveals itself and this leads to oscillations on entropy and heat capacity while α or Λ changing.

3.3 Size Dependency of 1D Fermi Gas

We examined the variations of thermodynamic quantities with chemical potential Λ and number of particles N, to show how the degeneracy affects the system. Now let's see how thermodynamic quantities react to a change in confinement. We analyzed the relationships of our four quantities (number of particles N, internal energy U, entropy S and heat capacity at constant volume C_V) with confinement parameter α_1 for 1D Fermi gas and obtained the Fig. (3.19) below:
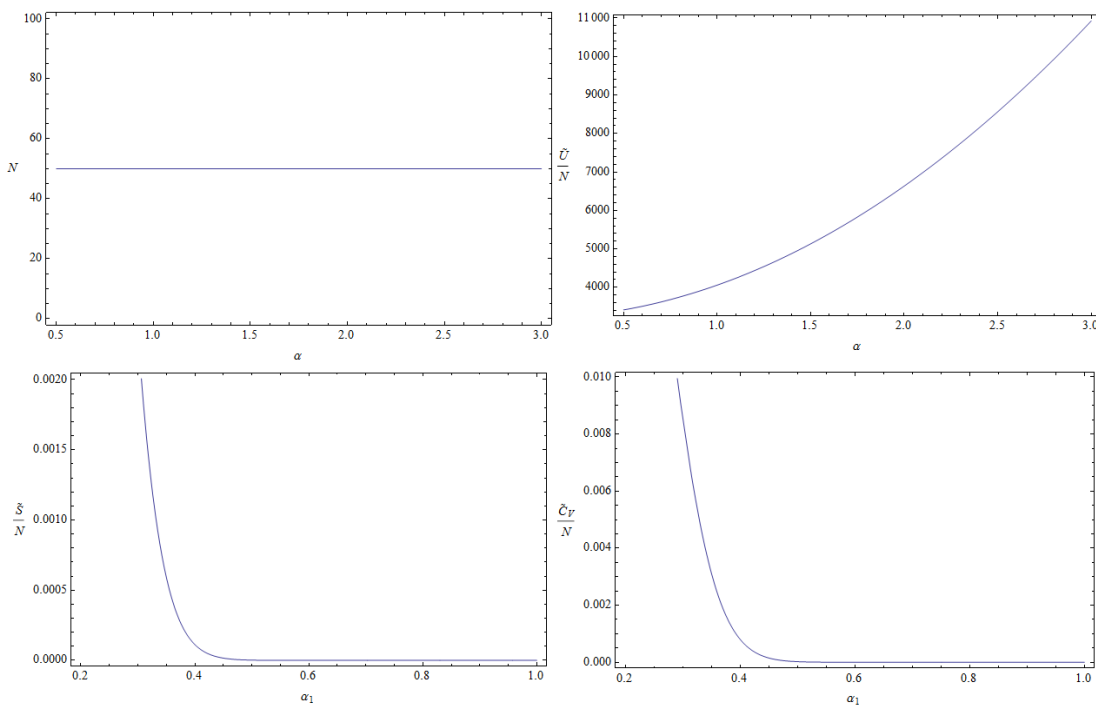
Figure 3.19: Number of particles, dimensionless specific internal energy, entropy and heat capacity changing with confinement parameter in the first direction for a 1D Fermi gas.

As of course, confining the domain has no effect on number of particles in the domain, particles are always there, unless we allow particle exchange. Dimensionless internal energy per particle is increasing when the domain size in the first direction decreasing. On the other hand, entropy and heat capacity drastically drops to zero when the domain size reduces.

As you noticed, when confinement changes, there are no oscillations in entropy and heat capacity since in 1D Fermi gas there is isotropic confinement (only the first

direction can be confined, remember second and third directions are already strongly confined).

4. 2D FERMI GAS CONFINED IN AN ANISOMETRIC DOMAIN

In this chapter, thermodynamic quantities of degenerate 2D Fermi gas are discussed considering an anisometric 2D domain like the one seen in Fig. (4.1).
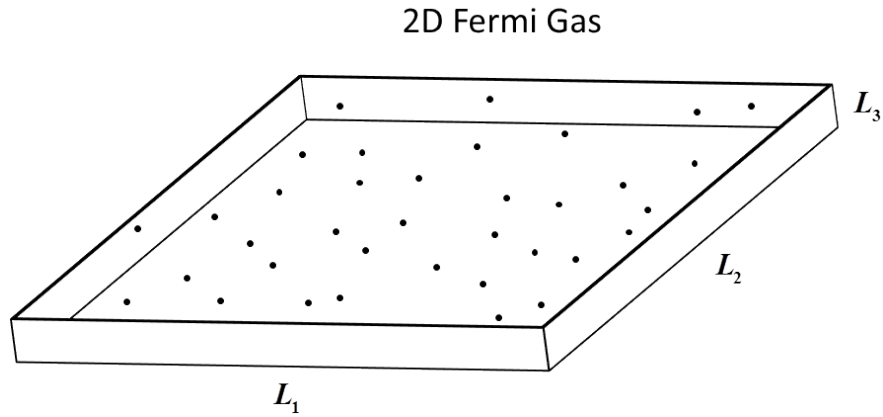
2D Fermi Gas

Figure 4.1: A prototype of an anisometric 2D domain with $\alpha_1 = 3$, $\alpha_2 = 3$ and $\alpha_3 = 40$.

Like we did in previous chapter for 1D Fermi gas, again we collect and examine thermodynamic quantities under two different headings; stepwise and peakwise, according to their behavior.

4.1 2D Thermodynamic Quantities with Quasi-irregular Stepwise Behavior

Let's consider an anisometric domain having 2D momentum space. Confinement parameters are chosen as $\alpha_1 = 3$, $\alpha_2 = 3$ and $\alpha_3 = 40$ for this domain. That means, the first and second directions are relatively weakly confined, whereas the third direction is strongly confined, so that no particles can be excited in third direction ($i_3 = 1$). Then, double summation is sufficient to express thermodynamic state functions of 2D Fermi gas for a definite range of Λ,

$$N_{2D} = \sum_{i_1=1}^{i_{1max}} \sum_{i_2=1}^{i_{2max}} \frac{1}{e^{[(\alpha_1 i_1)^2 + (\alpha_2 i_2)^2 - \Lambda'']} + 1} \tag{4.1}$$

where $\Lambda'' = \Lambda - \alpha_3^2$. Eq. (4.1) represents the 2D nature as long as $\Lambda < \Lambda_2 = (\alpha_1)^2 + (\alpha_2)^2 + (2\alpha_3)^2$. Like in 1D case, by using the first two terms of PSF, analytical expression for 2D number of particles is obtained as

$$N_{2D} \approx \frac{\pi \Lambda''}{4\alpha_1 \alpha_2} - \frac{\sqrt{\Lambda''}}{2}\left(\frac{1}{\alpha_1} + \frac{1}{\alpha_2}\right) + \frac{1}{4} \tag{4.2}$$

In previous chapter, for 1D Fermi gases, we have found an equation that represents the discrete nature without making summations at all. Instead this time, instead of that, we can reduce the number of sums and represent the discrete nature only by one summation, Eq. (4.3),

$$N_{2D} \cong \sum_{i_1=1}^{i_{1max}} \frac{\sqrt{\Lambda'' - (\alpha_1 i_1)^2}}{\alpha_2} - \frac{1}{2} + \frac{1}{\pi}\arctan\left[\cot\left(\frac{\pi\sqrt{\Lambda'' - (\alpha_1 i_1)^2}}{\alpha_2}\right)\right] \tag{4.3}$$

In 2D case, when we look at the behavior of number of particles varying with dimensionless chemical potential, in Fig. (4.2), we see that there are no longer regular steps as in 1D case. Blue curve in Fig. (4.2) is plotted by using Eq. (4.1), the yellow curve by Eq. (4.2), discrete steps with red lines by Eq. (4.3) and red dots are solved again numerically from Eq. (4.1). It is seen that Eq. (4.2) follows the trend and Eq. (4.3) represents the discrete steps quite well. The nature still discrete and stepwise though the skewness of steps changes and there are chemical potential values corresponding to the steepness of the $N - \Lambda$ function this time, in addition to the values corresponding to the plateaus.

In Fig. (4.3), $N - \Lambda$ is plotted for continuous case where $\alpha_1 = \alpha_2 = 0.1$. For nearly free domains, it is seen that Eq. (4.2) perfectly matches with the exact solution.
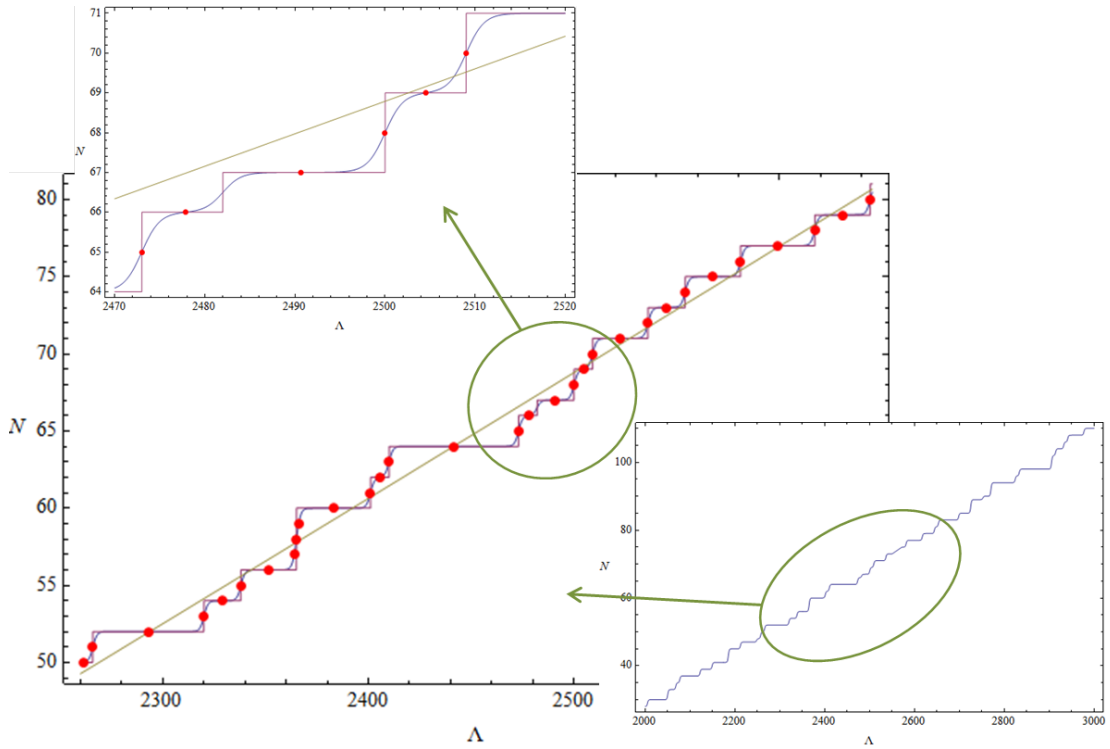
Figure 4.2: Number of particles vs dimensionless chemical potential for 2D Fermi gas with $\alpha_1 = 3$, $\alpha_2 = 3$ and $\alpha_3 = 40$.
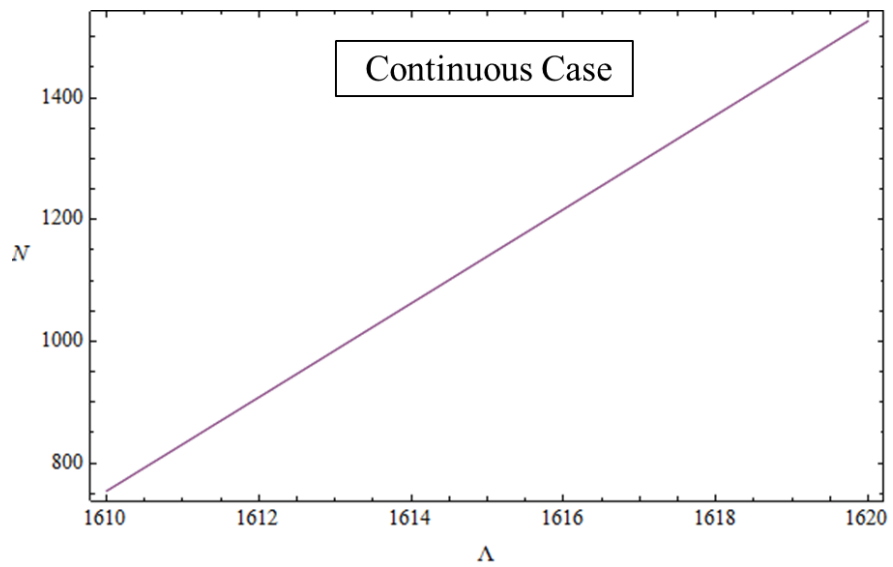

Figure 4.3: Number of particles vs dimensionless chemical potential for 2D Fermi gas with $\alpha_1 = 0.1$, $\alpha_2 = 0.1$ and $\alpha_3 = 40$.

For 2D Fermi gases, dimensionless internal energy in double summation is written as

$$\frac{U_{2D}}{k_B T} = \widetilde{U}_{2D} = \sum_{i_1=1}^{i_{1max}} \sum_{i_2=1}^{i_{2max}} \frac{(\alpha_1 i_1)^2 + (\alpha_2 i_2)^2 + (\alpha_3)^2}{e^{[(\alpha_1 i_1)^2 + (\alpha_2 i_2)^2 - \Lambda'']} + 1} \tag{4.4}$$

By using the first two terms of PSF, dimensionless internal energy for 2D Fermi gases can be approximated as

$$\widetilde{U}_{2D} \approx \frac{\pi \Lambda''^2}{8\alpha_1 \alpha_2} - \frac{\Lambda''^{3/2}}{6} \left(\frac{1}{\alpha_1} + \frac{1}{\alpha_2} \right) + \alpha_3^2 N_{2D} \tag{4.5}$$

where N_{2D} is the Eq. (4.2).

In Fig. (4.4), blue curve is obtained by dividing the exact 2D summation solution of internal energy Eq. (4.4) to Eq. (4.1) and red curve is obtained by dividing Eq. (4.5) to Eq. (4.2). As expected, the pattern is the same as in Fig. (4.2) where $N - \Lambda$ is plotted. Our approximate solution (represented by red curve) exactly matches with the solution in continuous case ($\alpha_1 = \alpha_2 = 0.1$) and represents the trend behavior in discrete case ($\alpha_1 = \alpha_2 = 3$).

Figure 4.4: Dimensionless internal energy per particle vs dimensionless chemical potential for discrete (left subfigure) and continuous (right subfigure) cases with $\alpha_1 = 3$ and $\alpha_1 = 0.1$ respectively. $\alpha_2 = 3$ and $\alpha_3 = 40$ for both cases.

When we look at the variations of dimensionless internal energy per particle with number of particles, its nature is not stepwise like in 1D, for both discrete and continuous cases. It seems like parametric plot of two stepwise functions compensate their stepwise behavior and as a result we observe smooth line even in discrete case in Fig. (4.5).
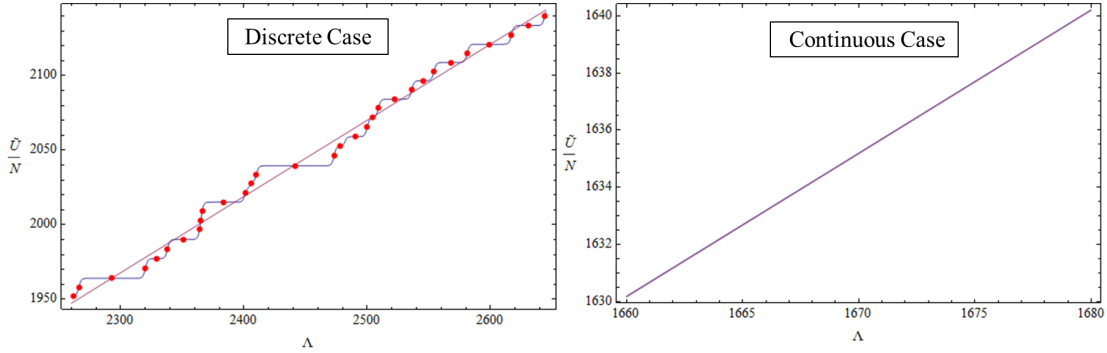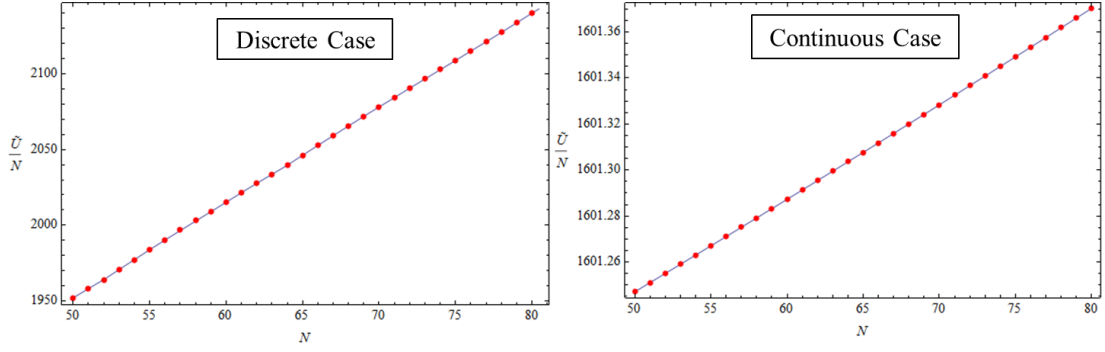
Figure 4.5: Dimensionless internal energy per particle vs number of particles for discrete (left subfigure) and continuous (right subfigure) cases with $\alpha_1 = 3$ and $\alpha_1 = 0.1$ respectively. $\alpha_2 = 3$ and $\alpha_3 = 40$ for both cases.

4.1.1 Diagonal and Non-diagonal Elements of the State Matrix

As it seen from Figs. (4.2) and (4.4), behaviors of thermodynamic state functions of 2D and (as we'll see in following chapter) 3D Fermi gases are interestingly different than that of 1D Fermi gases. To understand the reason of this difference, let's examine the nature of summations in detail. As we know, all thermodynamic quantities are represented by summations over momentum state variables $\{i_1, i_2, i_3\}$, which constitute a state matrix. Each element in the state matrix represents a momentum state of the system and all contributions to thermodynamic quantities are done over this momentum state variables. For 2D and 3D Fermi gases, it is possible to decompose the state matrix into diagonal $\{i_1 = i_2 = i_3\}$, and non-diagonal matrices. However, for 1D Fermi gas, since the state matrix becomes the state vector, there are no diagonal or non-diagonal elements but just a vector. Quasi-irregular behavior of thermodynamic state functions of 2D and 3D Fermi gases is the result of the contributions of the non-diagonal state matrix. In non-diagonal state matrix, multiplicity or degeneracy of energy levels can be different than one, in other words, contributions of states constantly changes during the progress of summation operator. This quasi-irregular[1] changes are mainly due to the combinatorial nature of summations. In Fig. (4.6), appearance of quasi-ness is charted.

---

[1] We are saying quasi-irregular because in fact the patterns are the result of a very definite, mathematically exact summation process. So they are not actually irregular, though they look like.

| Regular Discrete Nature | + | Degenerate Energy Levels | = | Quasi-irregular Discrete Nature |

Figure 4.6: Regular behavior becomes quasi-irregular in 2D and 3D Fermi gases, due to degeneracy of energy levels.

4.2 2D Thermodynamic Quantities with Quasi-irregular Peakwise Behavior

Peakwise behavior of entropy is obtained for 2D Fermi gas in Fig. (4.7) for the discrete case. Unlike 1D case, now its behavior is not regular but quasi-irregular.

Figure 4.7: Dimensionless entropy per particle vs dimensionless chemical potential for discrete (left subfigure) and continuous (right subfigure) cases with $\alpha_1 = 3$ and $\alpha_1 = 0.1$ respectively. $\alpha_2 = 3$ and $\alpha_3 = 40$ for both cases.
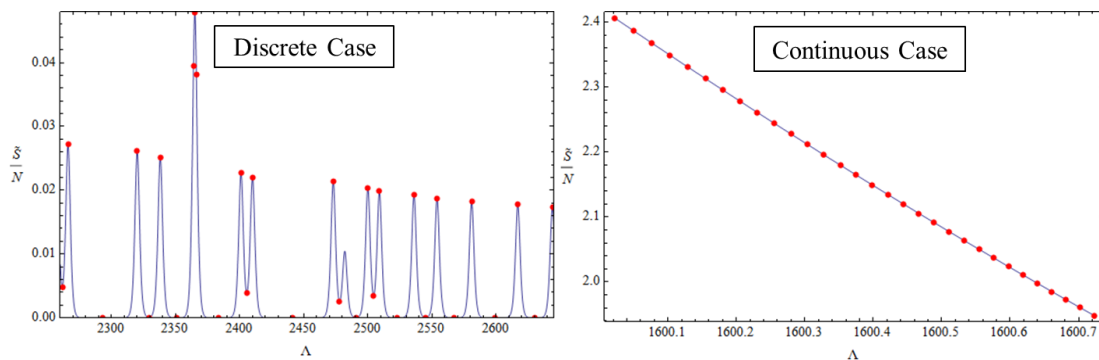

Figure 4.8: Dimensionless heat capacity per particle vs dimensionless chemical potential for discrete (left subfigure) and continuous (right subfigure) cases with $\alpha_1 = 3$ and $\alpha_1 = 0.1$ respectively. $\alpha_2 = 3$ and $\alpha_3 = 40$ for both cases.
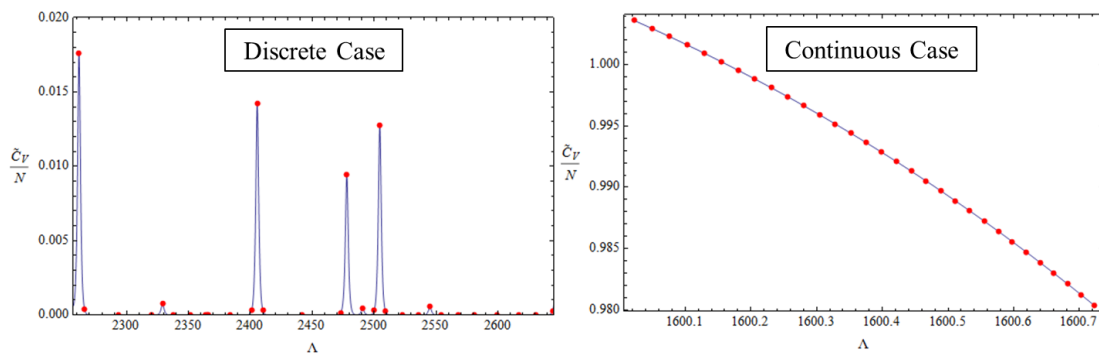
To understand the causes of the peaks, let's examine the nature of Fermi line in 2D Fermi gas.

4.2.1 Discrete Fermi Line

In 1D Fermi gas, contributions to entropy and heat capacity were coming from Fermi point. Likewise, in 2D Fermi gas, they are coming from the particles on an hypothetical line called Fermi line. Contributions coming from the outside of Fermi line is totally negligible, since contributions of particles on outside of the region of Fermi line, correspond to the bottoms of FD variance function where its value vanishes. Therefore, summation just over the states on Fermi line gives the values of the entropy and heat capacity for 2D Fermi gas. To define Fermi line, we need some mathematical tools like round, ceiling and floor functions. Here, we derived the analytical expressions of them for any x,

$$\text{Round}(x) = x + \frac{1}{\pi}\arctan\left[\cot\left(\pi\left(x + \frac{1}{2}\right)\right)\right] \tag{4.6}$$

by adding one half to x, we obtain ceiling function,

$$\text{Ceiling}(x) = x + \frac{1}{2} + \frac{1}{\pi}\arctan\left[\cot\left(\pi\left(x + 1\right)\right)\right] \tag{4.7}$$

by substracting one half from x, we obtain floor function,

$$\text{Floor}(x) = x - \frac{1}{2} + \frac{1}{\pi}\arctan\left[\cot\left(\pi\left(x\right)\right)\right] \tag{4.8}$$

Now, it is possible to arrange the lower and upper limits of the summations in entropy and heat capacity, according to Fermi line.

$$i_{1min} = 1 \tag{4.9}$$

$$i_{1max} = \frac{\sqrt{\Lambda''}}{\alpha_1} + \frac{1}{2} \tag{4.10}$$

$$i_{2min} = \text{Ceiling}\left[\frac{\sqrt{\Lambda'' - \left[\alpha_1\left(i_1 + \frac{1}{2}\right)\right]^2}}{\alpha_2} - \frac{1}{2}\right] \tag{4.11}$$

$$= \frac{\sqrt{\Lambda'' - \left[\alpha_1\left(i_1 + \frac{1}{2}\right)\right]^2}}{\alpha_2} + \frac{1}{\pi}\arctan\left[\cot\left(\frac{\pi\sqrt{\Lambda'' - \left[\alpha_1\left(i_1 + \frac{1}{2}\right)\right]^2}}{\alpha_2} + \frac{\pi}{2}\right)\right] \tag{4.12}$$

$$i_{2max} = \text{Floor}\left[\frac{\sqrt{\Lambda'' - [\alpha_1(i_1 - \frac{1}{2})]^2}}{\alpha_2} + \frac{1}{2}\right] \quad \text{(4.13)}$$

$$= \frac{\sqrt{\Lambda'' - [\alpha_1(i_1 - \frac{1}{2})]^2}}{\alpha_2} + \frac{1}{\pi}\arctan\left[\cot\left(\frac{\pi\sqrt{\Lambda'' - [\alpha_1(i_1 - \frac{1}{2})]^2}}{\alpha_2} + \frac{\pi}{2}\right)\right] \quad \text{(4.14)}$$

Then, the sum over momentum states through those limits gives the discrete Fermi line shown by solid blue line in Fig. (4.9). Summing from 1 to i_{1max} over $\sqrt{\Lambda'' - (\alpha_1 i_1)^2}/\alpha_2$ gives the idealized Fermi line represented by red dotted line in Fig. (4.9). Making summations from 1 to i_{1max} over $\sqrt{\Lambda'' - [\alpha_1(i_1 + 1/2)]^2}/\alpha_2 - 1/2$ and $\sqrt{\Lambda'' - [\alpha_1(i_1 - 1/2)]^2}/\alpha_2 + 1/2$ respectively gives lower and upper dashed brown lines enclosing the discrete Fermi line which are called the Fermi shell. As it happens, Fermi shell is the consequence of Heisenberg uncertainty principle and discrete Fermi line always stays inside the area enclosed by Fermi shell.
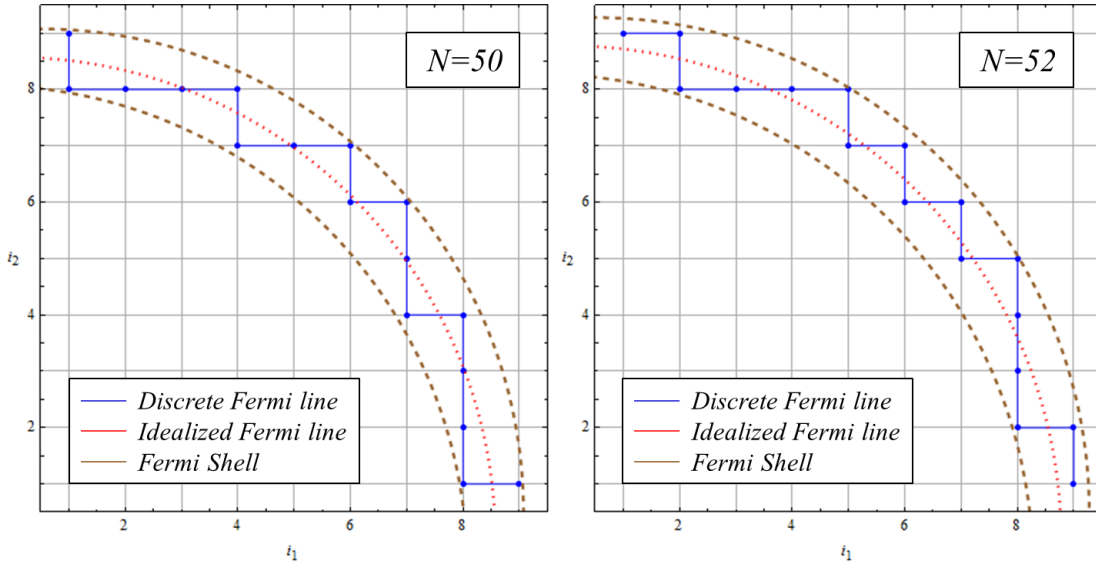
Figure 4.9: Idealized and discrete Fermi lines and Fermi shell for 2D Fermi gas with $\alpha_1 = 3, \alpha_2 = 3, \alpha_3 = 40$. On the left subfigure, N=50 and on the right subfigure, N=52.

As we've seen in previous chapter, the position of momentum states in functional space of variance function determines the magnitude of the contribution to entropy and heat capacity. Peaks of the variance correspond to the idealized Fermi line, so the closer the state to idealized Fermi line, the larger its contribution to entropy and heat capacity and vice versa.

In Fig. (4.10), behavior of entropy varying with particle number is seen. Interestingly, on the right subfigure entropy graph there are several modes for entropy.

Figure 4.10: Dimensionless entropy per particle (left subfigure) and entropy itself (right subfigure) changing with number of particles where $\alpha_1 = 3, \alpha_2 = 3, \alpha_3 = 40$.

When number of particles or chemical potential increase, Fermi line and consequently the Fermi shell extends while its thickness remains constant. There are oscillations in entropy and heat capacity, since the combination of proximities of momentum states in Fermi shell to the idealized Fermi line changes and results to a different contribution for a different combination of states. In shor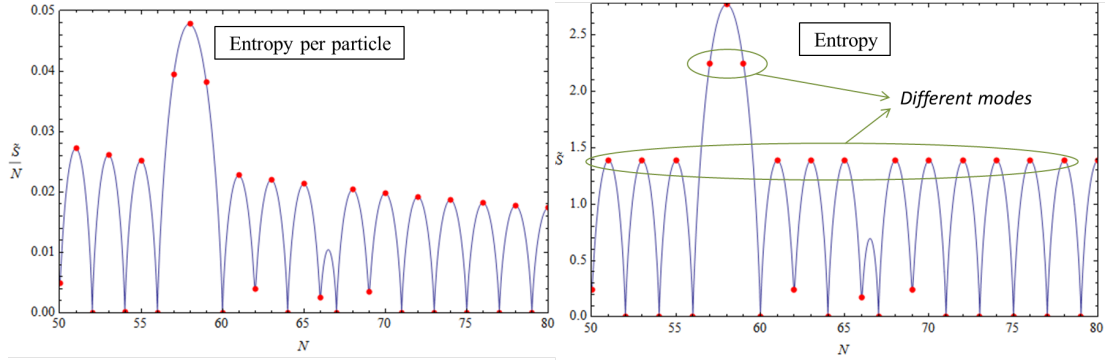t, the proximities of the states to the peaks of the variance function determines the contribution. For example, in Fig. (4.11), there is a peak at 50 particles and it vanishes when two more particles are added to the domain.

Comparison of the same domain with number of particles 50 and 52 represents with peak and without peak respectively, is shown in Fig. (4.9). For $N = 50$, there are more particle near to the idealized Fermi line and for $N = 52$, they are almost none. Remember that the thickness of the variance peak decreases when confinement and degeneracy increases. So even for a little deviation from the idealized Fermi line, the contribution of that state to the entropy and heat capacity almost vanishes for strongly confined and degenerate Fermi gases.

Although Fermi shell starts to contain more and more states when N or Λ increases, the contributions does not increase since FWHM of variance decreases also. Thereby, despite the oscillations, entropy and heat capacity goes to zero when $N \to \infty$ or $\alpha \to \infty$.
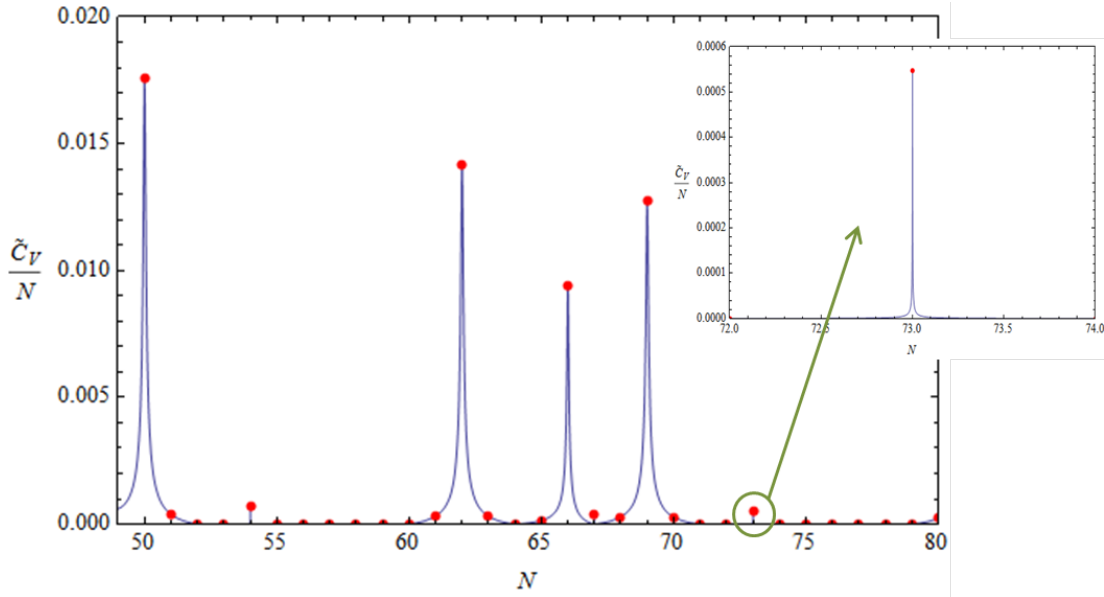
Figure 4.11: Dimensionless heat capacity per particle varying with number of particles for 2D Fermi gas with $\alpha_1 = 3$, $\alpha_2 = 3$ and $\alpha_3 = 40$.

4.3 Oscillatory Quantum Size Effects in 2D Entropy and Heat Capacity

In previous chapter, we've seen for the 1D case that entropy and heat capacity change smoothly when its first direction, which is the only allowed direction, is changed. However, for 2D case the situation is entirely different. In 2D case, there are two directions, the first and the second, are allowed.

4.3.1 Anisotropic Size Dependence

Unlike 1D domains, there are two ways for confinement of 2D domain; anisotropic and isotropic confinements. In both cases, effect of confinement on particle number and internal energy is the same and trivial, see Fig. (4.12). However, for entropy and heat capacity, behaviors are quite different.
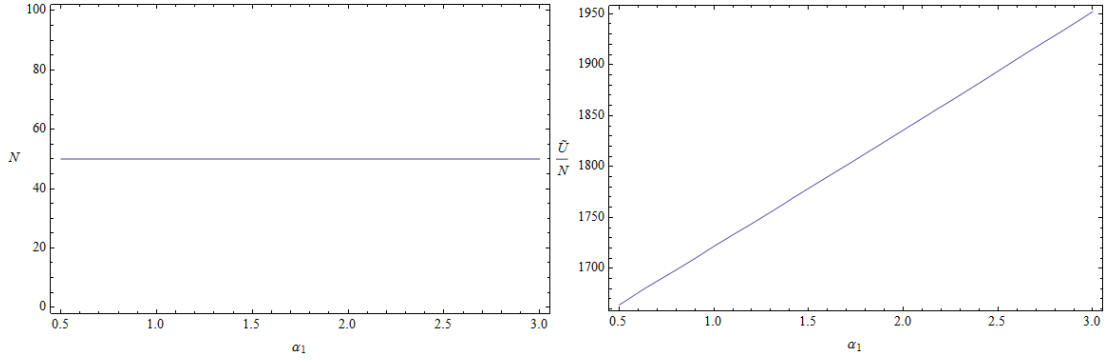
Figure 4.12: Number of particles (left subfigure) and dimensionless internal energy per particle (right subfigure) changing with confinement parameter in the first direction α_1.

In anisometric size confinement case, in Fig. (4.13), quasi-irregular, non-periodic oscillations in entropy and heat capacity is obtained when confinement changed only in one direction, α_1. Oscillatory behavior is the result of the discrete nature of Fermi line. When domain size changes anisotropically, distributions of states in Fermi shell as well as their contributions also change and cause oscillations.

Figure 4.13: Dimensionless entropy per particle (left subfigure) and specific heat (right subfigure) changing with confinement parameter in the first direction α_1.

4.3.2 Isotropic Size Dependence

On the other hand, when two allowed directions of 2D domain change isotropically (at once), sharp oscillations disappear yield themselves to very slowly varying smooth changes, see Fig. (4.14). The reason of the relatively smooth change in isotropic case is that the distances of integer momentum states to the idealized Fermi line (where the contribution is maximum), does not change while the sharpness of the variance function changes for all states in Fermi shell.
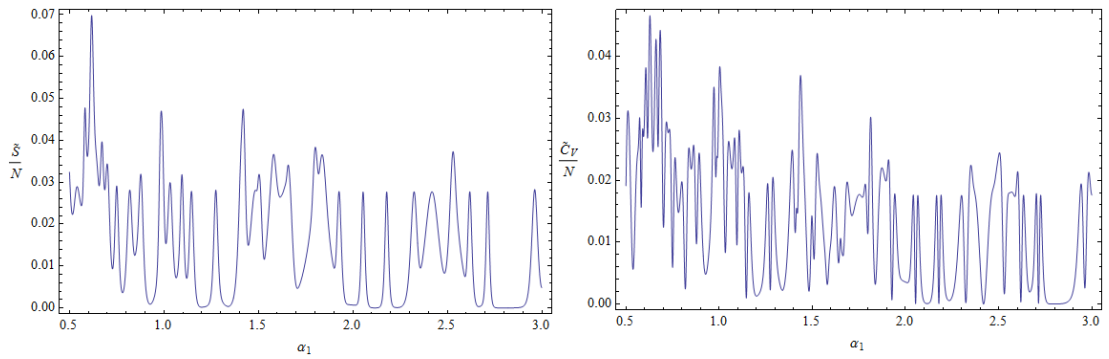
65
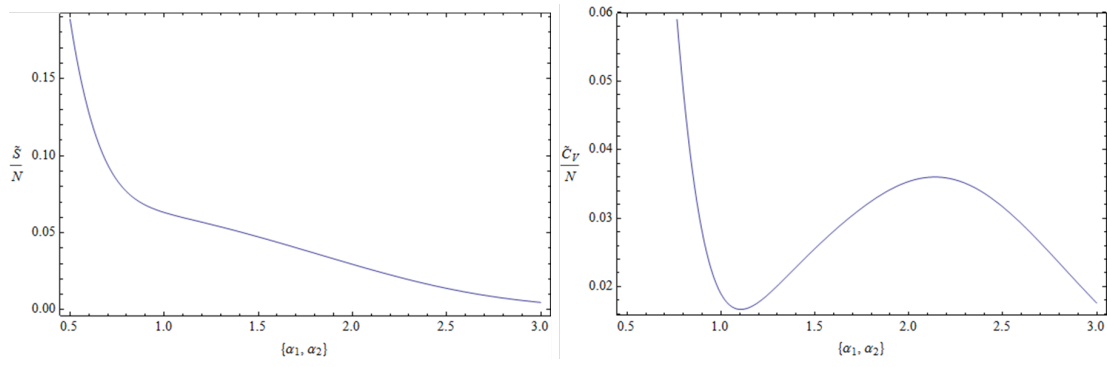
Figure 4.14: Dimensionless entropy per particle (left subfigure) and specific heat (right subfigure) changing with confinement parameter of first and second directions α_1, α_2.

5. 3D FERMI GAS CONFINED IN AN ISOMETRIC DOMAIN

Although confined structures behave as lower-dimensional for some certain chemical potential intervals, in the end, all structures in our universe are actually three-dimensional. In this chapter, we discuss an isometric 3D domain with relatively weakly confined in all directions like in Fig. (5.1). Confinement parameters are chosen for this kind of domain as $\alpha_1 = \alpha_2 = \alpha_3 = 3$.

3D Fermi Gas
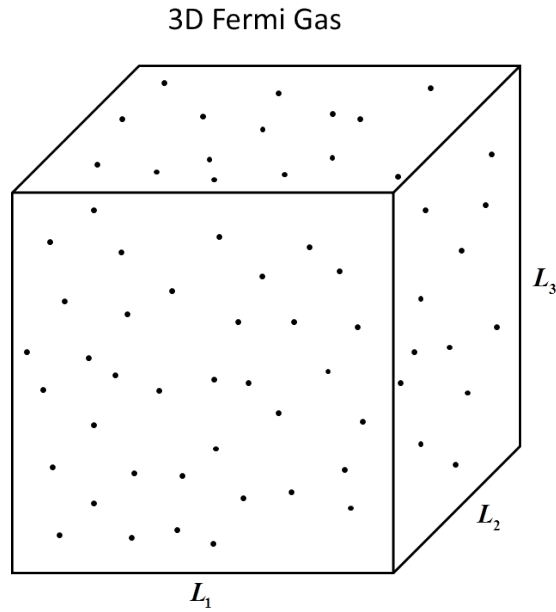
Figure 5.1: A prototype of an isometric 3D domain with $\alpha_1 = 3$, $\alpha_2 = 3$ and $\alpha_3 = 3$.

5.1 3D Thermodynamic Quantities with Quasi-irregular Stepwise Behavior

In 3D case, behaviors of thermodynamic quantities are very similar to 2D one. Due to the degeneracy of energy levels, patterns are quasi-irregular just like in the 2D case.

Without any restriction in the range of Λ this time, number of particles can be written as

$$N = \sum_{i_1=1}^{i_{1max}} \sum_{i_2=1}^{i_{2max}} \sum_{i_3=1}^{i_{3max}} \frac{1}{e^{[(\alpha_1 i_1)^2 + (\alpha_2 i_2)^2 + (\alpha_3 i_3)^2 - \Lambda]} + 1} \tag{5.1}$$

By using the first two terms of PSF, we can obtain number of particles approximately as

$$N_{3D} \approx \frac{\pi \Lambda^{3/2}}{6\alpha_1 \alpha_2 \alpha_3} - \frac{\pi \Lambda}{8} \left(\frac{1}{\alpha_1 \alpha_2} + \frac{1}{\alpha_2 \alpha_3} + \frac{1}{\alpha_1 \alpha_3} \right)$$
$$+ \frac{\sqrt{\Lambda}}{4} \left(\frac{1}{\alpha_1} + \frac{1}{\alpha_2} + \frac{1}{\alpha_3} \right) - \frac{1}{8}$$

(5.2)

where the first term represents the bulk (3D) contribution and second, third and fourth terms represent the surface, line and corner contributions respectively.

Quasi-irregular stepwise behavior is seen in the relationship of particle number and chemical potential in Fig. (5.2), where blue and red curves represent Eqs. (5.1) and (5.2) respectively. Likewise, red dots show the Λ values correspond to integer N.

Figure 5.2: Variation of number of particles with dimensionless chemical potential for a 3D domain with $\alpha_1 = 3$, $\alpha_2 = 3$ and $\alpha_3 = 3$.

From the first two terms of PSF, internal energy can be approximated as

$$\widetilde{U}_{3D} \approx \frac{\pi \Lambda^{5/2}}{10\alpha_1 \alpha_2 \alpha_3} - \frac{\pi \Lambda^2}{16} \left(\frac{1}{\alpha_1 \alpha_2} + \frac{1}{\alpha_2 \alpha_3} + \frac{1}{\alpha_1 \alpha_3} \right)$$
$$+ \frac{\Lambda^{3/2}}{12} \left(\frac{1}{\alpha_1} + \frac{1}{\alpha_2} + \frac{1}{\alpha_3} \right) - \frac{1}{8}$$

(5.3)

where again like in Eq. (5.2), dimensional contributions are represented by the relevant terms in the Eq. (5.3).

In Fig. (5.3), blue curve is obtained by dividing exact 3D internal energy sum to exact 3D number of particles sum and red curve is the result of Eq. (5.3) divided by Eq. (5.2). Red dots indicates the integer number of particles in internal energy-chemical potential functional space. Due to degeneracy of energy levels, behaviors of particle number and internal energy are not regular.
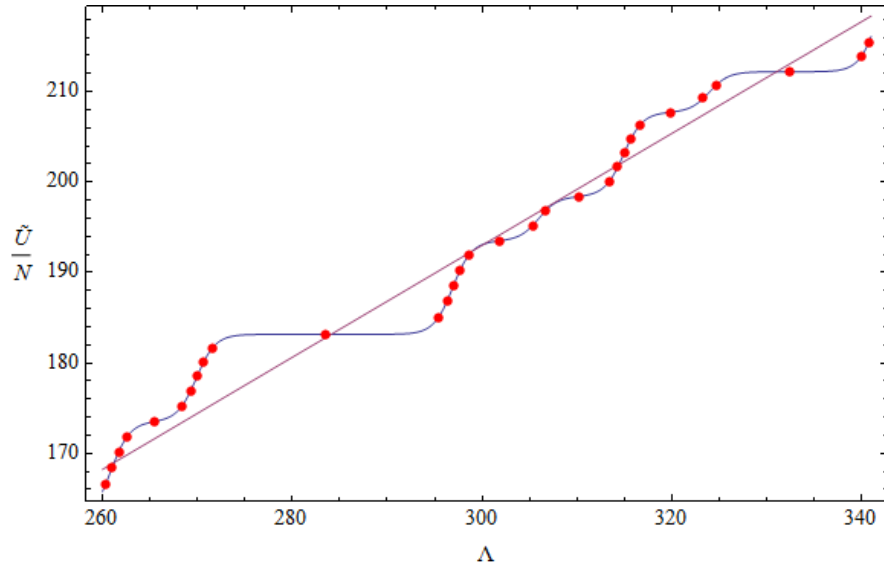
Figure 5.3: Variation of dimensionless internal energy per particle with dimensionless chemical potential for a 3D domain with $\alpha_1 = 3$, $\alpha_2 = 3$ and $\alpha_3 = 3$.

5.2 3D Thermodynamic Quantities with Quasi-irregular Peakwise Behavior

Like in 2D case, entropy has quasi-irregular peakwise behavior in confined 3D nano structures contain Fermi gas. In Fig. (5.4), peaks in entropy when it is changing with chemical potential is shown. Peakwise nature turns into a camber behavior in Fig. (5.5) where entropy is changing with particle number.

69

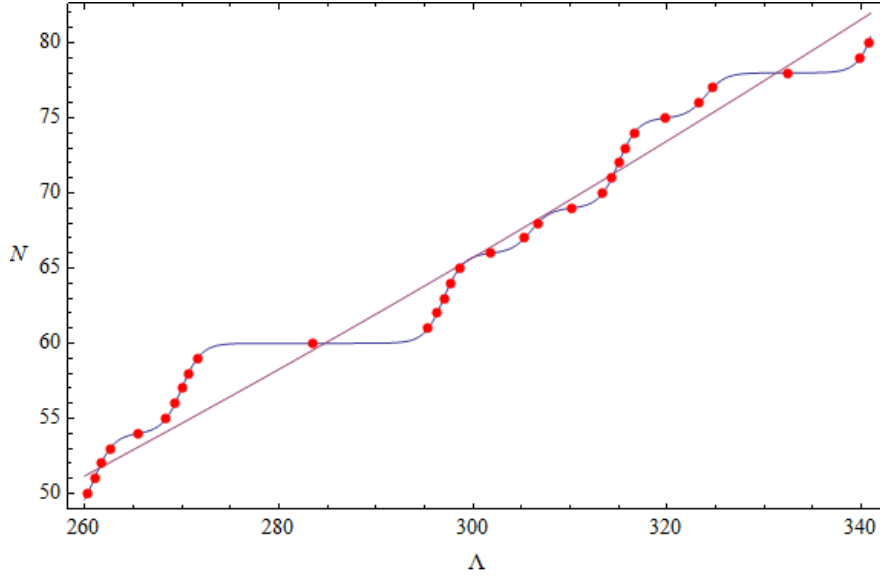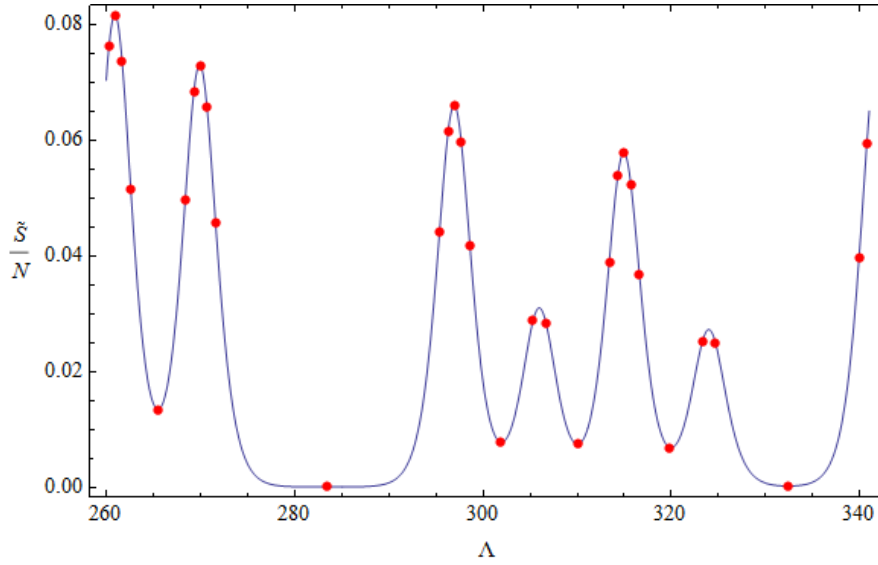**Figure 5.4**: Dimensionless entropy per particle varying with dimensionless chemical potential for a 3D domain with $\alpha_1 = 3$, $\alpha_2 = 3$ and $\alpha_3 = 3$.
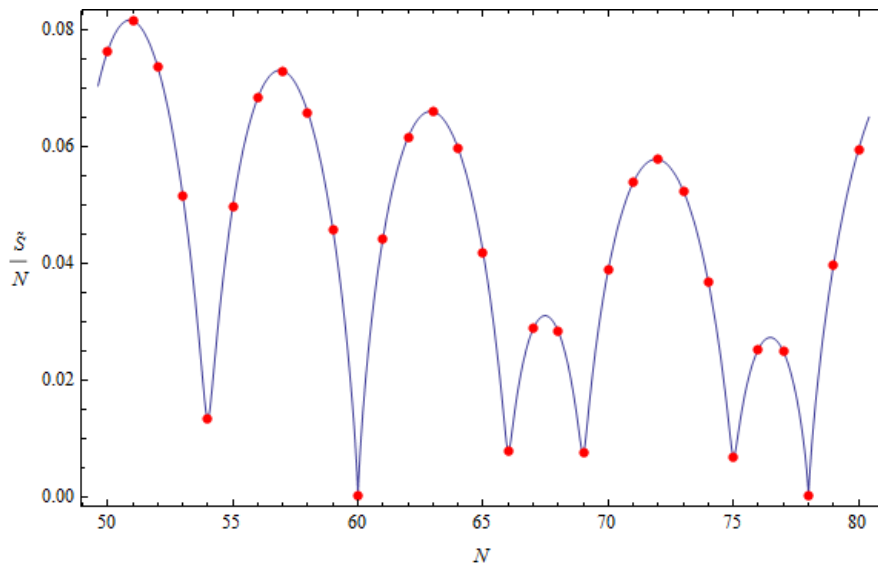
Figure 5.5: Dimensionless entropy per particle varying with particle number for a 3D domain with $\alpha_1 = 3$, $\alpha_2 = 3$ and $\alpha_3 = 3$.

Peakwise nature in the variation of specific heat with chemical potential and particle number of 3D Fermi gases is shown in Figs. (5.6) and (5.7) respectively. Reason of these peaks is similar to the 2D case. This time, they are the consequence of the discreteness of Fermi surface in confined 3D Fermi gases.
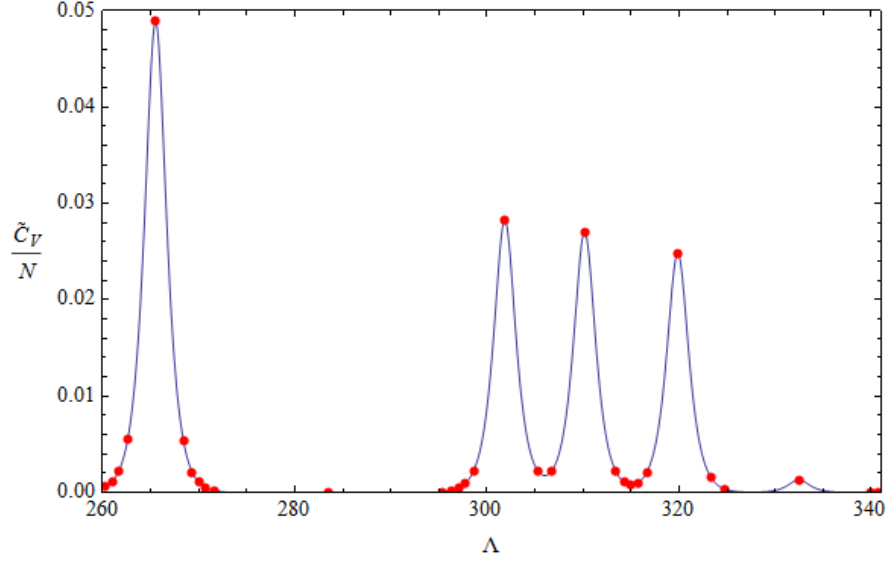
Figure 5.6: Dimensionless heat capacity per particle varying with dimensionless chemical potential for a 3D domain with $\alpha_1 = 3$, $\alpha_2 = 3$ and $\alpha_3 = 3$.
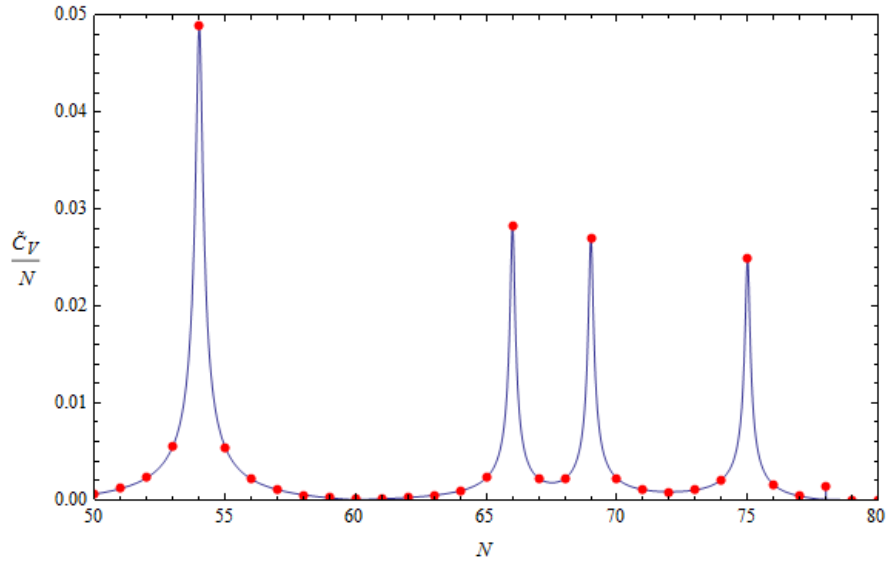
Figure 5.7: Dimensionless heat capacity per particle varying with particle number for a 3D domain with $\alpha_1 = 3$, $\alpha_2 = 3$ and $\alpha_3 = 3$.

5.2.1 Discrete Fermi Surface

In 3D Fermi gases, contribution to entropy and heat capacity comes from the integer momentum states on the Fermi surface. Entropy and heat capacity contributions are the consequence of the peaks of FD variance function. If there is a peak in the variation of variance with energy or chemical potential, then contribution is large and vice versa. Since peaks of the variance correspond to the discrete Fermi surface within Fermi shell,

71

it is enough to sum the momentum states on discrete Fermi surface. Then instead of summing from 1 to ∞, we can make summations between the following values of momentum states,

$$i_{1min} = 1 \tag{5.4}$$

$$i_{1max} = \frac{\sqrt{\Lambda''}}{\alpha_1} + \frac{1}{2} \tag{5.5}$$

$$i_{2min} = \text{Ceiling}\left[\frac{\sqrt{\Lambda'' - \left[\alpha_1\left(i_1 + \frac{1}{2}\right)\right]^2 - \left[\alpha_3\left(i_3 + \frac{1}{2}\right)\right]^2}}{\alpha_2} - \frac{1}{2}\right] \tag{5.6}$$

$$= \frac{\sqrt{\Lambda'' - \left[\alpha_1\left(i_1 + \frac{1}{2}\right)\right]^2 - \left[\alpha_3\left(i_3 + \frac{1}{2}\right)\right]^2}}{\alpha_2} \tag{5.7}$$

$$+ \frac{1}{\pi}\arctan\left[\cot\left(\frac{\pi\sqrt{\Lambda'' - \left[\alpha_1\left(i_1 + \frac{1}{2}\right)\right]^2 - \left[\alpha_3\left(i_3 + \frac{1}{2}\right)\right]^2}}{\alpha_2} + \frac{\pi}{2}\right)\right] \tag{5.8}$$

$$i_{2max} = \text{Floor}\left[\frac{\sqrt{\Lambda'' - \left[\alpha_1(i_1 - \frac{1}{2})\right]^2 - \left[\alpha_3(i_3 - \frac{1}{2})\right]^2}}{\alpha_2} + \frac{1}{2}\right] \tag{5.9}$$

$$= \frac{\sqrt{\Lambda'' - \left[\alpha_1\left(i_1 - \frac{1}{2}\right)\right]^2 - \left[\alpha_3(i_3 - \frac{1}{2})\right]^2}}{\alpha_2} \tag{5.10}$$

$$+ \frac{1}{\pi}\arctan\left[\cot\left(\frac{\pi\sqrt{\Lambda'' - \left[\alpha_1\left(i_1 - \frac{1}{2}\right)\right]^2 - \left[\alpha_3(i_3 - \frac{1}{2})\right]^2}}{\alpha_2} + \frac{\pi}{2}\right)\right] \tag{5.11}$$

$$i_{3min} = 1 \tag{5.12}$$

$$i_{3max} = \frac{\sqrt{\Lambda''}}{\alpha_3} + \frac{1}{2} \tag{5.13}$$

Discrete Fermi surface, idealized Fermi surface and its $\pm 1/2$ neighborhoods are shown in Fig. (5.8) by rainbow, orange and light blue colored surfaces respectively. States outside the Fermi shell, have almost no contribution to entropy and heat capacity of the 3D Fermi gas.
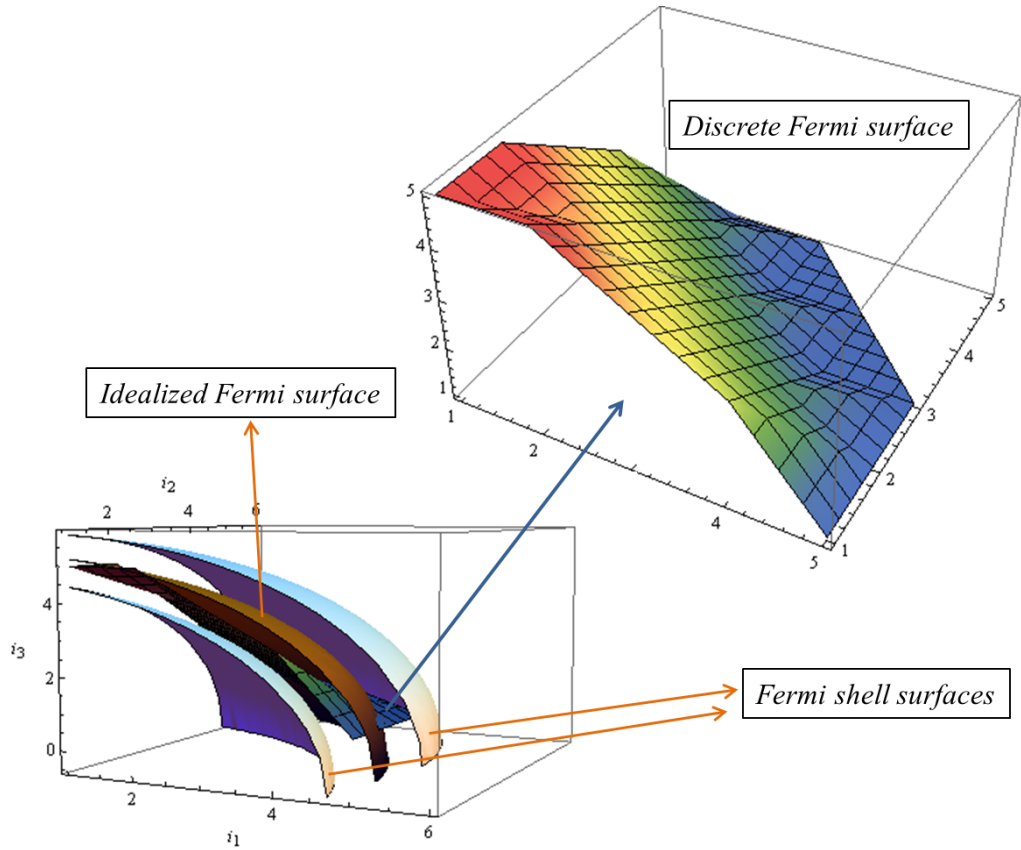
Figure 5.8: Idealized and discrete Fermi surface and Fermi shell surfaces for 3D Fermi gas with $\alpha_1 = 3, \alpha_2 = 3, \alpha_3 = 3$.

5.3 Oscillatory Quantum Size Effects in 3D Entropy and Heat Capacity

As we've seen in the 2D case, number of particles and internal energy do not show any special or unexpected behavior when the confinement changes. On the other hand, size dependencies in the entropy and heat capacity of confined 3D Fermi gases are extremely strong. As it is seen in Figs. (5.9) and (5.10), there are oscillatory behaviors in the variations of entropy and heat capacity with confinement parameter of the domain in the first direction.
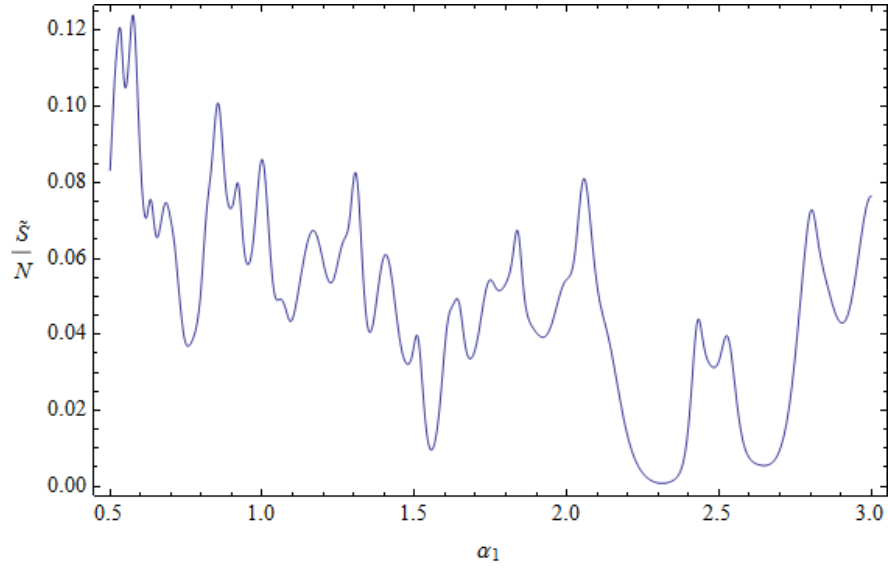
Figure 5.9: Oscillations in dimensionless entropy per particle varying with confine-
ment parameter in the first direction for $N = 50$, $\alpha_2 = 3$ and $\alpha_3 = 3$.
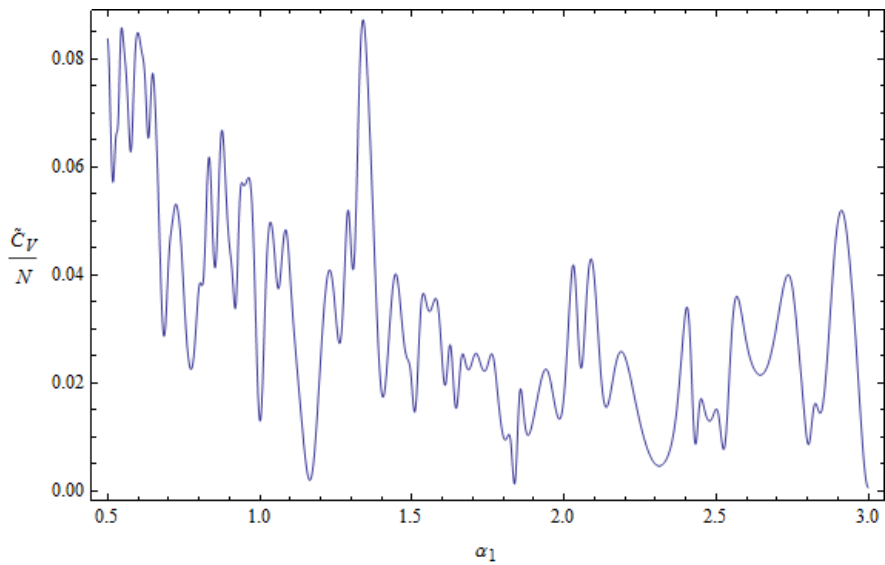
Figure 5.10: Oscillations in dimensionless heat capacity per particle varying with
confinement parameter in the first direction for $N = 50$, $\alpha_2 = 3$ and
$\alpha_3 = 3$.

When two of the three directions are subjected to change, oscillatory behavior can still
be observed, see Fig. (5.11). However, when all three directions are changed at once,
in Fig. (5.12), oscillations almost disappear and functions exhibits smooth changes
with confinement parameters.
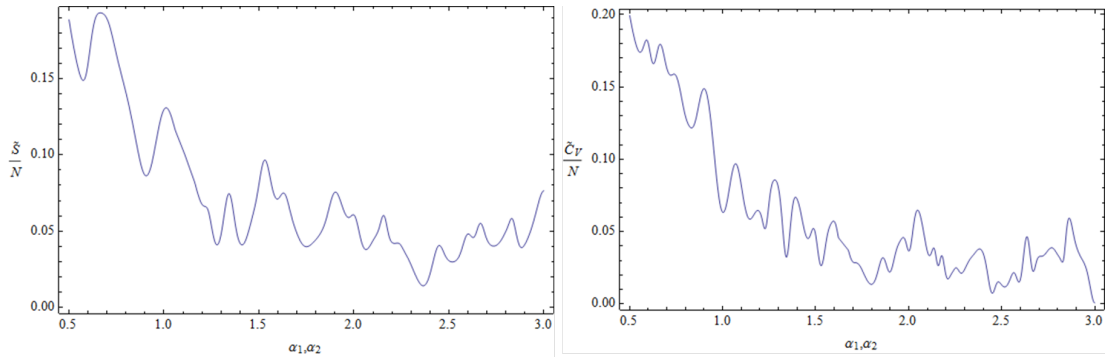
Figure 5.11: Dimensionless entropy per particle (left subfigure) and dimensionless heat capacity per particle (right subfigure) changing with isometric confinement in first and second directions while third one is constant ($\alpha_3 = 3$) for $N = 50$.
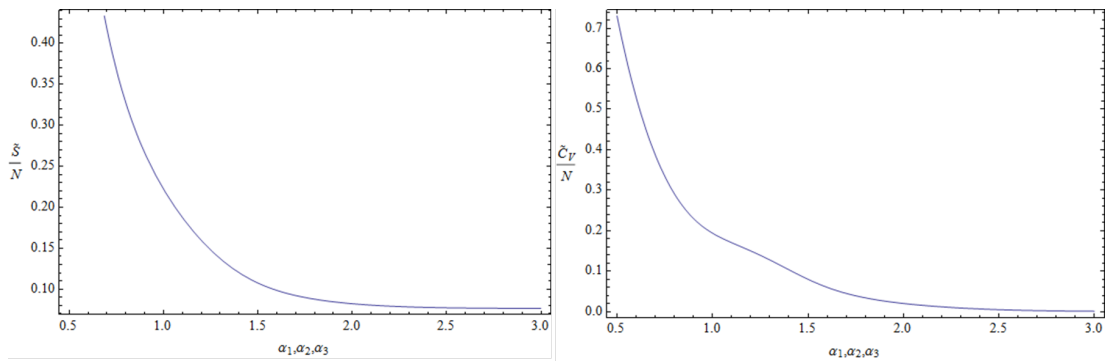
Figure 5.12: Dimensionless entropy per particle (left subfigure) and dimensionless heat capacity per particle (right subfigure) changing with isometric confinement in all directions.

As we see, entropy and heat capacity are affected severely by confinement.

6. EXCESS THERMAL ENERGY STORAGE AT NANO SCALE

Perhaps the best way to verify the results in this thesis is trying to measure the heat capacity of relatively weakly confined 3D Fermi gas. Confinement rates are easily obtainable in today's experimental capabilities. Since oscillations in heat capacity is a direct consequence of the discrete nature, experimental verification of heat capacity oscillations means also the verification of the discrete nature of thermodynamics.

In this study so far, only electronic contributions to heat capacity are discussed. In the heat capacity of metals, there are also lattice contributions and total heat capacity of metals is written as

$$C_V^{(T)} = C_V^{(e)} + C_V^{(L)} = \gamma_e T + \gamma_L T^3 \tag{6.1}$$

where γ_e and γ_L are proportionality constants and (T), (e) and (L) superscripts denote total, electronic and lattice contributions respectively. From Eq. (6.1), one can infer that in low temperatures electronic contributions, whereas in high temperatures lattice contributions are dominant. Also note that, decreasing temperature increases the confinement parameter α which is the case in this study. So it is consistent to expect the dominant contributions to degenerate and confined ideal Fermi gases come from the electronic one. That's why lattice contributions are neglected.

Let's consider a 3D isometric InSb nano structure with sizes $L_1 = L_2 = L_3 = 10$nm and conduction electron density around $9.35 \text{x} 10^{25}$ m^{-3} at 5K [28]. Changing the size of the domain in the first direction from 10 nm to 12 nm will result to the oscillations in the electronic heat capacity of the substance as in Fig. (6.1).
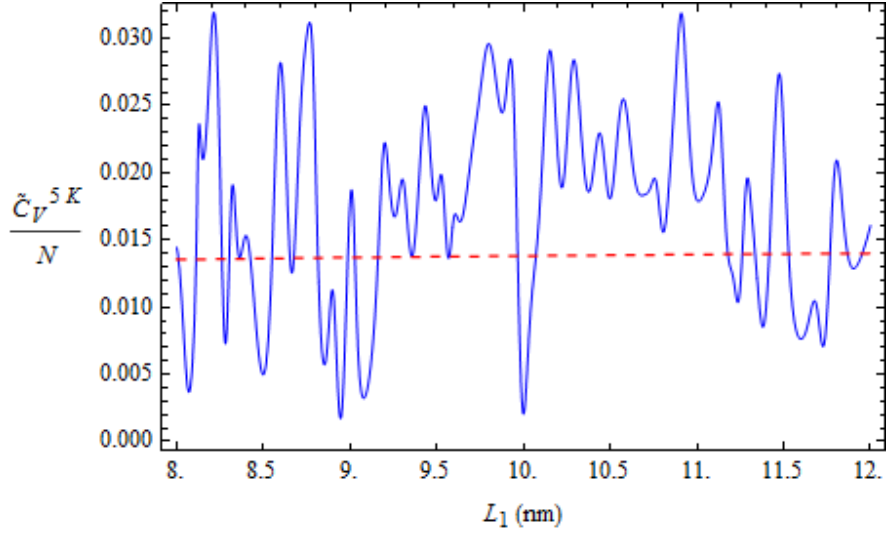
Figure 6.1: Dimensionless specific heat varying with domain size in the 1st direction for $T = 5$K.

In Fig. (6.1) and then in Figs. (6.2) and (6.3), blue curve represents the exact summation equation of heat capacity (Eq. 2.38) divided by exact number of particles (Eq. 5.1) and red line represents the specific heat capacity under continuum approximation from Eq. (2.78) that is $\widetilde{C}_V/N = \pi^2/2\Lambda$. The same experimental setup but in different temperature, say 7K will change the oscillation pattern as in Fig. (6.2).
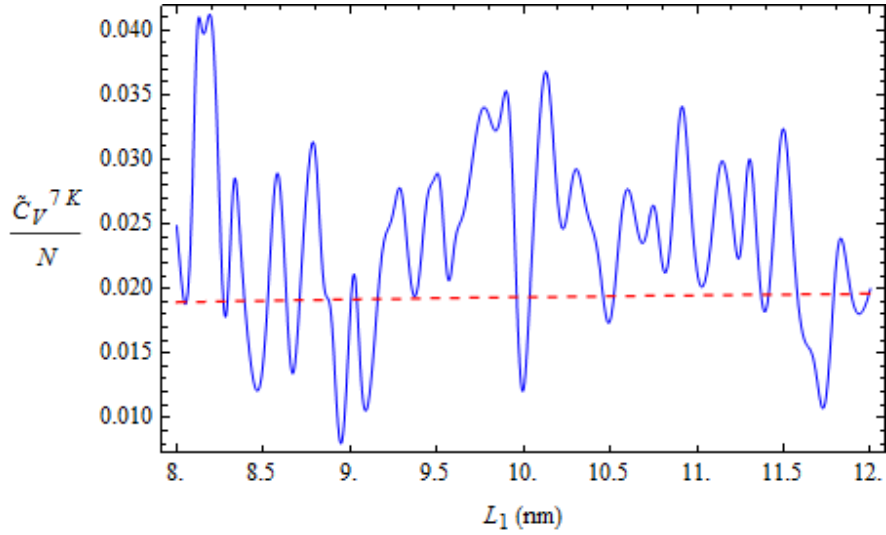
Figure 6.2: Dimensionless specific heat varying with domain size in the 1st direction for $T = 7$K.

Due to several natural reasons there might be errors in the experiments and experimental results may not exactly the same with the Figs. (6.1) or (6.2). However,

we can divide two results to each other and get a relative result of the heat capacity of structure. In this case, even if there is an experimental error, if the experiment is done properly, the proportional result of heat capacities of two cases (5K and 7K) should be the same as in Fig. (6.3). As it is seen from Figs. (6.1), (6.2) and (6.3), there are experimentally recognizable rise and falls in the specific heat while domain size changes.
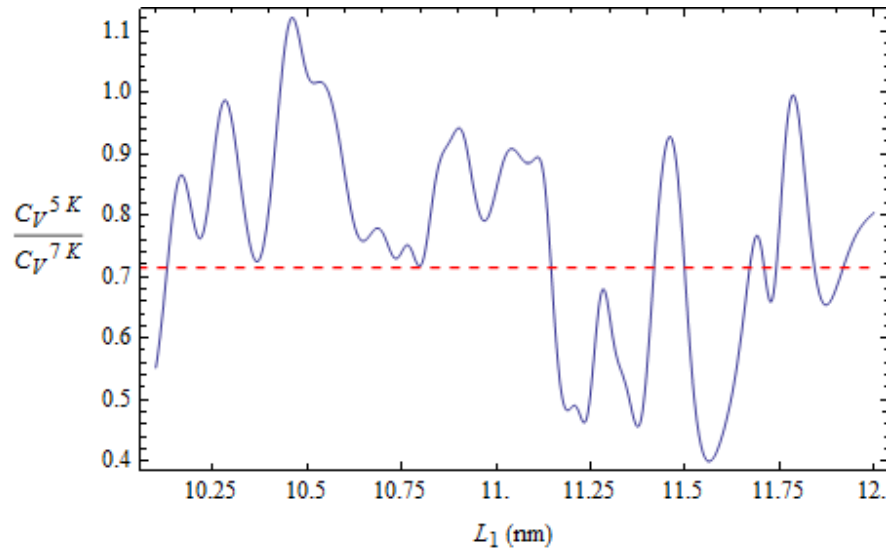
Figure 6.3: Ratio of the C_V vs L_1 results for $T = 5$K and $T = 7$K.

One can also experimentally verify the results by measuring the Fermi surface and observing its discreteness [29].

Thermal energy storage is directly related to the heat capacity. The higher heat capacity means the more thermal energy storage. According to the heat capacity equation (Eq. 2.38), heat capacity of nano structures are lower than the macro ones. However, when oscillations and peaks that we observed are considered, the situation may change.

Finely tuning confinement to the values where heat capacity of the nano structure makes its peak and gathering many of them may lead to a macroscopic substance with a pretty larger specific heat capacity than the ordinary one. Making a nano device based on heat capacity oscillations, will be the manifestation of excess thermal energy storage at nano scale by quantum size effects.

Apart from the industrial potential, discreteness of thermodynamics broadens our perspective on nature and intuitively show us even the most well-established concepts

like continuity of thermodynamic quantities can be considered as an asymptotic approximation of more general concepts. Almost every breakthrough in science corroborates the importance of thinking phenomena in opposite limits of conventional cases. Considering this point of view in fundamental areas like thermodynamics may take us closer to the reality of nature.

REFERENCES

[1] **Sisman, A. and Müller, I.**, 2004. The Casimir-like size effects in ideal gases, *Phys. Lett. A*, **320**, 360–366.

[2] **Sisman, A.**, 2004. Surface dependency in thermodynamics of ideal gases, *J. Phys. A- Math. Gen.*, **37**, 11353–11361.

[3] **Sisman, A. and Babac, G.**, 2012. Quantum Size Effects on Classical Thermosize Effects, *Continuum Mech. Thermodyn.*, **24**, 339–346.

[4] **Aydin, A. and Sisman, A.**, 2013. Discrete Nature of Thermodynamic Properties, Proceedings of 12th Joint European Thermodynamics Conference, Brescia, Italy, pp.425–429.

[5] **Aydin, A. and Sisman, A.**, 2014. Discrete Nature of Thermodynamics in Confined Ideal Fermi Gases (Accepted), *Phys. Lett. A*.

[6] **Kittel, C. and Kroemer, H.**, 1980. Thermal Physics, 2nd Ed., W. H. Freeman.

[7] **Reif, F.**, 1965. Fundamentals of Statistical and Thermal Physics, McGraw-Hill.

[8] **Landau, L. and Lifshitz, E.**, 1980. Statistical Physics, 3rd Ed., Pergamon Press.

[9] **Molina, M.I.**, 1996. Ideal gas in a finite container, *Am. J. Phys.*, **64**, 503–505.

[10] **Pathria, R.K.**, 1998. An ideal quantum gas in a finite-sized container, *Am. J. Phys.*, **66**, 1080–1085.

[11] **Dai, W.S. and Xie, M.**, 2003. Quantum statistics of ideal gases in confined space, *Phys. Lett. A*, **311**, 340–346.

[12] **Dai, W.S. and Xie, M.**, 2004. Geometry effects in confined space, *Phys. Rev. E*, **70**, 016103.

[13] **Pang, H.; Dai, W.S. and Xie, M.**, 2006. The difference of boundary effects between Bose and Fermi systems, *J. Phys. A- Math. Gen.*, **39**, 2563–2571.

[14] **Tayurskii, D., A. and Minnullin, A., R.**, 2003. Thermodynamic and magnetic properties of the confined neutral Fermi systems, *Physica B*, **329–333**, 152–153.

[15] **Schneider, J. and Wallis, H.**, 1998. Mesoscopic Fermi gas in a harmonic trap, *Phys. Rev. A*, **57**, 1253–1259.

[16] **Chen, L.; Su, G. and Chen, J.**, 2012. Ultracold finite-size Fermi gas in a quartic trap, *Phys. Lett. A*, **376**, 2908–2910.

[17] **Sisman, A.; Ozturk, Z.F. and Firat, C.**, 2007. Quantum boundary layer: a non-uniform density distribution of an ideal gas in thermodynamic equilibrium, *Phys. Lett. A*, **362**, 16–20.

[18] **Firat, C. and Sisman, A.**, 2009. Universality of quantum boundary layer for a Maxwellian gas, *Phys. Scripta*, **79**, 065002.

[19] **Firat, C.; Sisman, A. and Ozturk, Z.F.**, 2010. Thermodynamics of gases in nano cavities, *Energy*, **35**, 814–819.

[20] **de Oliveira, I. N.; Lyra, M.L. and Albuquerque, E.L.**, 2004. Specific heat anomalies of non-interacting fermions with multifractal energy spectra, *Physica A*, **343**, 424–432.

[21] **Moreira, D. A.; Albuquerque, E.L. and Anselmo, D.H.A.L.**, 2008. Specific heat spectra of non-interacting fermions in a quasiperiodic ladder sequence, *Phys. Lett. A*, **372**, 5233–5238.

[22] **Ozturk, Z.F. and Sisman, A.**, 2009. Quantum Size Effects on the Thermal and Potential Conductivities of Ideal Gases, *Phys. Scripta*, **80**, 065402.

[23] **Firat, C. and Sisman, A.**, 2013. Quantum forces of a gas confined in nano structures, *Phys. Scr.*, **87**, 045008.

[24] **Griffiths, D.J.**, 2004. Introduction to Quantum Mechanics, 2nd Ed., Prentice Hall.

[25] **Yan, Z.**, 2000. General thermal wavelength and its applications, *Eur. J. Phys.*, **21**, 625–631.

[26] **Firat, C.**, 2008. Quantum Size Effects in the Thermodynamic Behaviors of Gases, Ph.D. thesis, Istanbul Technical University.

[27] **Warner, J.H.**, **Schaffel, F.**, **Rummeli, M. and Bachmatiuk, A.**, 2012. Graphene: Fundamentals and emergent applications, 1st Ed., Elsevier.

[28] **Gueron, M.**, 1964. Density of the conduction electrons at the nuclei in Indium Antimonide, *Phys. Rev.*, **135**, A1.

[29] **Kordyuk, A.A.**, **Borisenko, S.V.**, **Golden, M.S.**, **Legner, S.**, **Nenkov, K.A.**, **Knupfer, M.**, **Fink, J.**, **Berger, H.**, **Forro, L. and Follath, R.**, 2002. Doping dependence of the Fermi surface in $(Bi,Pb)_2Sr_2CaCu_2O_{8+\delta}$, *Phys. Rev. B*, **66**, 014502.

APPENDICES

APPENDIX A: MATHEMATICAL SUPPLEMENT
APPENDIX B: THERMODYNAMIC SUPPLEMENT

APPENDIX A: MATHEMATICAL SUPPLEMENT

1.1 Derivation of Boltzmann Entropy Formula

Entropy is fundamentally defined as a measure for the number of microscopic configurations (denoted by Ω) in a system of objects. In physical processes, this measure governs a purely physical quantity that is called heat. There is a direct proportionality between heat and entropy change in a system with a factor called temperature,

$$dS \geq \frac{dQ}{T} \tag{A.1}$$

It is apparent from the equation above that, since heat is an extensive (additive) quantity, entropy also have to be. Hence, we cannot directly calculate entropy by measuring how many microscopic configurations a system has, since as a statistical fact, combining two systems into one system will result to the multiplication of the number of microscopic configurations of two systems ($\Omega_1 \times \Omega_2 = \Omega_{1,2}$), which is a non-additive operation. For consistency with the physical definition, entropy would be calculated as an extensive quantity, so that multiplication of probabilities or configurations of systems corresponds to the addition of their entropies ($S_1 + S_2 = S_{1,2}$), see Fig. (A.1).

$$\Omega_1 \quad \times \quad \Omega_2 \quad = \quad \Omega_{1,2}$$
$$S_1 \quad + \quad S_2 \quad = \quad S_{1,2}$$
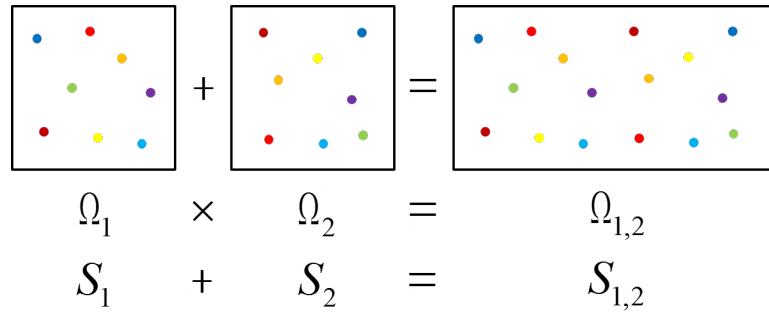
Figure A.1: Entropy have to be additive while multiplicity is not.

So, we want a function that satisfies,

$$f(xy) = f(x) + f(y) \tag{A.2}$$

Suppose f is a differentiable and continuous function. Taking the derivative of above equation with respect to x and y gives respectively,

$$yf'(xy) = f'(x) \longrightarrow f'(xy) = \frac{f'(x)}{y} \tag{A.3a}$$

$$xf'(xy) = f'(y) \longrightarrow f'(xy) = \frac{f'(y)}{x} \tag{A.3b}$$

so,

$$f'(xy) = \frac{f'(x)}{y} = \frac{f'(y)}{x} \tag{A.4}$$

arranging and equating them to a constant k,

$$xf'(x) = yf'(y) = k \tag{A.5}$$

which can be written as

$$f'(x) = \frac{k}{x} \quad \text{and} \quad f'(y) = \frac{k}{y} \tag{A.6}$$

integrating them with respect to x and y respectively,

$$\int f'(x)dx = k \int \frac{dx}{x} \quad \text{and} \quad \int f'(y)dy = k \int \frac{dy}{y} \tag{A.7}$$

that proves $f(x)$ and $f(y)$ are nothing but the logarithm function,

$$f(x) = k \log x + c \quad \text{and} \quad f(y) = k \log y + c \tag{A.8}$$

As it is seen, only differentiable and continuous function that satisfies the condition is logarithm function. Statistically, inverse of the number of microstates correspond to a macrostate gives the probability of a microstate ($1/\Omega_i = p_i$). If all possible microstates are not equally likely, taking the average of the logarithm of number of configurations will give entropy and it is written in its general form as[1]

$$S = -\sum_i p_i \log p_i \tag{A.9}$$

where p_i is the probability of ith state. When all states are equally probable and naturally $\sum_i p_i = 1$, above formula reduces to the Boltzmann's entropy formula,

$$S = \log \Omega \tag{A.10}$$

where temperature scale constant k_B is taken as unity ($k_B = 1$) for brevity.

---

[1]In fact even this is not the most general form, but a close and thermodynamically sufficient one. The most general form of entropy is known as Von Neumann entropy in quantum statistical mechanics, and written as $S = \text{Tr}(\rho \log \rho)$ where Tr is trace and ρ is the density matrix.

1.2 Derivation of Poisson Summation Formula

Poisson summation formula is stated as

$$\sum_{i=-\infty}^{\infty} f(i) = \sum_{s=-\infty}^{\infty} \widehat{f}(s) \tag{A.11}$$

where $\widehat{f}$ is the Fourier transform of f. Then from the definition of Fourier transform,

$$\sum_{i=-\infty}^{\infty} f(i) = \sum_{s=-\infty}^{\infty} \int_{-\infty}^{\infty} f(i)e^{-2\pi Isi}di \tag{A.12}$$

where I is imaginary unit. From Euler's identity we can write this as

$$\sum_{i=-\infty}^{\infty} f(i) = \sum_{s=-\infty}^{\infty} \int_{-\infty}^{\infty} f(i)[\cos(2\pi si) - I\sin(2\pi si)]di \tag{A.13}$$

For even functions, summation and integral on the right hand side can take the form below:

$$f(i) = f(-i) \ \rightarrow \ \sum_{i=-\infty}^{\infty} f(i) = 2\sum_{s=1}^{\infty} \left[2\int_{0}^{\infty} f(i)\cos(2\pi si)di \right] + 2\int_{0}^{\infty} f(i)di \tag{A.14}$$

It is possible to express the summation as

$$\sum_{i=-\infty}^{\infty} f(i) = 2\sum_{i=1}^{\infty} f(i) + f(0) \tag{A.15}$$

Then,

$$\sum_{i=1}^{\infty} f(i) = \frac{1}{2}\sum_{i=-\infty}^{\infty} f(i) - \frac{f(0)}{2} \tag{A.16}$$

Writing Eq. (A.14) into Eq. (A.16) gives PSF for even functions,

$$\sum_{i=1}^{\infty} f(i) = \int_{0}^{\infty} f(i)di - \frac{f(0)}{2} + 2\sum_{s=1}^{\infty} \int_{0}^{\infty} f(i)\cos(2\pi si)di \tag{A.17}$$

1.3 Useful Integrals

Evaluations of some common integrals that are used in quantum statistics are given below:

$$\int_{0}^{\infty} \frac{(\alpha i)^n}{e^{(\alpha i)^2 - \Lambda} \pm 1}di = \mp\frac{\Gamma[(n+1)/2]}{2\alpha}Li_{(n+1)/2}(\mp e^\Lambda) \tag{A.18}$$

$$\int_{0}^{\infty} \frac{(\alpha i)^n e^{(\alpha i)^2 - \Lambda}}{\left(e^{(\alpha i)^2 - \Lambda} \pm 1\right)^2}di = \mp\left(\frac{n-1}{4\alpha}\right)\Gamma\left(\frac{n-1}{2}\right)Li_{(n-1)/2}(\mp e^\Lambda) \tag{A.19}$$

$$\int_0^\infty (\alpha i)^n \ln\left[1 \pm e^{\Lambda - (\alpha i)^2}\right] di = \mp \frac{\Gamma[(n+1)/2]}{2\alpha} Li_{(n+3)/2}(\mp e^\Lambda) \qquad \textbf{(A.20)}$$

Integrals above are true except the points where Gamma function goes to infinity.

1.4 Polylogarithm Functions and Their Series Expansions

Polylogarithm Functions are special functions defined as

$$Li_n(z) = \sum_{k=1}^\infty \frac{z^k}{k^n} \qquad \textbf{(A.21)}$$

where n is order and z is the argument of the function. It has a beautiful property that it responses to integration or differentiation with increase or decrease in order respectively. This property makes it practical in such operations.

$$\Lambda >> 1 \Rightarrow Li_n(-e^\Lambda) \cong -\frac{\Lambda^n}{\Gamma[n+1]}\left[1 + \frac{\pi^2 n(n-1)}{6\Lambda^2}\right] + O(n^4) \qquad \textbf{(A.22)}$$

where Γ indicates the Gamma function and O denotes the order of unwritten terms of the expansion. Most encountered polylogarithm functions in Fermi-Dirac statistics are given below with their series expansions

$$Li_{5/2}(-e^\Lambda) \cong -\frac{8\Lambda^{5/2}}{15\sqrt{\pi}}\left[1 + \frac{5\pi^2}{8\Lambda^2}\right] \qquad \textbf{(A.23)}$$

$$Li_2(-e^\Lambda) \cong -\frac{\Lambda^2}{2}\left[1 + \frac{\pi^2}{3\Lambda^2}\right] \qquad \textbf{(A.24)}$$

$$Li_{3/2}(-e^\Lambda) \cong -\frac{4\Lambda^{3/2}}{3\sqrt{\pi}}\left[1 + \frac{\pi^2}{8\Lambda^2}\right] \qquad \textbf{(A.25)}$$

$$Li_1(-e^\Lambda) \cong -\Lambda \qquad \textbf{(A.26)}$$

$$Li_{1/2}(-e^\Lambda) \cong -\frac{2\Lambda^{1/2}}{\sqrt{\pi}}\left[1 - \frac{\pi^2}{24\Lambda^2}\right] \qquad \textbf{(A.27)}$$

$$Li_0(-e^\Lambda) \cong -1 \qquad \textbf{(A.28)}$$

$$Li_{-1/2}(-e^\Lambda) \cong -\frac{1}{\sqrt{\pi\Lambda}}\left[1 + \frac{\pi^2}{8\Lambda^2}\right] \qquad \textbf{(A.29)}$$

Even for $\Lambda = 10$, errors of above equations are under $2\mathrm{x}10^{-4}$ and drastically decrease with increasing Λ.

For the integrals encountered in BE statistics below formula can be used,

$$\Lambda \to^- 0 \Rightarrow Li_n(e^\Lambda) = \Gamma(1-n)(-\Lambda)^{n-1} + \sum_{k=0}^{\infty} \frac{(-\Lambda)^k \zeta(n-k)}{k!} \qquad \text{(A.30)}$$

where ζ is the Riemann zeta function. Even for $\Lambda = -0.1$, errors of above equation are under $3\text{x}10^{-5}$ and again decrease rapidly with increasing Λ.

1.5 First Order Temperature Corrections To Chemical Potential

1.5.1 Derivation in 3D

From Eq. (2.46), we can write number of particles for 3D by expanding polylogarithms to zeroth order correction we have,

$$N_3 = \frac{V}{\lambda_{th}^3} \frac{4\Lambda^{3/2}}{3\sqrt{\pi}} \qquad \text{(A.31)}$$

We want to find the temperature correction to chemical potential, but we don't know it yet. So let's assume chemical potential differs with a small term of δ_3,

$$\mu = \mu_F(1+\delta_3) \qquad \text{(A.32)}$$

or equivalently,

$$\Lambda = \Lambda_F(1+\delta_3) \qquad \text{(A.33)}$$

Now the aim is to find the value of δ_3. Inserting the above relation to the first order temperature correction of number of particles equation in Eq. (2.46) gives,

$$N_3 = \frac{V}{\lambda_{th}^3} \frac{4[\Lambda_F(1+\delta_3)]^{3/2}}{3\sqrt{\pi}} \left[1 + \frac{\pi^2}{8[\Lambda_F(1+\delta_3)]^2} \right] \qquad \text{(A.34)}$$

Dividing the one with first order correction Eq. (A.34) to zeroth order one Eq. (A.31) gives,

$$1 = (1+\delta_3)^{3/2} \left(1 + \frac{\pi^2}{8\Lambda_F^2(1+\delta_3)^2} \right) \qquad \text{(A.35)}$$

We may neglect the correction term in the denominator and use the approximation of $(1+x)^n \approx 1+nx$ which gives

$$1 = \left(1 + \frac{3\delta_3}{2} \right) \left(1 + \frac{\pi^2}{8\Lambda_F^2} \right) \qquad \text{(A.36)}$$

Neglecting the fourth order term coming from the multiplication above leads,

$$1 = 1 + \frac{3\delta_3}{2} + \frac{\pi^2}{8\Lambda_F^2} \qquad \text{(A.37)}$$

Then temperature correction to chemical potential in 3D domians, δ_3 becomes,

$$\delta_3 = -\frac{\pi^2}{12\Lambda_F^2} \tag{A.38}$$

and we write for 3D domains,

$$\Lambda = \Lambda_F \left(1 - \frac{\pi^2}{12\Lambda_F^2} \right) \tag{A.39}$$

or equivalently,

$$\mu = \mu_F \left(1 - \frac{\pi^2 k_B^2 T^2}{12\mu_F^2} \right) \tag{A.40}$$

This is A very useful result that by using this it is possible to obtain entropy and heat capacity for continuous 3D domains.

1.5.2 Derivation in 2D

First order correction of number of particles in 2D does not contain temperature correction, so $\mu = \mu_F$ for 2D case. Entropy and heat capacity in 2D can be derived by using the first order temperature corrections of other relevant thermodynamic quantities. See (2.2.4).

1.5.3 Derivation in 1D

In the same manner we do in 3D case, zeroth order and first order corrections for number of particles in 1D are written respectively as

$$N_1 = \frac{2C}{h}\sqrt{2m}\sqrt{\mu_1} \tag{A.41}$$

$$N_1 = \frac{2C}{h}\sqrt{2m}\sqrt{\mu_1(1+\delta_1)} \left(1 - \frac{\pi^2}{24\Lambda_F^2} \right) \tag{A.42}$$

Dividing Eq. (A.42) to Eq. (A.41) and making relevant approximations leads,

$$1 = 1 + \frac{\delta_1}{2} - \frac{\pi^2}{24\Lambda_F^2} \tag{A.43}$$

Then temperature correction of chemical potential for 1D domains,

$$\delta_1 = \frac{\pi^2}{12\Lambda_F^2} \tag{A.44}$$

Then the chemical potential in 1D continuous domains can be written along with its temperature correction as

$$\mu = \mu_F \left(1 + \frac{\pi^2 k_B^2 T^2}{12\mu_F^2} \right) \tag{A.45}$$

APPENDIX B: THERMODYNAMIC SUPPLEMENT

2.1 Glossary of Thermodynamics

- **Energy:** A property that changes at least one of the state variables of the system.

- **Entropy:** An extensive measure of the number of microscopic configurations that an equilibrium thermodynamic system can be found. It can be interpreted as the quantity of *"unknown"* or the magnitude of *"disorder"*. So entropy is a property of macrostate, not of the microstate.

- **Heat:** A form of energy that spontaneously transfers itself from higher temperature object to the lower one to balance the entropy difference in between objects.

- **Work:** A form of energy that can be used in mechanical forms.

- **Microstate:** An instant state of particles in a system that corresponds to their degrees of freedom (like positions and momentums) and quantum numbers (like spins, angular momentums) of individual particles.

- **Macrostate:** An instant state of a system that corresponds to the macroscopic properties (like pressure, temperature and volume) of particles. Different microstates can lead to the same macrostate.

- **Thermal equilibrium:** A condition that two systems in contact reach to the same constant temperature.

- **Statistical ensemble:** A bunch of systems that represents a specific probability distribution.

- **Microcanonical ensemble:** An isolated system with fixed total energy and number of particles.

- **Canonical ensemble:** A closed system with fixed temperature and number of particles.

- **Grand canonical ensemble:** An open system with neither energy nor number of particles is fixed.

- **Maxwell-Boltzmann statistics:** An equilibrium statistical concept that particles are assumed to be non-interacting and system is in its high temperature and/or low density limit.

- **Fermi-Dirac statistics:** An equilibrium statistical concept for non-interacting particles which obey the Pauli exclusion principle.

- **Bose-Einstein statistics:** An equilibrium statistical concept for non-interacting particles which have tendency to condensate into the same energy state.

- **Partition function:** An abstract statistical concept introduced for describing the statistical properties of a system in thermodynamic equilibrium. Useful for simplifying and manipulating thermodynamic functions.

- **Chemical potential:** A form of potential energy that causes to the movement of particles in a system.

- **Temperature:** A measure of infinitesimal change in entropy with respect to infinitesimal change in energy.

$$\frac{1}{T} = \left(\frac{\partial S}{\partial U} \right)_{V,N}$$

- **Helmholtz free energy:** A form of potential energy that can be converted to work.

- **Pressure:** A force per unit area due to kinetic energies of particles (energetic pressure) and their tendency to evolve into a more probable configuration (entropic pressure).

- **Heat capacity:** Heat energy required to change the temperature of an object by a given amount.

- **Thermal fluctuations:** Quasi-random deviations of a system from its equilibrium state. Disappear at absolute zero temperature.

- **Degeneracy:** A condition of a system with extremely high density or low temperatures so that quantum mechanical effects determine the physical characteristics of the system.

- **Multiplicity:** Number of momentum state configurations which correspond to the same energy level. In other words, the degeneracy of energy levels.

2.2 Glossary of Related Quantum Mechanical Concepts

- **Quantum state:** Quantum mechanical state (like position, spin or momentum) of a system denoted by quantum numbers.

- **Momentum state:** A quantum state of particles that characterize their energies.

- **Wave function:** A function that describes the statistical probabilities of a quantum state. According to the standard interpretation of quantum mechanics, it contains all the information about its quantum state.

- **Spin:** An intrinsic quantum state of elementary particles. It specifies the statistical behavior of particles as stated by spin-statistics theorem. For example, particles having half-integer spin exhibits the nature of FD statistics, whereas particles having integer spin displays the character of BE statistics.

- **Thermal de Broglie wavelength:** A quantity defined in the calculation of partition function and related with the de Broglie wavelength of particles.

- **Most probable de Broglie wavelength:** Wavelength of particles which makes distribution function maximum.

- **Pauli exclusion principle:** A principle states that two or more identical fermions cannot occupy the same quantum state simultaneously.

- **Quantum confinement:** When domain size is smaller than the most probable de Broglie wavelength of particles, they're said to be quantum mechanically confined in the domain.

- **Quantum fluctuations:** Random and temporary change in the amount of energy in a region of spacetime due to creation and annihilation of particle-antiparticle pairs allowed by energy-time uncertainty principle.

$$\Delta E \Delta t \approx \frac{h}{2\pi}$$

2.3 Laws of Thermodynamics

- **0th law of thermodynamics:** If a system A is in *thermal equilibrium* with systems B and C, then B and C are also in thermal equilibrium with each other. It represents the *associative* property of the heat. Mathematically,

$$A \equiv B \ \text{ and } \ B \equiv C \ \longrightarrow \ A \equiv C$$

- **1th law of thermodynamics:** Heat is a form of *energy* and energy is *conserved* for closed systems.[1] Then change in the internal energy of a closed system corresponds to a change in heat and/or work.

$$dU = dQ + dW$$

- **2th law of thermodynamics:** *Entropy* of an isolated system cannot decrease.[2]

$$dS \geq 0$$

- **3th law of thermodynamics:** Entropy of a system with *temperature* at absolute zero Kelvin is *zero* and it is *not* possible to reach absolute zero with finite number of processes. Quantum mechanically, this is the consequence of the existence of a lowest energy state for any particle.

$$T \to 0 \ \implies \ S(T) = 0$$

---

[1]Quantum fluctuations are neglected.

[2]At least within a given time on the order of human observation. On the other hand, since entropy in fact is a purely statistical notion, fluctuations always happen and according to Poincaré recurrence theorem, even for an isolated system, if there is sufficiently long (i mean *really* long) time, entropy *will* eventually decrease and system returns to a state very close to its initial state [].

CURRICULUM VITAE

Name Surname: Alhun AYDIN

Place and Date of Birth: Bursa, 04/05/1989

Address: Istanbul Technical University, Energy Institute, 34469, Istanbul, Turkey

E-Mails: aydinalh@itu.edu.tr, alhunaydin@gmail.com

B.Sc.: Physics, Koç University

Professional Experience: Research Assistant

PUBLICATIONS/PRESENTATIONS ON THE THESIS

▪ **Aydin A.** and Sisman A., *Discrete Nature of Thermodynamics in Confined Ideal Fermi Gases*, Phys. Lett. A, 2014 (Accepted)

▪ **Aydin A.** and Sisman A., *Discrete Nature of Thermodynamic Properties*, 12th Joint European Thermodynamics Conference, Proceedings of JETC 2013, pp: 425-429, 1-5 July 2013, Brescia, Italy